SIMULTANEOUS TARGETING OF PARP1 AND RAD52 TRIGGERS DUAL SYNTHETIC LETHALITY IN BRCA-DEFICIENT CANCERS

A Dissertation
Submitted to
the Temple University Graduate Board

In Partial Fulfillment
of the Requirements for the Degree
DOCTOR OF PHILOSOPHY

---

by
Katherine S. Reed
May 2018

Examining Committee Members:

Tomasz Skorski, M.D., Ph.D. (Advisor), Department of Microbiology and Immunology
Xavier Graña, Ph.D., Department of Medical Genetics and Molecular Biochemistry
Dianne Soprano, Ph.D., Department of Medical Genetics and Molecular Biochemistry
Dan Liebermann, Ph.D., Department of Medical Genetics and Molecular Biochemistry
Richard Pomerantz, Ph.D., Department of Medical Genetics and Molecular Biochemistry
Neil Johnson, Ph.D., Fox Chase Cancer Center
Alex Mazin, Ph.D., (External Examiner), Drexel University College of Medicine

ABSTRACT

PARP inhibitors (PARPi) have been used to induce synthetic lethality in BRCA-deficient tumors in clinical trials with limited success due to the development of resistance to PARPi. BRCA-deficient cells are unable to repair DNA double strand breaks by the accurate homologous recombination repair (HR), and therefore rely on alternative DNA repair pathways for survval. We hypothesized that RAD52-mediated DNA repair mechanisms remain active and are thus protecting some PARPi-treated BRCA-deficient tumor cells from apoptosis, and that targeting RAD52 should enhance the synthetic lethal effect of PARPi. We show here that RAD52 inhibitors (RAD52i) attenuated single-strand annealing (SSA) and residual HR activity in BRCA-deficient cells. Simultaneous targeting of PARP1 and RAD52 with small molecule inhibitors or via expression of dominant-negative mutants induced an accumulation of DSBs and selective eradication of BRCA-deficient solid tumor and leukemia cells, while BRCA-proficient cells were unaffected. *Parp1-/-Rad52-/-* transgenic mice are healthy and indistinguishable from wild-type mice due to the presence of the BRCA-pathway, and *Parp1-/-Rad52-/-* mice with inducible BRCA1-deficient leukemia displayed significantly prolonged survival when compared to *Parp1-/-* and *Rad52-/-* counterparts. Finally, PARPi + RAD52i selectively targeted BRCA1-deficient solid tumors in immunodeficient mice with minimal toxicity to normal cells and tissues which are protected by the BRCA-pathway, indicating minimal side effects. In conclusion, our data indicate that combination treatment of RAD52i and PARPi will significantly improve therapeutic outcome of BRCA-deficient malignancies compared

to treatment with PARPi monotherapy, while leaving healthy cells and tissues unharmed.

This work is dedicated to my parents,

who instilled in me a love of knowledge and science

at a young age, and are two of the most positive,

hard-working, and inspirational people I know.

ACKNOWLEDGMENTS

First, I would like to thank my advisor, Dr. Tomasz Skorski. It has been a privilege to work for someone who is so dedicated and passionate about his research, and such an exceptional mentor. He was always willing to discuss experimental plans and data at any time, and after working with him for so long I will never forget the most important part of an experiment ("controls, controls, and more controls"). He also strongly encouraged his students to submit abstracts to and present at conferences, and I am incredibly grateful for those opportunities which have ultimately improved my confidence at presenting and discussing current data. While I am sad that my time in this lab is nearing its end, I will always be thankful for the opportunity to work under the guidance of such a wonderful mentor the past few years, and I leave the lab a better scientist and person because of that.

I would also like to thank the members of the Skorski lab, both past and present. First and foremost, I want to thank Elisabeth Gillespie for her extraordinary patience and skill as a mentor when I first joined the lab. I'd also like to thank Kimberly Morales, Margaret Nieborowska-Skorska, Yashodhara Dasgupta, Silvia Maifrede, Paulina Podszywalow-Bartnicka, Samantha Granger, Bac Viet Le, Konstantin Golovine, and Monika Toma for your mentorship and support, and for being so generous with your time and knowledge when it came to discussion experimental design and troubleshooting. I also want to thank the two enthusiastic and talented undergraduates whose excellent work contributed specifically to this project: Micheal Sicilano and Morgan Moore. It has been a pleasure to train and to work with such hardworking and pleasant individuals. Additionally, I'd like to say thank you to everyone in my lab listed above for your

friendship and support over the years. I'm so lucky to have had the opportunity to work in a lab where everyone who comes and goes gets along so well. I will certainly miss working with you all. Finally, over the past few years I've grown particularly close to Yasho and Silvia. I not only look up to you two as mentors and talented researchers, but I also will always cherish our friendship.

This research could not have been done without the guidance and advice from the members of my advisory committee, Tomasz Skorski, M.D., Ph.D., Xavier Graña, Ph.D., Dianne Soprano, Ph.D., Dan Liebermann, Ph.D., Richard Pomerantz, Ph.D., and Neil Johnson, Ph.D., in addition to Alex Mazin, Ph.D., my external committee member. Thank you all for the time, support, valuable advice, and encouragement you have provided over the years. I have learned a lot from our meetings over the years and I am abundantly grateful for your guidance and expertise.

I would also like to thank the friends I've made outside the lab at Temple in the Biomedical Sciences program, as well as my colleagues at the Fels Institute for Cancer Research & Molecular Biology and the Microbiology & Immunology department at Lewis Katz School of Medicine. I truly enjoyed getting to know many of you over the years and I am grateful to work with such an exceptional group of people. Additionally, I want to thank my friends from high school, college, etc. outside of the Temple community, who cannot all be named here. I appreciate having such a positive, motivational group of people in my life.

I would also like to extend my gratitude to my family. To my mother-in-law Diane and my father-in-law Jerry, thank you both for your encouragement and understanding over the years. I am so lucky to have you for in-laws. To my parents Tom

and Jane Sullivan, thank you for being so supportive over the years. When times were tough you always knew what to say to motivate me to buck up and keep working through it and I truly appreciate everything you have done the past few years. Last but not least, to my wonderful husband Ron, you have repeatedly gone above and beyond to help eliminate stress and have always been so supportive through both the ups and the downs that come with research. Thank you for always being there for me.

TABLE OF CONTENTS

Page

LIST OF ABBREVIATIONS

53BP1	p53 Binding Protein 1
6-OH-dopa	6-Hydroxy-DL-Dopa
A5MP	Adenosine 5'-Monophosphate
AICAR/ZMP	5-Aminoimidazole-4-Carboxamide Ribonucleotide 5' Phosphate
AML	Acute Myeloid Leukemia
ALL	Acute Lymphoblastic Leukemia
ALT-NHEJ	Alternative Non-Homologous End-Joining
AP Site	Apurinic/Apyrimidinic Site
B/A	BCR-ABL
BA	Basophils
BARD1	BRCA1 Associated RING Domain 1
BER	Break Excision Repair
BM	Bone Marrow
BMCs	Bone Marrow Cells
BL	Burkitt Lymphoma
BRCT	BRCA1 C-terminal domain
CI	Combination Index
C-NHEJ	Canonical Non-Homologous End-Joining
CML	Chronic Myeloid Leukemia
CML-BP	Chronic Myeloid Leukemia – Blast Phase
CML-CP	Chronic Myeloid Leukemia – Chronic Phase
DAPI	4'6'-diamidino-2-phenylindole
DNR	Daunorubicin
Dopa	6-Hydroxy-DL-Dopa
DNA-PKcs	DNA-PK Catalytic Subunit

DSB	Double Strand Break
dsDNA	Double-Stranded DNA
EBV	Epstein-Barr Virus
EO	Eosinophils
F79	Phenylalanine 79 Aptamer
FDA	Food and Drug Administration
H&E	Hematoxylin and Eosin
HB	Hemoglobin
HCT	Hematocrit
hCD45	Human CD45
HR	Homologous Recombination
HSC	Hematopoetic Stem Cell
iGFP	Internal GFP
IM	Imatinib
Indels	Small Insertions and Deletions
IR	Ionizing Radiation
i.p.	Intraperitoneal
i.v.	Intravenous
LCL	Lymphoblastoid Cell Line
LSK	Linage-Sca1+C-Kit1
LY	Lymphocytes
MCH	Mean Corpuscular Hemoglobin
MCV	Mean Red Blood Cell Volume
MDS	Myelodysplastic Syndrome
MO	Monocytes
MRN	MRE11/RAD50/NBS1
NAD+	Nicotinamide Adenine Dinucleotide

NCI	National Cancer Institute
NE	Neutrophils
NHEJ	Non-Homologous End-Joining
Ola	Olaparib
P-gp	P-Glycoprotein
PALB2	Partner and Localizer of BRCA2
PAR	Poly (ADP-Ribose)
PARP	Poly (ADP-Ribose) Polymerase
PARPi	Poly (ADP-Ribose) Polymerase 1 Inhibitor
PB	Peripheral Blood
PBMC	Peripheral Blood Mononuclear Cells
PDX	Paient-Derived Xenograft
PLT	Platelets
RAD52i	RAD52 Inhibitor
RBC	Red Blood Cell
RFS	Relapse Free Survival
RPA	Replication Protein A
SCL	Stem Cell Locus
SCLC	Small Cell Lung Cancer
scRAD52	*Saccharomyces cerevisiae* RAD52
scRNAseq	Single-Cell RNA Sequencing
SD	Standard Deviation
SE	Standard Error
SLFN11	Schlafen 11
SP	Spleen
SSA	Single-Strand Annealing
SSB	Single Strand Break

ssDNA	Single-Stranded DNA
XRCC1	X-ray repair cross-complementing protein 1
t-MDS	Therapy-Related Myelodysplastic Syndrome
Tala	Talazoparib
Tet-off	Tetracyline-off
ttA	Tetracycline-Controlled Transactivator
TRE	Tetracycline Response Element
WBCs	White Blood Cells

LIST OF TABLES

LIST OF FIGURES

CHAPTER 1

INTRODUCTION

Synthetic Lethality

Cancer cells commonly accumulate high levels of spontaneous and drug-induced DNA mutations and small insertions and deletions (indels) that ultimately cause genomic instability and inactivate apoptosis/senescence/DNA checkpoint pathways, but they survive due to protection provided by enhanced/altered DNA repair pathways[1]. While these compensatory repair pathways may promote tumorigenesis, they also provide a distinct weakness that can be therapeutically exploited through a concept known as synthetic lethality. Synthetic lethality occurs when the inactivation of one or more genes leads to cell death, while a deficiency in only one of the genes does not. This phenomenon occurs because the two genes code for proteins that are involved in pathways that serve redundant functions and can thus compensate for each other if one of the pathways is inactivated by a mutation[2]. This interaction between two genes was first described in 1922 after it was first observed in *Drosophila melanogaster* that some non-allelic genes were lethal in combinations in offspring while the parents, who were homozygous for both genes, were healthy[3]. The term "synthetic lethality" was coined in 1946 when the same observation was made in *Drosophila Pseudoobscura*[4].

Cancer cells in which one of these gene products is inactivated become dependent on the second gene for cell survival, providing a weakness that can be targeted therapeutically. This therapeutic approach is particularly advantageous as it provides a

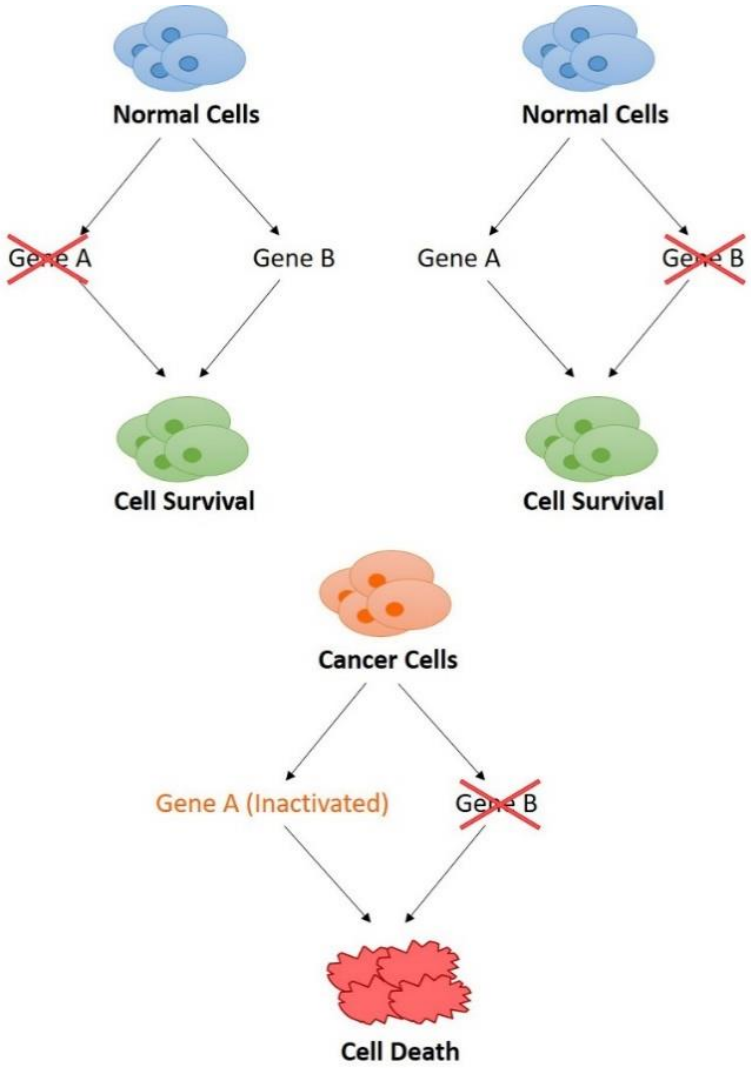

Figure 1: Concept of synthetic lethality. Synthetic lethality occurs when two redundant pathways promote cell survival in normal cells, but one of these pathways is inactivated in cancer cells. Cancer cells rely preferentially on the alternative pathway for cell survival. Therefore, targeting this alternative pathway (mediated by Gene B) will selectively result in cancer cell death while normal cells will be protected by Gene A.

way to specifically target cancer cells in a patient while having minimal toxic effects in normal, healthy cells. We are interested in using synthetic lethality as an approach to develop a combination therapy that will specifically inhibit multiple redundant DNA double strand break (DSB) repair pathways in BRCA-deficient cancer cells while leaving normal cell unharmed.

BRCA-Deficient Cancers

BRCA1 and *BRCA2* are tumor suppressor genes that were first isolated in 1994 and 1995, respectively[5,6]. Both BRCA1 and BRCA2 play crucial roles in the accurate repair of DNA DSBs and arrested replication forks via homologous recombination (HR). Individuals who carry mutations in either BRCA1 or BRCA2 have an elevated risk of 60-70% and 45-55%, respectively, of developing breast cancer and a risk of 40% and 20%, respectively, of developing ovarian cancer[7].

Germline and Spontaneous Mutations in BRCA1 and BRCA2

Germline mutations in BRCA1 or BRCA2 account for about 10% of breast cancers and 15% of ovarian cancers[8]. These mutations are inherited in an autosomal dominant fashion, meaning that only a single copy of the mutated allele is needed for disease to develop. The remaining single wild type allele eventually needs to develop mutations for cancer to occur, a phenomenon called loss of heterozygosity. Loss of heterozygosity at the wild type allele is observed in the majority of breast and ovarian cancer patients with germline mutations in either *BRCA1* or *BRCA2*[9,10]. Recent studies

have also reported that patients harboring germline mutations in BRCA1 or BRCA2 have increased risk in developing other cancers in addition to breast and ovarian cancer, such as uterine, cervical, colon, male breast, prostate, pancreatic cancers, and melanoma[11]. BRCA1/2-deficient cancers are typically highly aggressive, high grade cancers that are very difficult to eradicate.

In addition to germline mutations, BRCA1 and BRCA2 mutations may also arise spontaneously, resulting in sporadic cancer. Approximately 90% of breast cancers and 85% of ovarian cancer cases are sporadic and can be caused by a multitude of factors[8]. In these cases, the patient is not born with a BRCA1/2 mutation, but the mutation instead eventually arises from the accumulation of mutations that naturally occur throughout the person's lifetime. Other factors such as the individual's environment can further promote the accumulation of cancer-predisposing mutations over time. In the case of spontaneous BRCA mutations, while the cause of the mutation may not be known the patient's tumor can still be screened for mutations in these genes.

Epigenetic Downregulation of BRCA1 and BRCA2

Sporadic breast and ovarian cancers have additionally been reported to be caused by aberrant methylation of the BRCA1 promoter. A meta-analysis of 40 individual studies reporting aberrant methylation of the BRCA1 promoter in patients with sporadic breast cancer found a statistically significant increase in BRCA1 promoter methylation in breast cancer patients compared to healthy controls[12]. Additionally, a study of a cohort of 256 primary high-grade serious ovarian cancer patients found hypermethylation of the

BRCA1 promoter in 14.8% of the patients[13]. The role of BRCA2 promoter hypermethylation in the development of breast cancer was also explored in another study, but there was no significant difference between the mean BRCA2 promoter methylation rates of the breast cancer and control cohorts[14]. More studies are needed to further determine the impact of epigenetic silencing of BRCA2 in cases of sporadic breast and ovarian cancers.

Oncogene-Induced BRCA-Deficient Cancers

BRCA1/2-deficiency can also be induced in some cancers by the expression of certain oncogenes. For example, the oncogene BCR-ABL, which causes chronic myeloid leukemia (CML) and is also found in some patients with acute lymphoblastic leukemia (ALL) or acute myeloid leukemia (AML), downregulates BRCA1 protein expression via inhibition of BRCA1 mRNA translation[15]. Our lab has previously reported that this downregulation is caused by a BCR-ABL-mediated endoplasmic reticulum stress response that ultimately results in the cytosolic localization of the mRNA-binding protein TIAR, which binds to the 3'UTR region of BRCA1 mRNA and inhibits its translation[16]. The oncogene AML1-ETO, which is expressed in 22% of all AML patients, is associated with downregulated expression of BRCA2 mRNA, although the exact mechanism is not yet known[17,18]. Additionally, cancers that are caused by overexpressed c-myc have upregulated miR-1245 which subsequently inhibits the translation of BRCA2 mRNA by directly binding to the 3'UTR of the BRCA2 transcript[19]. Recently, Maifrede et al. demonstrated that primary human Burkitt lymphoma/leukemia cells carrying the

IGH/MYC translocation were deficient in BRCA2 protein expression, which was associated with an upregulation of miR-1245 as expected[20].

BRCA Pathway-Deficient Cancers

A tumor exhibits a "BRCA-deficient" phenotype if a mutation occurs in any gene in the BRCA-mediated HR pathway (BRCA1-BARD1-CtIP-PALB2-BRCA2-RAD51 paralogs–RAD54) as the genes in this pathway are epistatic, meaning that the pathway can only proceed if all of the proteins are expressed and functioning normally[21-27]. While individual mutations in these genes are rare, germline or somatic mutations collectively in genes in the BRCA pathway genes other than BRCA1/2 occur in 7-8% of ovarian cancer cases, and the presence of these mutations has been reported to sensitize the tumor cells to inhibitors of the DNA repair protein poly (ADP-ribose) polymerase 1 (PARP1)[28]. Female germline mutation carriers in PALB2 have an estimated lifetime risk of 33% in developing breast cancer for those with no family history of breast cancer, and 58% for those with a family history[29]. Collectively from studies conducted in populations from multiple countries, loss-of-function PALB2 mutations are found in 0.6-3.9% of families with a history of breast cancer[29]. PALB2 has also been linked to male breast, pancreatic, and ovarian cancers[30]. Additionally, germline mutations in the RAD51 paralogs RAD51B, RAD51C, RAD51D, and XRCC2 have been linked with a moderate risk of breast and/or ovarian cancer[31,32]. Moreover, it has been reported that 10-12% of lethal prostate cancers harbor mutations in genes critical to BRCA-mediated HR including BRCA1/2, and PALB2[33,34]. Finally, a retrospective analysis of CtIP expression levels in

384 paraffin-embedded breast cancer biopsies found a correlation between low/no CtIP expression and high-grade breast cancer[35]; However, another group was unable to detect any germline mutations in *CtIP* following a screen of 210 probands of breast cancer families indicating that the de-regulated CtIP expression associated with high-grade breast cancer is caused by another mechanism that remains to be elucidated[36].

DNA Repair Pathways

DSBs are one of the most dangerous types of DNA lesion to a cell. DSBs can be generated by exposure to exogenous sources such as ionizing radiation (IR), reactive oxygen species, and genotoxic chemical compounds, or they can result from natural cellular processes such as V(D)J recombination in the immune system, as intermediates during mitotic and meiotic recombination, or as the result of stalled replication forks[37]. If left unrepaired, DSBs can lead to chromosomal loss and/or cell death[38]. Faulty repair of these breaks may give rise to additional mutations, chromosomal translocations, and complex chromosomal rearrangements, and eventually lead to the development of cancer. Multiple DSB repair pathways have evolved to prevent these detrimental effects from occurring, such as HR and non-homologous end-joining (NHEJ).

HR

HR is an evolutionarily conserved process that is the only DSB repair mechanism that relies on DNA from a sister chromatid in mitotic cells or homologous chromosome during meiosis as a template for DNA synthesis, allowing for extremely accurate repair

of the break[39]. Thus, in regards to the cell cycle HR is only active in proliferating cells when sister chromatids are available to use as templates. Accordingly, the HR pathway is crucial for the repair of DSBs that occur at the replication fork[40]. DSB repair by HR is primary mediated by the BRCA pathway (Figure 2), which consists of a group of proteins that work together to ultimately recruit and load RAD51 onto the resected single-stranded DNA (ssDNA) ends, described in more detail below.

HR repair is initiated when the DSB is recognized by the MRE11/RAD50/NBS1 (MRN) complex, which is a major sensor of DNA damage[41]. Once a DSB is detected, the MRN complex functions by tethering the DNA ends together and by recruiting ATM kinase to the DSB[41,42]. ATM is essential for the phosphorylation of histone H2AX to form γH2AX foci, a rapid and early marker of DSBs that can be seen as early as 30 minutes after ionizing radiation[43]. The formation of γH2AX foci promotes the recruitment of the BRCA1-BARD1 (BRCA1-Associated RING Domain 1) heterodimer to the DSB by interacting with the two consecutive BRCT domains (BRCA1 C-terminal domain) on BRCA1[44,45]. BARD1 is the permanent binding partner of BRCA1 and is required for BRCA1 to function[46].

BRCA1-BARD1 heterodimer has multiple functions essential to the HR pathway. The first is mediating efficient and prolonged end resection of the double stranded DNA ends to generate 3'ssDNA ends[46]. As cells enter the S phase of the cell cycle, CtIP is phosphorylated on serine residue 327, which promotes binding by BRCA1 to form the BRCA1-C complex[46]. BRCA1 protects and stabilizes CtIP, allowing CtIP to generate longer 3'ssDNA ends than if CtIP were operating alone. The MRN complex has

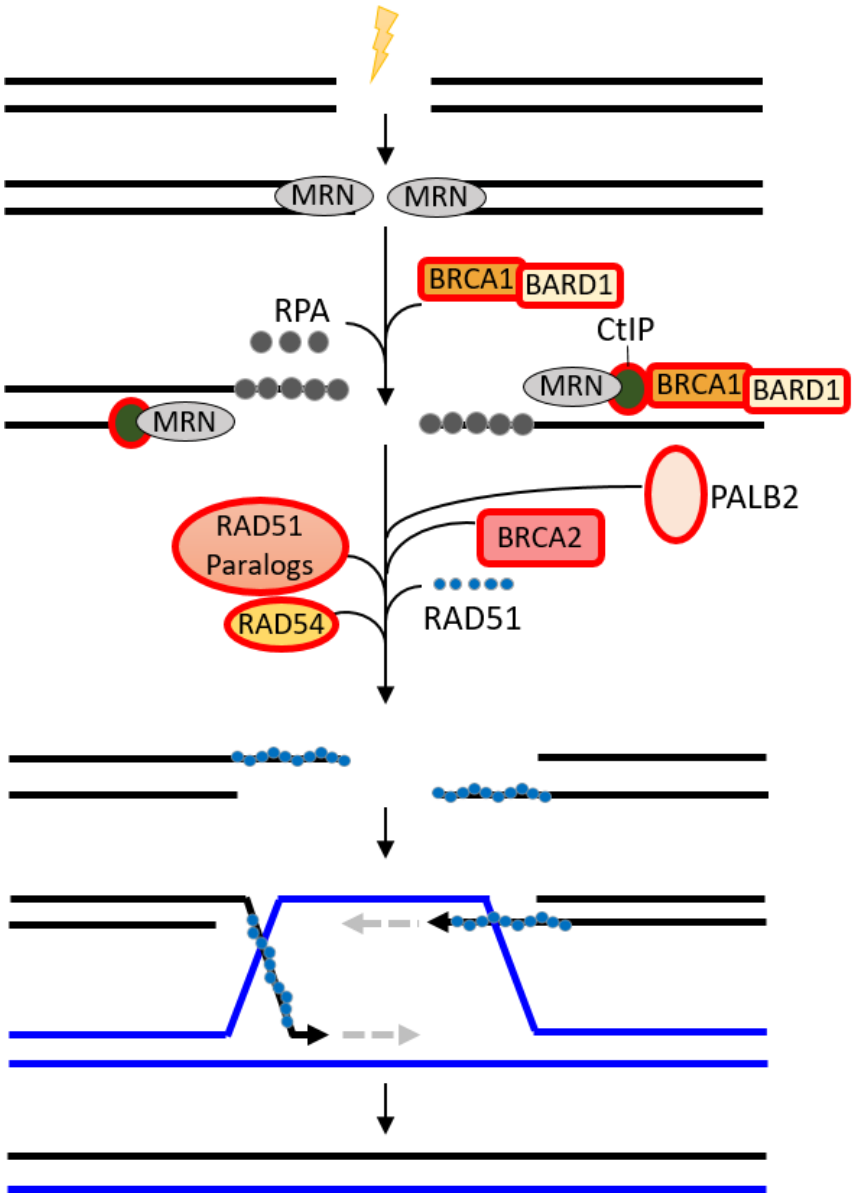

Figure 2. BRCA-mediated homologous recombination. The proteins outlined in red are essential for the BRCA pathway to facilitate the loading of RAD51 onto the free ssDNA ends.

exonuclease and endonuclease capabilities via Mre11, so MRN works in concordance with BRCA1-CtIP to facilitate end-resection[47]. Replication Protein A (RPA) then binds to and stabilizes the 3'ssDNA ends until displaced when RAD51 recombinase is loaded onto the DNA. In addition to its role in promoting stable CtIP-mediated end-resection, the second main function of BRCA1 is to recruit the repair machinery needed to ultimately recruit and load RAD51 by serving as a scaffold[25]. BRCA1 promotes the recruitment of BRCA2 to DSBs by binding to the scaffold protein PALB2 (partner and localizer of BRCA2) which in turn interacts with BRCA2, and RAD51. PALB2 is essential for the recruitment of BRCA2 to the repair complex. BRCA2 is crucial for loading RAD51 onto the RPA-coated ssDNA ends[48].

After RAD51 is loaded, BRCA2 works in tandem with the RAD51 paralogs (RAD51B, RAD51C, RAD51D, XRCC2, and XRCC3) to stabilize the RAD51 nucleoprotein filament during the search for a homologous template and strand invasion. The specific functions of the individual RAD51 paralogs at different steps in HR are still unclear. It has been reported that they form two main complexes *in vivo* that are both absolutely essential for BRCA-mediated HR: Rad51B-Rad51C-Rad51D-XRCC2 and Rad51C-XRCC3[21,49]. It appears that the Rad51B-Rad51C-Rad51D-XRCC2 complex specifically functions downstream of BRCA2 but upstream of RAD51 recruitment, and is involved in stabilizing the RAD51 nucleoprotein filament[21]. RAD51C-XRCC3 is required for HR to continue after RAD51 is recruited by binding to, remodeling, and stabilizing RAD51-ssDNA pre-synaptic nucleoprotein filament so that it is in a more "open" and stable conformation to promote efficient RAD51 strand exchange

activity[50,51].

Finally, after the RAD51 nucleoprotein filament is formed, RAD54 functions by stabilizing the interaction between ssDNA and RAD51 and by transiently unwinding the double stranded DNA (dsDNA) to promote RAD51-mediated strand invasion in search of a homologous template[52,53]. Additionally, it has been recently demonstrated that both BRCA1 and BARD1 directly interact with RAD51 and enhance its recombinase activity[25]. The stabilized RAD51 nucleoprotein filament catalyzes strand invasion of unbroken, homologous DNA to complete the repair process[54]. As RAD51 recruitment and loading onto ssDNA end is required for HR repair, RAD51 nuclear foci formation at sites of DNA damage provides a useful biomarker for HR-mediated repair[55].

It is well documented that each protein in the BRCA pathway (Figure 2; proteins essential to the BRCA pathway outlined in red) is required for the loading of RAD51, and BRCA-mediated HR cannot proceed if any proteins in the pathway are downregulated or inactivated. Cell lines knocked down in each of the five RAD51 paralogs have been confirmed to behave similarly to cells deficient in BRCA1/2[56,57]. SiRNA-mediated partial knockdown of PALB2 in MCF7 cells resulted in approximately 50% inhibition in the number of cells forming RAD51 foci in response to 10 Gy of ionizing radiation[23]. Moreover, expression of an oncogenic splice variant of BARD1 not only impairs HR activity, but *BARD1*-null mice are also embryonic lethal[58,59]. Furthermore, HeLa, HCC1937, and U20S cells expressing mutant CtIP were unable to form RAD51 foci[60].

RAD52-Mediated HR

HR can also proceed through a backup pathway mediated by RAD52, which operates independently of the BRCA-pathway. The notion that an additional BRCA-independent HR pathway may be present in eukaryotes was first made following the observation that RAD52 in budding yeast *Saccharomyces cerevisiae* (scRAD52) is imperative for HR, and the absence of scRAD52 is lethal for the organism; however, murine embryonic stem cells with inactivated RAD52 showed reduced levels of HR activity but they were not hypersensitive to DNA damaging agents[61]. ScRAD52 mediates HR by physically associating with RPA, RAD51, as well as ssDNA and dsDNA and thus is thought to facilitate the recruitment and loading of RAD51 onto DNA[62].

BRCA2, which is not present in yeast, appears to have evolved in higher organisms to play a major role in this process, mostly likely because more complex regulation is needed in higher organisms to respond to the increased level of mutations experienced by the genome[62]. Thus the RAD52-mediated HR pathway remains functional as a backup pathway to BRCA-mediated HR. Despite the clear evidence of the importance of scRAD52 to RAD51-mediated recombination, reconstituted human RAD52 (hRAD52) did not show activity as a recombination mediator in biochemical assays, indicating that there may be additional proteins in the pathway and/or posttranslational modifications needed that remain to be identified[63]; however, RAD52 is currently the only known essential gene to mediate the redundant HR pathway in cancer cells deficient in BRCA1, BRCA2, or PALB2.

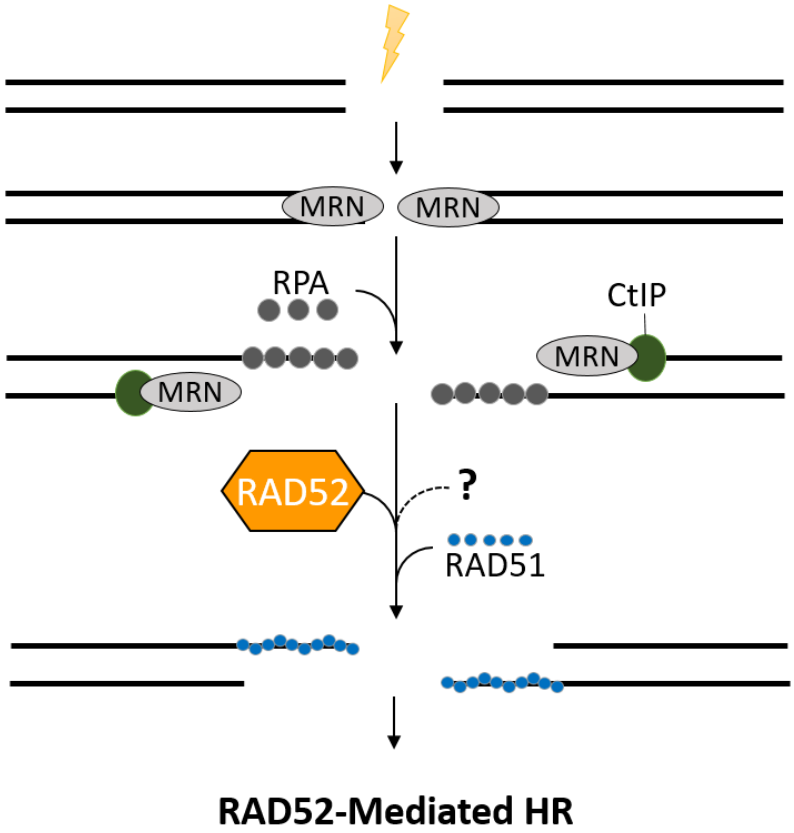

Figure 3. RAD52-mediated HR pathway. RAD52 is the major player in a redundant HR pathway that loads RAD51 onto ssDNA, ends independent of the BRCA pathway. It is a distinct pathway from SSA, which is RAD51-independent.

Single-Strand Annealing (SSA)

SSA is another DSB repair pathway that requires sequence homology, but it is otherwise distinct from HR. SSA is a RAD52-dependent pathway that can proceed following end resection if there are enough repetitive sequences on both sides of the DSB. Similar to HR, the MRN complex detects the DSB, resects the DNA ends to generate 3'ssDNA ends, and recruits RPA to stabilize the ssDNA[54]. In SSA, RAD52 is recruited to the DSB site where it promotes the annealing of the complementary sections of ssDNA. The ssDNA flaps generated from this step are subsequently trimmed off by the ERCC1/XPF endonuclease complex, resulting in a loss of DNA. Unlike HR, SSA is a RAD51-independent process despite RAD52 having a RAD1-binding domain[64]. SSA is therefore a mutagenic DSB repair process in comparison to HR, although it is preferable when the DSB is not able to be repaired by either HR or NHEJ[65].

NHEJ

There are two NHEJ pathways: canonical-NHEJ (C-NHEJ) and alternative NHEJ (ALT-NHEJ) (Figure 4). C-NEHJ is the only DSB repair pathway active during all phases of the cell cycle, and it is mediated by a set of proteins that are also important for V(D)J recombination during antibody maturation, including Ku70/80 heterodimer, the catalytic subunit of DNA-PK (DNA-PKcs), Artemis, and the XRCC4/Ligase IV/XLF complex (Figure 4A)[66]. The process is initiated when Ku70/80 heterodimer binds to DSB ends and immediately recruits and binds to DNA-PKcs to form the DNA-PK holoenzyme[67,68]. The DNA-PK holoenzyme works in conjunction with the nuclease

Artemis and additional enzymes to process the DNA ends and catalyze their synapsis, which are subsequently ligated by the DNA ligase IV/XRCC4 complex[68-70]. Since the broken ends undergo processing and subsequent ligation, C-NHEJ frequently results in small sequence changes resulting in small insertions of at least 1 nucleotide, and between 1-10 nucleotide deletions, or the generation of point mutations at the junction that makes C-NHEJ repair more error prone than HR[66]. Additionally, C-NHEJ does not have any built-in safeguards to ensure the original DSB ends are rejoined, meaning that C-NHEJ is more chromosomal translocations[67].

ALT-NHEJ (Figure 4B) is thought to serve in part as a backup pathway following the failure of C-NHEJ[69]. Like C-NHEJ, ALT-NHEJ is error prone because it has no way to restore the original DNA sequence in the immediate area surrounding the DSB, but ALT-NHEJ is more likely to result in sequence alterations than C-NHEJ and has a much higher probability of translocation formation[71]. The presence of functional PARP1 is required for ALT-NHEJ to occur, and it has been reported that PARP1 serves a similar function in ALT-NHEJ to the role of DNA-PKcs in C-NHEJ since DNA-PKcs is not involved in ALT-NHEJ. In ALT-NHEJ repair, PARP1 works in conjunction with MRE11 of the MRE11-RAD50-NBS1 (MRN) complex, DNA polymerase Θ, and WRN helicase to process the DNA ends, which are subsequently ligated by Ligase I and/or Ligase III[69,72].

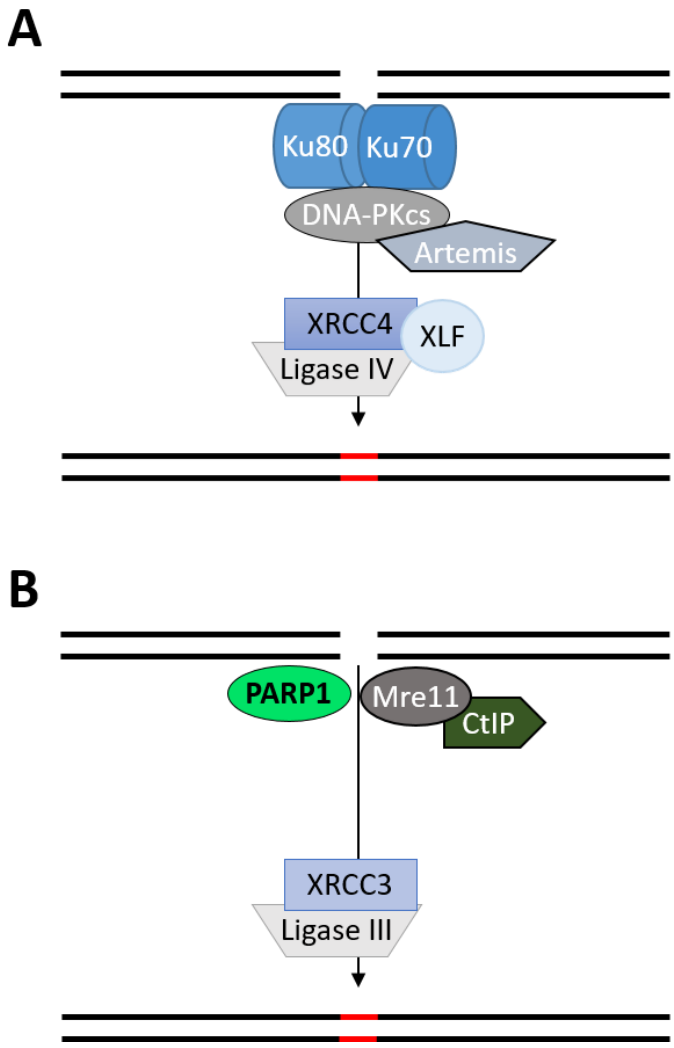

Figure 4. NHEJ-mediated repair of DSBs. NHEJ promotes the repair of DSBs by directly ligating the broken ends together following minimal end-processing. (**A**) Canonical NHEJ (C-NHEJ). (**B**) Alternative NHEJ (ALT-NHEJ).

Regulation of Choice Between DSB Repair Pathways

The regulation of choice between DSB repair pathways is largely cell cycle-dependent. ALT-NHEJ activity is suppressed by both Ku70/80 and DNA-PK, and it is significantly elevated in C-NHEJ-deficient cells, which is consistent with reports that Ku70/80 and PARP1 directly compete for DSB[37,73,74]. ALT-NHEJ also operates at a slower rate than C-NHEJ, which supports its role as a backup pathway to both C-NHEJ and HR[75]. Furthermore, PARP1 activity is hyperactivated in the S-phase of HR-deficient cells, highlighting the importance of ALT-NHEJ in protecting HR-deficient proliferating cells from accumulating a lethal number of DSBs[76].

Despite the relatively error prone nature of both C-NHEJ and ALT-NHEJ in comparison to HR, both repair pathways are essential processes when it comes to maintaining genomic stability in cells, as they are the only DSB repair mechanisms active in both proliferating and quiescent cells. C-NHEJ operates with faster kinetics compared to both HR and ALT-NHEJ, solidifying its role as a DSB repair pathway that is indispensable in the protection against genomic instability and the prevention of carcinogenesis[77].

PARP Family of Proteins

There are 17 members of the PARP family of proteins in humans, but PARP1 is the most abundant and best characterized. PARPs are nuclear enzymes that, once activated, catalyze the covalent attachment of long polymers of ADP-ribose called poly(ADP-ribose) (PAR) on itself and other acceptor proteins, a process called

PARylation[78]. PARP proteins are only considered to be "true PARPs" if they are capable of PARylation. Thus, the majority of proteins in the PARP family are not considered true PARPs as they can only either transfer a single ADP-ribose moiety onto acceptor proteins (mono-ADP-ribosylation) or are catalytically inactive[79]. Based on this standard, the only "true PARPs" in the PARP family of proteins are PARP1, PARP2, PARP3 and tankyrase1; however, PARP1, PARP2, PARP3, and Tankyrases 1 and 2 are the main PARPs in the DNA damage response[80-82].

Despite the fact that multiple PARP superfamily members are involved in the DNA damage response, PARP1 is estimated to be responsible for approximately 90% of PARylation in mammalian cells with the remaining 10% mediated mainly by PARP2 and to a lesser degree by PARP3[83,84]. PARP1 and PARP2 have highly homologous carboxy-terminal PARP domains and display genuine polymerase activity, but they have distinct DNA binding domains indicating that they may target different substrates[85,86]. While PARP3 does not contain a defined DNA binding domain, it has been reported that PARP3 is capable of being activated by DNA; however, its precise role in DNA repair is still unknown[87]. While PARP3 has been reported to be capable of PARylation, the majority of its known activity regarding DNA damage at this time involves mono-ADP-ribosylation[88,89]; However, it has been demonstrated that PARylation catalyzed by PARP3 stimulates the activity of PARP1 in response to DNA damage[79]. One hypothesis is that PARP3 activity may promote ALT-NHEJ repair of DSBs, although there is also evidence that PARP3 may promote C-NHEJ[87].

While PARP3 does play some small role in DNA repair that remains to be

elucidated, PARP1 and PARP2 play a much more significant role, with PARP1 being the primary PARP involved in DNA repair. *Parp1-/-Parp2-/-* mice are embryonic lethal, highlighting the importance of PARylation during embryonic development[90]. PARP1 functions by scanning DNA for damage and upon detecting a break it binds with a high affinity, resulting in the activation of PARP1. Once activated, PARP1 rapidly catalyzes the covalent attachment of long PAR derives the ADP-ribose monomers from nicotinamide adenine dinucleotide (NAD+) to itself (auto-PARylation) and onto nearby proteins and DNA to recruit such as X-ray repair cross-complementing protein 1 (XRCC1)[91]. These polymers signal to DNA repair proteins such as XRCC1 to rapidly relocate to the site of the damage[92].

Roles of PARP1 and PARP2 in DNA Repair

As described in more detail earlier, PARP1 mediates the backup, error-prone DSB pathway ALT-NHEJ. Interestingly, in addition to its role in ALT-NHEJ, PARP1 binds to and is activated by stalled replication forks in dividing cells[93]. PARP1 activity has been found to be required for to protect stalled replication forks from MRE11-mediated degradation, as PARP1 inhibition is associated with hyperactivation of MRE11 and a subsequent significantly increased degradation at stalled forks[94]. Additionally, PARP1 functions in promoting the reactivation of stalled replication forks via the recruitment of MRE11 for end resection[95].

PARP1 in Single Strand Break Repair

PARP1 also functions in initiating single strand break repair by recruiting proteins involved in the base excision repair (BER) pathway. BER functions in repairing bases damaged through mechanisms such as oxidation, alkylation, and deamination, all of which can commonly be formed by endogenous cellular metabolism[92]. The overall process involves the recognition and excision of the damaged bases by a variety of glycosylases depending on the type of damage, generating an apurinic/apyrimidinic (AP) site. The AP site is cleaved by an AP endonuclease, resulting in the formation of a SSB intermediate. PARP1 scans DNA and is activated when it binds to a SSB, causing rapid autoPARylation and swift recruitment of SSB repair proteins, such as the XRCC1 complex, DNA polymerase β, DNA Ligase III. The nucleotide gap is then either rapidly sealed and ligated via short patch repair to repair a single nucleotide, or long patch repair to replace two or more nucleotides[96].

PARP2 is also thought to function in the repair of SSBs, although its exact role remains to be elucidated. PARP2-/- mice display significantly increased sensitivity to alkylating agents and ionizing radiation, and PARP2 has been shown to interact with SSB repair proteins such as XRCC1, DNA polymerase β, and ligase III. PARP2 was shown to have a delayed recruitment in response to microirradiated damage sites compared to the immediate recruitment of PARP1, indicating that PARP2 most likely functions later in the SSB repair process[97].

Additional Roles of PARP1 in Cells

Notably, PARP1 plays a key role in chromatin modification as core histones, histone H1, and polynucleosomes are all substrates for PARylation, allowing for PARP to promote chromatin relaxation or condensation depending on type of DNA damage[79,98,99]. This highlights the importance of PARylation on the epigenetic aspect of DNA repair. In addition to the role that PARP1 plays in DNA repair, PARP1 also functions in transcriptional regulation, mitotic spindle formation, and in pathways that mediate apoptosis[100]. Moreover, PARP1 plays a role in regulating cell cycle checkpoints and maintaining the expression genes involved in the stress response[101,102].

PARPi-Mediated Synthetic Lethality in BRCA-Deficient Cancers

The classic and most well-known example of inducing synthetic lethality in BRCA-deficient cancer cells involves the use of PARP inhibitors (PARPi) to target preferentially PARP1, in addition to PARP2 and PARP3. Within the past decade, PARPis have emerged as a promising new class of anti-cancer drugs that specifically targets cancers containing mutations in homologous recombination repair. The success of PARPi in BRCA1 and BRCA2-deficient breast tumors in preclinical studies has established a proof-of-concept for personalized cancer therapy using synthetic lethality[103].

In cells with impaired BRCA-mediated HR, inhibition of PARP1 compromises the ability to repair SSBs, resulting in an accumulation of DSBs due to collapsed replication forks at SSBs during the S phase of the cell cycle. HR is essential for the repair of DSBs that occur at the replication fork, making HR-deficient cells markedly

susceptible to PARPi. Moreover, PARPi suppresses the repair of the accumulated DSBs via ALT-NHEJ since this pathway is mediated by PARP1. Although the backup RAD52-mediated HR pathway is still capable of repairing DSBs in BRCA-deficient cells treated with PARPi, the overwhelming increase in number of DSBs is toxic to the majority of BRCA-deficient cancer cells[104].

Until recently, it was believed that the antitumor activity of PARPi was attributed solely to their ability of inhibiting the catalytic activity of PARP1 and to a lesser degree PARP2 and PARP3, resulting in an accumulation of SSBs that would become DSBs in actively dividing cells. However, it was demonstrated recently that catalytic inactivation is not the only mechanism that makes PARP inhibitors cytotoxic; Most PARPi also physically trap PARP1, and possibly PARP2, onto the damaged DNA, resulting in fixed PARP-DNA complexes that completely block DNA replication and transcription. The effect is extremely cytotoxic and exceedingly more potent than catalytic inactivation of PARP. The ability to trap PARP to DNA varies among current PARP inhibitors.

Although this study is focused on targeting cancers deficient in BRCA pathway-mediated HR, PARPi can also exert a synthetic lethal effect against cancers deficient in C-NHEJ proteins. It was recently reported by Czyż et al. that the PARPi olaparib induced synthetic lethality in ligase IV-deficient melanomas without exerting any toxic effects on normal melanocytes[105]. Ligase IV is required for C-NHEJ-mediated repair of DSBs, which is the main DSB repair pathway in phases of the cell cycle except for the S phase, when HR becomes the prominent predominant DSB repair mechanism. They confirmed using γ-H2AX immunofluorescence that this synthetic lethal effect observed in ligase IV-

deficient was associated with a significant accumulation of lethal DSBs[105].

Additionally, our lab used PARPi to induce synthetic lethality in quiescent leukemia stem cells deficient in DNA-PKcs[106]. As described earlier, non-dividing cells rely exclusively on NHEJ pathways to repair lethal DSBs since HR is only active during S and G2 phases of the cell cycle. Since DNA-PKcs is essential for C-NHEJ-mediated repair, DNA-PKcs-deficient quiescent leukemia stem cells must solely rely on PARP1-mediated ALT-NHEJ for DSB repair. We demonstrated this phenomenon by using a precision medicine approach that employed Gene Expression and Mutation Analysis to select leukemia patients with DNA-PK based on qRT-PCR and microarrays, who we predicted would be sensitive to PARPi. Quiescent DNA-PK-deficient cells were sensitive to PARPi *in vitro* and *in vivo,* while the DNA-PK-proficient counterparts were unaffected[106].

PARPis Currently Under Clinical Development

Currently, the majority of reported PARPis are analogs of nicotinamide and function by competing with NAD+ for access to the catalytic site of PARP1, resulting in inhibition of PARylation[107]. *In vitro* assays measuring PARP1 catalytic activity determined that most PARPi are extremely efficacious with highly similar IC50 values, with the exception of talazoparib, which is estimated to be between 20-200-fold more potent than other currently known PARPi inhibitors[108]. This increased potency of talazoparib is attributed to its remarkable trapping ability, as it is the most effective and potent PARP trapper of all currently known PARPi[101]. Talazoparib is currently being

tested in clinical trials in breast cancer patients that harbor germline BRCA mutations in addition to other cancer types associated with defective DNA damage response, and was found to significantly extend progression-free survival in a phase 3 trial of metastatic breast cancer patients[109]. Velaparib is another orally available PARP inhibitor that is currently being tested in clinical trials. It is the most selective PARP inhibitor to date, with strong selectivity towards PARPs1-3, though it also is the least effective PARPi at trapping PARPs[110,111].

FDA Approved PARPis

Olaparib (Lynparza®) is an oral PARP inhibitor that was the first PARPi to enter clinical trials, and it is the most investigated PARPi in BRCA-deficient cancers thus far. Olaparib made history in December 2014 by becoming the first PARPi to be approved by the U.S. Food and Drug Administration (FDA)[112]. The FDA specifically approved it for the treatment of pre-treated, relapsed ovarian cancer that harbors BRCA mutations[112]. Additionally, the FDA approved olaparib in August 2017 for the maintenance treatment for patients with recurrent fallopian tube, peritoneal, or epithelial ovarian cancer, who are in a complete or partial response to platinum-based chemotherapy[113]. In January 2018 olaparib made history once again when the FDA approved olaparib to treat germline BRCA-mutated metastatic breast cancer patients who have undergone chemotherapy, making olaparib the first FDA-approved drug to specifically treat patients with inherited breast cancer[114].

In 2016, the FDA granted accelerated approval of the intravenous PARP inhibitor

rucaparib (Rubraca®) to treat women with advanced ovarian cancer harboring BRCA mutations who were also previously treated with two or more chemotherapies[115]. Finally, in March 2017 the FDA approved the oral PARP inhibitor niraparib (Zejula®) as a treatment for patients with recurrent ovarian, fallopian tube, or primary peritoneal cancer, who are in partial or complete response to platinum-based chemotherapy[116]

Mechanisms of Resistance to PARPi

Despite very promising preclinical data using PARPi in BRCA-deficient cancers, these therapeutics have had relatively limited success in clinical trials, with patients ultimately relapsing despite initially responding to treatment[117-124]. Additionally, some patients eventually develop resistance to PARPi over time. There are multiple documented mechanisms by which PARPi resistance can occur. For example, one group used BRCA1-methylated breast cancer patient-derived xenograft (PDX) models to demonstrate resistance to PARPi through epigenetic re-expression of BRCA1 due to loss of methylation in the BRCA1 promoter[125]. Another mechanism involves increased drug export from the cells mediated by P-glycoprotein (P-gp). Rottenberg et al. observed that long-term treatment of olaparib in a BRCA1-deficient breast cancer mouse resulted in upregulated expression of the *Abcb1 a/b* genes encoding P-gp, which actively pumps olaparib and other drugs out of the cells[126]. Treatment with the P-glycoprotein inhibitor, tariquidar, reversed the resistance to olaparib[126]. This resistance mechanism only develops if the drug is a substrate of P-gp, such as olaparib. Fortunately, additional potent PARPi, such as velaparib are emerging that are poor substrates for P-gp[127].

PARPi resistance can also be caused through aberrant expression of other proteins that regulate the DNA damage response. For example, multiple reports have shown that the loss of p53 binding protein 1 (53BP1) caused by truncating mutations *TP53BP1* in BRCA-deficient breast cancer partially restores the capacity to perform HR by allowing CtIP with unobstructed access to DSB breaks, resulting in hyperactivation of DNA end resection activity[128,129]. Loss of 53BP1 expression also significantly attenuates the ATM-dependent checkpoint response and G2 arrest in response to DNA damage accumulation[130]. Additionally, loss of 53BP1 expression has been reported to be associated with the presence of BRCA1/2 mutations, with triple-negative phenotype, and with poorer survival in breast cancer patients[130].

Currently, the most well documented resistance mechanism is the development of a secondary in-frame deletion mutation that restores function lost by the original BRCA1/2 mutation. The secondary in-frame deletion mutation either corrects the original mutation or bypasses it in some way, restoring the capacity of the cell to repair DSBs via HR[131]. Multiple groups have demonstrated the restoration of the BRCA2 open reading frame as a prominent resistance mechanism to PARPi in BRCA2-deficient breast, pancreatic, and ovarian cancer cell lines[132-134]. An additional study identified specific secondary somatic mutations in both BRCA1 and BRCA2 that restored their function in BRCA1- and BRCA2- deficient ovarian cancer cell lines[135].

PARPi Resistance in Clinical Trials

Until recently, the majority of data regarding the various mechanisms behind the

development of resistance to PARPi was obtained from *in vitro* and *in vivo* studies, as opposed to clinical trials. The first observation of clinical resistance to PARPi by comparing tumor biopsies taken from the same patient at diagnosis and after developing resistance to PARPi was reported in 2013, where tumor-specific BRCA2 secondary mutations were identified using massively parallel sequencing in two breast cancer patients who had developed resistance to olaparib while still receiving treatments. In both patients, the secondary mutations restored the BRCA2 open reading frame[136].

In September 2017, Goodall et al. published a study where they analyzed samples obtained from patients participating in the Phase II clinical trial (TOPARP-A) of olaparib in metastatic prostate cancer patients that resulted in the FDA awarding olaparib with 'Breakthrough Designation' by the FDA in 2016 for advanced prostate cancer with defects in BRCA2/ATM[34]. They compared tumor biopsy DNA and circulating cell-free DNA isolated from each patient in the study, and they found that BRCA2 reversion mutations were responsible for restoring the BRCA2 open reading frame as a major cause of resistance to talazoparib and olaparib in tumors with germline BRCA2 mutations as well as in tumors with somatic loss of BRCA2 and PALB2[34]. Quigley et al. analyzed solid and liquid tumor biopsies from the same clinical trial and further identified multiple separate BRCA2 reversion mutations in samples from individual patients, highlighting the usefulness of circulating cell-free DNA in identifying reversion mutation heterogeneity not discernable in solid tumor samples[137]. In November 2017, Weigelt et al. also reported on the utility of circulating cell-free DNA on identifying reversion mutations in BRCA1 and BRCA2 in breast and ovarian cancer patients resistant to

PARPi and/or platinum therapy[138].

Additionally, in June 2017 a study was published analyzing samples collected from patients participating in a Phase II clinical trial (ARIEL2 Part 1) of epithelial ovarian carcinomas harboring mutations in BRCA1/2 genes[139]. After sequencing genes involved in the BRCA-mediated HR pathway in twelve patients, they found that six of the twelve patients had truncation mutations in BRCA1, or RAD51 paralogs RAD51C or RAD51D. In post-progression analyses, five of the six biopsies contained at least one secondary mutation that restored the open reading frame. In particular, four separate mutations were observed that restored function in RAD51C[28].

It is clear that while PARPi are initially effective at targeting BRCA-deficient cancers in clinical trials, they do not target all of the cancer cells and eventually long-term exposure selects for a population of cancer cells that are resistant to treatment. This highlights the need to combine PARPi with drugs that further impairs the DNA damage response in this subgroup of cells to more efficiently target all of the cancer cells in the population.

RAD52-Mediated Synthetic Lethality

Synthetic lethality can also be induced in BRCA-deficient cells by targeting RAD52. In this case, inhibiting RAD52 completely prevents HR-mediated repair of DSBs in BRCA-deficient cancer cells, in addition to repair via SSA, which is entirely dependent on RAD52 (Figure 5).

RAD52-mediated synthetic lethality was first demonstrated in 2011 when Feng et

al. reported that RAD52 stimulated the formation of RAD51 nuclear foci in BRCA2-deficient cell lines, and that the depletion of RAD52 via shRNA in BRCA2-deficient cells[140]. In 2013 the same lab confirmed that inactivation of RAD52 also induces

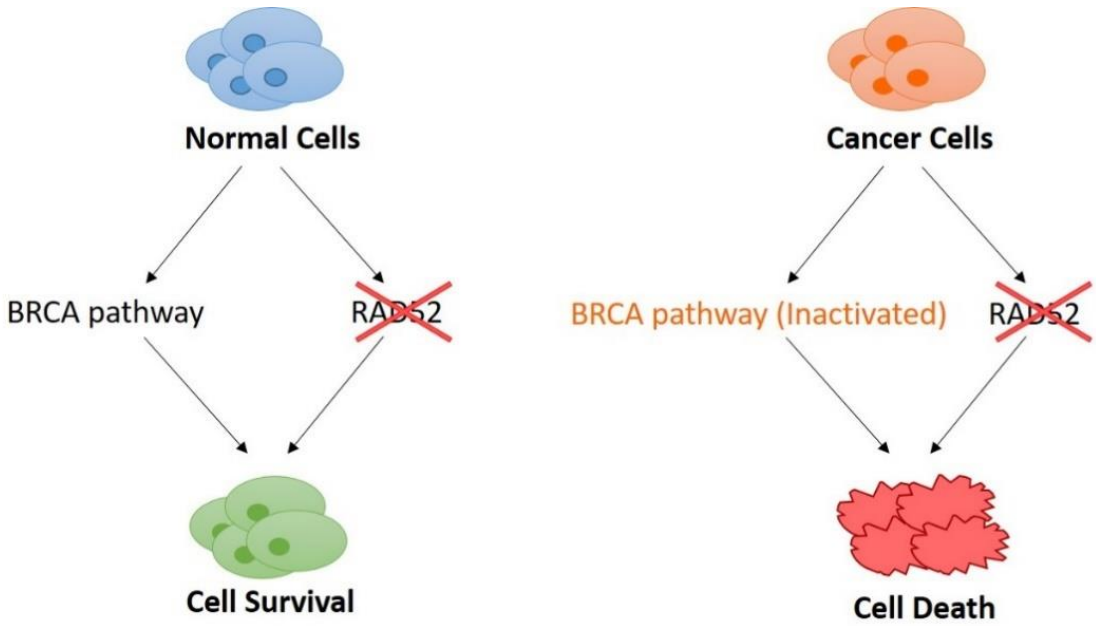

Figure 5. RAD52-mediated synthetic lethality in BRCA-deficient cancers. BRCA-deficient cells are unable to accurately repair DSBs with BRCA-mediated HR, but the backup RAD52-mediated error-free HR and RAD52-dependent SSA pathways are still active. Inactivation of RAD52 completely prevents BRCA-deficient cells from repairing DSBs via HR and SSA, leading to a lethal accumulation of DSBs. Normal cells have functional BRCA-mediated HR and are thus unaffected by inactivation of RAD52.

synthetic lethality in cell lines deficient in BRCA1 and PALB2, while exerting negligible effects on their BRCA1- and PALB2-proficient counterparts[23]. Additionally, while inactivation of RAD52 show no significant phenotype in mammals, suppression of RAD52 is lethal when in combination with mutations in additional genes that cause hereditary breast and ovarian cancer like PALB2 and RAD51C[141]. Inhibition of RAD52 also prevents the repair of DSBs by the error-prone SSA annealing, as this pathway is entirely dependent on RAD52 function. While RAD52 inhibition only prevents HR- and SSA-mediated repair, error-prone NHEJ-mediated DSB repair and SSB repair activities are still overwhelmed by the cytotoxic effects an accumulation of toxic DSBs following DNA replication in the majority of BRCA-deficient cancer cells[26,142].

RAD52 Small Molecule Inhibitors

Until recently, there were no published RAD52-specific small molecule inhibitors. Cramer-Morales et al. was the first to demonstrate synthetic lethality via a targeted approach using a peptide aptamer designed to target phenylalanine 79 (F79) residue in RAD52 DNA binding domain I in leukemias harboring inactivating mutations in BRCA1/2[26]. Between 2015-2016, we along with our collaborators separately published three RAD52 small molecule inhibitors of various specificity.

Our lab performed virtual computer screens of two chemical libraries containing FDA-approved drugs, and National Cancer Institute (NCI) drug-like compounds to identify candidates to block hRAD52 DNA binding domain I based on the RAD52 crystal structure. This screen resulted in the identification of adenosine 5'-

monophosphate (A5MP), and also its mimic 5-aminoimidazole-4-carboxamide ribonucleotide 5' phosphate (AICAR/ZMP) as an inhibitor of RAD52 activity *in vitro*, which exerted synthetic lethality against BRCA1 and BRCA2–mutated cancer cell lines[142]; however, the off-target effects of these inhibitors in vivo may be broad as it also inhibits autophagy[143]. While these two hits may not be viable options *in vivo* due to limitations in specificity and in membrane permeability for AICAR/ZMP, they offer a starting point for candidate inhibitors that may be further developed into anti-RAD52 drugs to treat patients with BRCA-deficient tumors[142].

Chandramouly et al. identified the RAD52 inhibitor (RAD52i) 6 hydroxy-DL-dopa (6-OH-dopa) via high throughput screening of the Sigma Lopac collection of pharmacologically active compounds for small molecules that block the interaction between RAD52 and ssDNA[144]. In this case, 6-OH-dopa acts as an allosteric inhibitor of the ssDNA binding activity. This allosteric inhibition results in the dissociation of the RAD52 undecamer ring structure which is required for RAD52 to bind ssDNA. While 6-OH-dopa inhibits RAD52 *in vitro* and in cells, it is not yet known how specific it is at targeting RAD52 *in vivo.* It is a known inhibitor of APE1, a major player in repairing SSBs via the BER pathway which may further enhance its effectiveness at targeting BRCA-deficient cells [145,146]; However, it is structurally similar to the Parkinson's disease treatment L-DOPA and it has been used to treat Parkinson's disease mouse models *in vivo*, indicating 6-OH-Dopa may have too many off-target effects in vivo to be a viable therapeutic option[147].

Additionally, Huang et al. also conducted a high throughput screen of two

libraries (Broad's diversity-oriented synthesis library and a Molecular Libraries Probe Center Network library) for compounds capable of blocking the interaction between RAD52 and ssDNA[148]. This led to the identification of multiple candidate inhibitors including D-I03 and D-G23, with D-I03 exerting the strongest inhibitory effect on human primary BRCA-deficient cells as well as the lowest genotoxicity in BRCA-proficient cells; however, in this case more work is needed to elucidate the precise mechanism by which D-I03 and D-G23 block the ssDNA annealing activity of RAD52[148].

Inducing Dual Synthetic Lethality in BRCA-Deficient Cancers

As discussed, PARPis have only had modest success thus far at targeting BRCA-deficient cells in clinical trials despite showing excellent promise in preclinical studies. As a reminder, PARPis induce synthetic lethality by promoting the accumulation of lethal DSBs in cells deficient in BRCA-mediated HR via inhibition of BER/SSB repair pathways, and ALT-NHEJ-mediated repair of DSBs, culminating in the death of the majority of the BRCA-deficient cells. However, a few resilient BRCA-deficient cells within a tumor may still survive due to protection from the RAD52-mediated HR back-up pathway and RAD52-dependent SSA repair. With the growing number of patients in clinical trials developing resistance to PARPi during or shortly after treatment in clinical trials, we hypothesized that the backup RAD52-mediated HR pathway in addition to RAD52-dependent SSA repair are together preventing PARPi from efficiently eradicating a small number of tumor cells.

It has already been well established that individually targeting PARP1 or RAD52

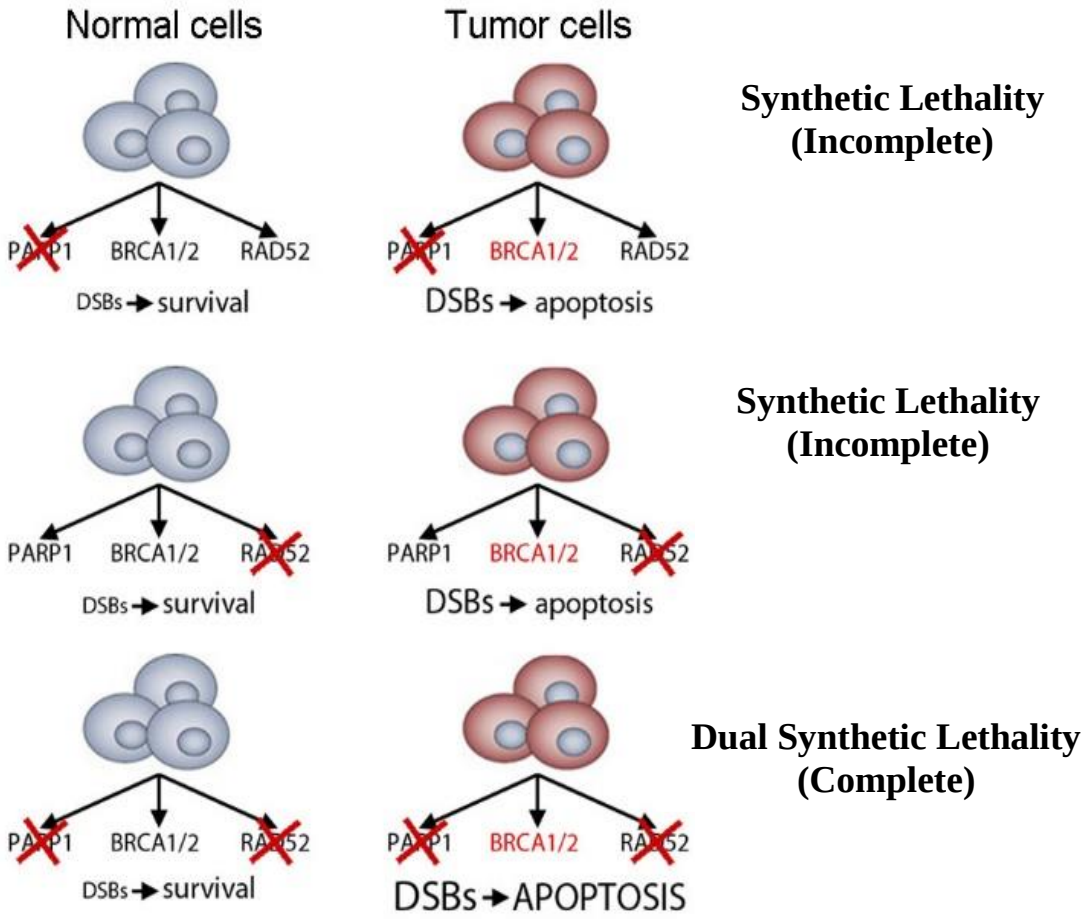

Figure 6. Dual synthetic lethality in BRCA-deficient cancers mediated by PARPi and RAD52i. Although RAD52i and PARPi both individually induce synthetic lethality in BRCA-deficient cancers, but in both cases some cells are still protected from cell death by alternative repair pathways. We hypothesized RAD52i will significantly enhance the selective killing of PARPi-treated BRCA-deficient cells via inducing dual synthetic lethality.

induces at least a partial synthetic lethal effect in cells lacking BRCA-mediated HR. Therefore, we propose that simultaneous inhibition of PARP1 and RAD52 will greatly improve the clinical effectiveness of PARPi to selectively target BRCA pathway-deficient cells by inducing dual synthetic lethality (Figure 6).

CHAPTER 2

MATERIALS AND METHODS

Cell Lines

BRCA1-/- and *BRCA1+/+* murine embryonic stem (ES) cells carrying a DR-GFP reporter cassette, *BRCA2-/-* VC8 and *BRCA2+/+* V79 hamster cell lines carrying DR-GFP reporter cassette, and BRCA*2+/+* and *BRCA2-/-* murine ES cell lines carrying SA-GFP reporter cassette were all obtained from Maria Jasin and Jeremy Stark (Sloan Kettering Cancer Center, New York, NY)[149-151]. The pancreatic carcinoma cell line, Capan1, with truncated *BRCA2* as well as Capan1 cells with restored BRCA2 expression were obtained from Simon Powell[140]. The human ovarian carcinoma cell line UWB1.289 carrying a germ-line *BRCA1* mutation within exon 11 (2594delC) and a deletion of the wild-type allele (*BRCA1-null*), and UWB1.289 cells in which BRCA1 expression has been restored (UWB1.289 BRCA1+) were purchased from ATCC. The BRCA1-null breast cancer cell line HCC1937 (5382insC germ-line mutation generating the truncated protein and no wild-type allele) and cells with restored BRCA1 expression (BRCA1+) were obtained from Ralph Scully[152]. The triple-negative breast cancer cell line MDA-MB-436 which contains a BRCA1 5396 + 1G>A mutation in the splice donor site of exon 20 that results in a BRCT domain-truncated protein, and MDA-MB-436 cells with restored BRCA1 were obtained from Neil Johnson (Fox Chase Cancer Center, Philadelphia, PA, USA)[153]. EUFA423 cells, which are immortalized fibroblasts derived from a Fanconi anemia patient with biallelic mutations (7691 insAT and 9900 insA)

in *BRCA2* that result in two different truncated forms of BRCA2, and EUFA423 cells with restored BRCA2 expression were obtained from Simon Powell[140]. The human pre-B cell line Nalm-6 parental and *RAD54-/-* isogenic cells were purchased from Horizon (Cambridge, UK). Burkitt lymphoma-derived Epstein-Barr virus (EBV)-positive B-cell lines Mutu and Raji and EBV-immortalized lymphoblastoid cell lines (LCLs) from healthy donors as previously described[20].

Primary Cells

FLT3(ITD)-positive AML samples were obtained from the Department of Internal Medicine I, Division of Hematology & Hemostaseology, Medical University of Vienna, Austria. BCR-ABL1 –positive CML, AML1-ETO –positive AML, IGH/MYC –positive Burkitt lymphoma primary samples and BRCA1/2 deficient and proficient AML samples were characterized before[20,106]. Samples of normal hematopoietic cells were purchased from Cambrex Bio Science (Walkersville, MD, USA). Lin-CD34+ cells were obtained from mononuclear fractions by magnetic sorting using the EasySep negative selection human progenitor cell enrichment cocktail followed by human CD34 positive selection cocktail (StemCell Technologies) as described before[106]. All primary cells were cultured in StemSpan H3000 media supplemented with a cocktail of growth factors (100 ng/mL stem cell factor, 20 ng/mL interleukin3 [IL-3], 100 ng/mL fms-related tyrosine kinase 3 ligand, 20 ng/mL granulocyte colony-stimulating factor, 20 ng/mL IL-6).

Transfections

All transfections were performed using Lipofectamine 2000 reagent (Invitrogen, Carlsbad, CA, USA) according to manufacturer's instructions. MDA-MB-436 and EUFA423 cells and their BRCA1 and BRCA2 reconstituted counterparts were transfected with pLSXP-GFP-RAD52wt, pLSXP-YFP-RAD52(F79A), pMIG-mCherry-PARP1wt and pMIG-mCherry-PARP1(E988K). Double-positive cells were sorted 72 h after transfection with BD Biosciences Influx™ Sorter, cultured in 96-well plate and counted after 14 days.

HR and SSA Reporter Assays

BRCA2-/- VC8 and BRCA2+/+ V79 hamster cell lines and BRCA1-/- (clone 17) and BRCA1+/+ (clone 92B) mES cells carrying DR-GFP reporter cassette and BRCA2-/- murine ES clone 42E cells (BRCA2-) and BRC21 wild-type clone 40b cells (BRCA2+) carrying SA-GFP cassette were co-transfected with pCBASce1 (encoding I-Sce1) and pDsRed (transfection efficiency control) plasmids using Lipofectamine 2000 (Invitrogen) as previously described[66,154]. Transfected cells were treated with Olaparib (AZD2281, Selleckchem), Talazoparib (Selleckchem), 6-OH-dopa, (Sigma) or vehicle (DMSO) immediately after removal of the transfection complexes. The percentage of GFP+DsRed+ cells in DsRed+ population was detected after 72 hours by flow cytometry to assess HR repair activity.

RAD51 Foci

HCC1937 BRCA1-deficient and –proficient cell lines were plated in six well plates containing coverslips coated with gelatin and allowed 24 hours to attach. Once attached, the cells were treated for 24 hours with 3 µg/ml cisplatin combined with 5µM olaparib (Ola) and/or 10µM 6-OH-dopa (Dopa). To detect RAD51 foci, cells were stained with an anti-RAD51 antibody (Thermo Scientific), followed by a secondary antibody conjugated with AlexaFluor 594. Negative controls were performed without addition of primary antibody. DNA was counterstained with 4'6'-diamidino-2-phenylindole (DAPI). Nuclei were analyzed and scored as either containing low foci (0-9 foci) or high foci (>10 foci) per nucleus. Coverslips were mounted onto polylysine-coated slides using an anti-fade reagent (SlowFade Gold, Invitrogen, Carlsbad, CA). Nuclear foci were visualized with an inverted Olympus IX70 fluorescence microscope equipped with a Cooke SensiCam QE camera (The Cooke Corp., Auburn Hills, MI). Images from at least 100 individual cells were analyzed per experimental group and were acquired with Slidebook 3.0 (Intelligent Imaging Innovations, Denver, CO). A series of three-dimensional images was converted to a single two-dimensional image. Deconvolution was applied using Slidebook 3.0 to each two-dimensional image to increase contrast and resolution.

Neutral Comet Assay

MDA-MB-436 BRCA1+ and BRCA1- cells and Nalm6 parental and *RAD54-/-* cells were treated for 24 hours with the indicated concentrations of Ola and/or Dopa. Comet assays were performed under neutral conditions using the Oxiselect Comet Assay Kit (Cell Biolabs) according to the manufacturer's instructions. Images were acquired by an inverted Olympus IX70 fluorescence microscope using a FITC filter, and the percentage of tail DNA of individual cells was calculated using the OpenComet plugin of ImageJ. 100-150 cells were used per treatment group.

Transgenic/Knockout Mice

Rad52-/- mice were obtained from Maria Jasin (Memorial Sloan-Kettering Cancer Center, New York, NY, USA), PARP1-/- mice (provided by Roberto Caricchio, Lewis Katz School of Medicine at Temple University) and SCLtTA;p210BCR-ABL1 mice (tet-off model of CML-CP)[155] were used before in our lab[106,156]. Rad52-/- were cross-bred with PARP1-/- mice to generate PARP1-/-Rad52-/-, PARP1-/-;wt, Rad52-/-;wt and wt/wt mice. These animals were cross-bred with SCLtTA;p210BCR-ABL1 mice to generate SCLtTA;p210BCR-ABL1;PARP1-/-Rad52-/-, SCLtTA;p210BCR-ABL1;PARP1-/-, SCLtTA;p210BCR-ABL1;Rad52-/-, and SCLtTA;p210BCR-ABL1;wt;wt mice. Transgenic/knockout mice were identified by polymerase chain reaction (PCR) of tail snip DNA. DNA isolation and purification from mice tails were performed using the REDExtract-N-Amp Tissue PCR Kit (Sigma-Aldrich). Genotyping for the SCLtTA and p210BCR-ABL1 transgenes and PARP1 was performed using transgene/knockout-

specific primers (Operon) and 2X GoTaq polymerase Master Mix (Promega). BCR-ABL1-specific primers (forward: 5'-GAGCGTGCAGAGTGGAGGGAGAACA-3'; reverse: 5'-GGTACCAGGAGTGTTTCTCCAGACTG-3') amplified a 500 basepair-long fragment using amplification conditions of 40 cycles at 94°C for 45 seconds, 55°C for 1 minute, and 72°C for 1 minute. SCLtTA-specific primers (tTA: 5'-TTTCGATCTGGACATGTTGG-3'; SCL: 5'-AGAACAGAATTCAGGGTCTTCCTT-3') yielded a 750 basepair product using amplification conditions consisting of 40 cycles at 94°C for 40 seconds, 60.5°C for 1 minute, and 72°C for 1 minute. PARP1 specific primers: forward: 5'-CATGTTCGATGGGAAAGTCCC- '3; wild type reverse: 5'-CCAGCGCAGCTCAGAGAAGCCA- '3; mutant reverse: 5'-CATGTTCGATGGGAAAGTCCC- '3. The primers amplified a 112 basepair fragment if wild type, a 350 basepair fragment if PARP1 null, and both 112 and 350 basepair fragments if heterozygous using amplification conditions consisting of 35 cycles at 94°C for 1 minute, 60°C for 1 minute, and 72°C for 3 minutes. The RAD52-specific primers were: forward: 5'-AGCCAGTATACAGCGGATG- '3; wild type reverse: 5'-CAACTAGATACATGCCCACG- '3; mutant reverse: 5'-CGCATCGCCTTCTATCGCCT- '3. The amplification conditions consist of 35 cycles at 93°C for 1 minute, 55°C for 1 minute, and 72°C for 3 minutes. PCR products (120 basepair fragment if wild type, a 320 basepair product if RAD52 null, and both 120 and 320 basepair fragments if heterozygous for RAD52) were run in a 1.5% agarose gel containing ethidium bromide, and visualized using the Gel DocTM XR+ Molecular Imager® System (Bio-Rad). Mice were provided with drinking water supplemented with

0.5 g/L tetracycline hydrochloride (Sigma-Aldrich) and leukemia was induced by withdrawal of tetracycline. CML-CP –like leukemia was characterized by splenomegaly, and leukocytosis associated with expansion of mature myeloid cells assessed by immunophenotyping as described below.

Immunophenotyping

To assess for leukocytosis, mouse bone marrow cells (BMCs) and peripheral blood mononuclear were isolated and stained with FITC-conjugated GR-1 (granulocyte marker), PE-conjugated MAC-1 (macrophage marker), APC-conjugated B220 (pan B cell marker) and PE-Cy7-conjugated CD3 (pan T cell marker). To assess for bone marrow stem and progenitor cell populations, BMCs were stained with rat anti-mouse APC–conjugated anti-lineage antibody cocktail (CD3e, CD11b, CD45R/B220, Ly-76, Ly-6G, and Ly6C), PE–conjugated CD117 (c-Kit), and PE-Cy7–conjugated Ly-6A/E (Sca-1). All cells were incubated with a murine Fc block (BD Pharmingen) for 10 minutes prior to staining. Murine immunophenotyping antibodies were all purchased from BD Pharmingen. Compensation controls were generated with single stains. Stained cells were analyzed by flow cytometry with BD FACSCanto II (BD Biosciences).

***In Vitro* Treatment**

PARPi olaparib and BMN673 (Selleckchem), RAD51i F79 aptamer[26], 6-OH-dopa[144], and I03[148], daunorubicin (Selleckchem), and BCR-ABL1 tyrosine kinase inhibitor imatinib (Selleckchem) were added to indicated cells for 3-5 days. Cell

count/viability was determined by Trypan blue exclusion. Clonogenic activity was assessed 7 days after re-plating of treated cells. Cell death and γ-H2AX staining were examined by flow cytometry after staining with Fixable Viability Dye eFluor® 780 (eBioscience) and Alexa Fluor® 647 anti-γ-H2AX (BD Biosciences) as described before[157]. For long-term experiments fresh inhibitors were added every 3-4 days and cells were expanded in fresh medium every 7 days.

Clonogenic Assay

Freshly harvested Lin- murine bone marrow cells were plated in serum-free MethoCult-SF H4236 (StemCell Technologies, Vancouver, Canada) supplemented with TET System Approved Fetal Bovine Serum (Takara Bio USA) with and without 10μg/mL tetracycline hydrochloride in the presence of a threshold concentrations (0.1 unit/ml) of recombinant murine IL-3, IL-6, and SCF as described before[158]. Colonies were counted after 5 to 7 days.

***In Vivo* Treatment**

NSG mice were total body irradiated (250 cGy) and inoculated i.v. with 1 x 10^6 BRCA deficient AML primary leukemia xenograft cells. Two weeks later mice were treated with vehicle (control), talazoparib [0.33mg/kg/day by oral gavage for 7 days[106]], F79 aptamer [2.5 mg/kg i.v.[26]] and a combination of talazoparib + F79 aptamer. Leukemia burden was analyzed by flow cytometry 7 days after the end of treatment. Human leukemia cells were detected by anti-human CD45 (hCD45) antibody as

described before[106]. Median survival time was determined. Nude mice were injected s.c with 5 x 106 BRCA deficient MDA-MB-436 cells. Once tumors reached a volume of 100mm3, mice were treated with vehicle (control), talazoparib [0.33mg/kg/day by oral gavage[106]], I03 [50mg/kg/day i.p], and a combination of talazoparib and I03 for 7 days. Tumors were measured weekly and tumor volumes were calculated using the ellipsoid volume formula (π/6 x L x W x H). C57BL/6 mice were treated with vehicle (control), or a combination of talazoparib [0.33mg/kg/day by oral gavage[106]] and I03 [50mg/kg/day i.p] daily for 7 days. Peripheral blood and bone marrow cell samples were taken 7 days after the end of treatment to assess for potential toxicity. Additionally, the indicated organs were fixed and stained with hematoxylin and eosin.

Statistics

Data are expressed as mean ± standard deviation (SD) and were compared using the unpaired Student t test; p values less than 0.05 were considered significant. Mean survival time of the mice ± standard error (SE) was calculated by Kaplan-Meier Log-Rank Survival Analysis. The response additivity approach was used to study the synergistic effects[159]. This approach shows a positive drug combination effect when the observed combination effect (EAB) is greater than the expected additive effect by the sum of the individual effects (EA + EB). The combination index (CI) was calculated as CI= (EA + EB)/EAB. The p-value for the possible synergistic effect is given by the significance of the interaction effect in a factorial analysis of variance of the individual and combination effects.

Study Approval

Human studies were approved by the appropriate Institutional Review Boards and met all requirements of the Declaration of Helsinki. Animal studies were approved by the Temple University Institutional Animal Care and Use Committee.

CHAPTER 3

RESULTS

Residual HR activity Attenuated by RAD52i in PARPi-Treated BRCA-Deficient Solid Tumor Cell Lines

To first demonstrate that the RAD52-mediated HR pathway is active in BRCA1- and BRCA2-deficient cells treated with PARPi, we assayed for HR activity by using BRCA1/2-deficient and proficient cell line pairs with a DR-GFP recombination reporter integrated into their genome. DR-GFP consists of two mutated GFP genes: SceGFP and

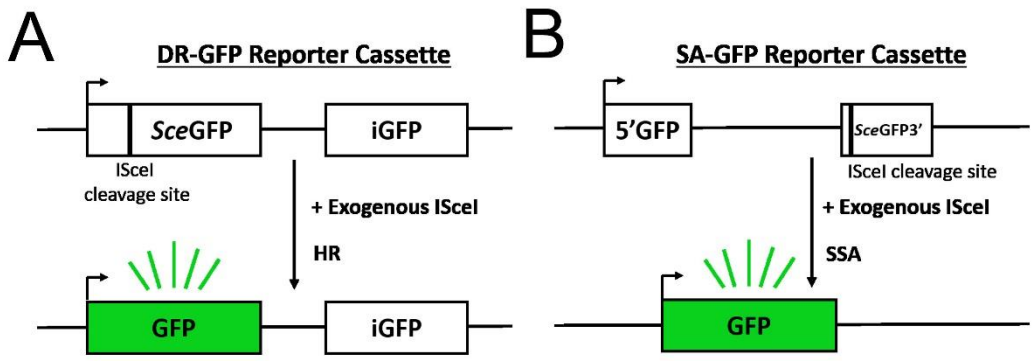

Figure 7. DR-GFP and SA-GFP reporter cassette schematics. (**A**) Ectopic expression of ISceI introduces a DSB in the upstream SceGFP of the DR-GFP reporter cassette. The DSB can be repaired by HR by using the downstream iGFP as a template, resulting in restored expression of GFP. (**B**) To measure SSA activity, ectopically expressed ISceI generates a DSB in SceGFP3'. 5'GFP and SceGFP3' fragments have 266 bp sequence homology, promoting repair of ISceI-induced DSB by SSA, restoring functional GFP expression.

iGFP (internal GFP) (Figure 7A). HR repair activity is measured following introduction of a DSB in the upstream SceGFP gene by the rare-cutting endonuclease ISceI, which can be repaired with HR machinery using the downstream iGFP gene as a template. The cell lines carrying DR-GFP cassettes were co-transfected with pCBA-Sce1 expression plasmid and pDsRed1-Mito as a control for transfection efficiency.

As expected, BRCA1- and BRCA2- deficient cells exhibited reduced HR activity compared to their BRCA1/2-proficient counterparts as measured by percentage of GFP+ cells in DsRed+ population (Figure 8A-B). Nevertheless, there was still residual activity in BRCA1/2-deficient cells that clearly could not be attributed to the BRCA pathway. Treatment with PARPis olaparib and talazoparib did not affect HR activity in either BRCA-deficient or proficient cells, which was expected as PARP1 is not involved in HR-mediated repair; However, the previously described RAD52i 6-hyrodxy-DL-dopa (Dopa)[144] significantly abrogated residual HR activity in both untreated and PARPi-treated BRCA-deficient cells while having no effect on their BRCA-proficient counterparts.

Detection of RAD51 foci by immunofluorescence is commonly used as a surrogate marker for HR activity since the loading of RAD51 onto ssDNA ends is an essential step in HR[23]. We used BRCA1-deficient HCC1937 cells, in which the formation of RAD51 foci is dependent on RAD52, and observed that treatment with RAD52i Dopa inhibited the formation of cisplatin-induced RAD51 foci in BRCA1-deficient HCC1937 but not in their BRCA1-proficient counterparts (Figure 8C). PARPi olaparib had no effect on RAD51 foci formation in BRCA-deficient cells as expected, although olaparib

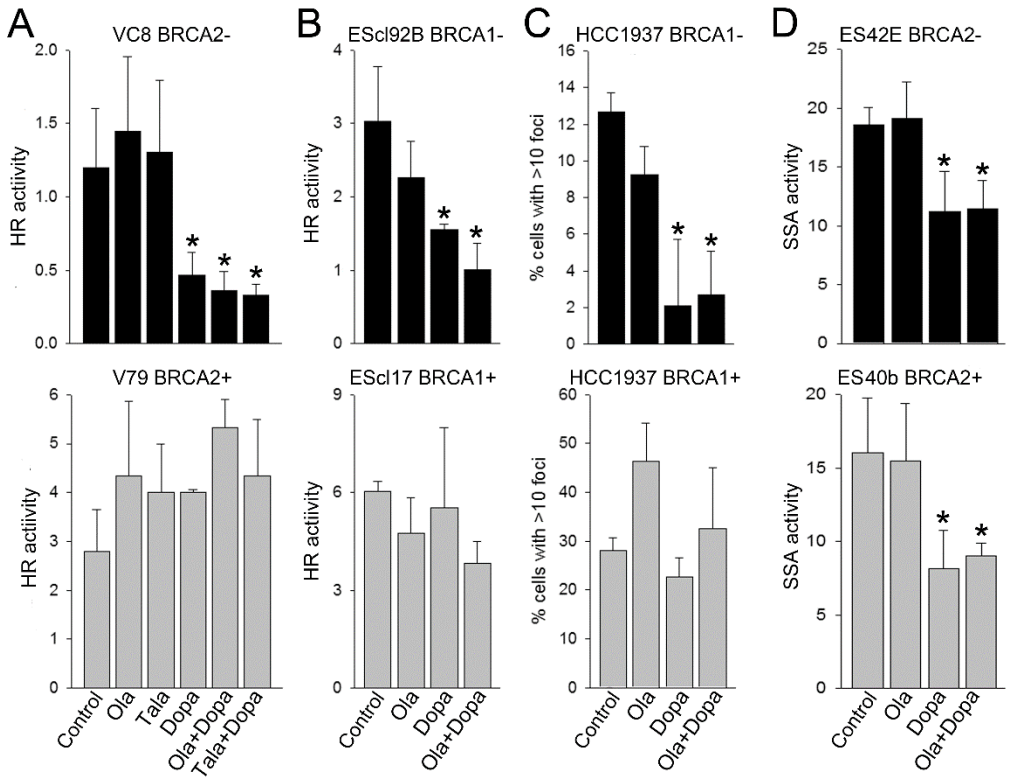

Figure 8. **RAD52i 6-OH-dopa attenuated HR and SSA in BRCA1/2-deficient cells treated with PARPi olaparib.** (**A**) BRCA2-mutated VC8 cells (BRCA2-) and BRCA2 wild-type V79 cells (BRCA2+) and (**B**) BRCA1-/- murine ES clone 17 cells (BRCA1-) and BRCA1 wild-type clone 92B cells (BRCA1+) contained DR-GFP reporter cassette for HR activity were co-transfected with plasmids encoding ISceI and DsRed, followed by treatment with 5μM olaparib (Ola), 5 nM Talazoparib (Tala) and/or 10μM 6-OH-dopa (Dopa), or left untreated (Control). Results represent mean % of GFP+DsRed+ cells in DsRed+ population ± SD from 3 independent experiments; *$p<0.05$ in comparison to untreated control. (**C**) BRCA1-mutated HCC1937 cells (BRCA1-) and HCC1937 expressing wild-type BRCA1 (BRCA1+)

[Figure 8 continued] ... 3 µg/ml cisplatin (Control), or cisplatin combined with 5µM olaparib (Ola) and/or 10µM 6-OH-dopa (Dopa). Results represent percent of cells with >10 RAD51 foci from 3 independent experiments (100 cells/experiment were evaluated); *p<0.05 in comparison to untreated control. (**D**) BRCA2-/-murine ES clone 42E cells (BRCA2-) and BRC21 wild-type clone 40b cells (BRCA2+) carrying SA-GFP cassette were co-transfected with ISceI and DsRed cDNAs followed by treatment with 1.25µM Ola and/or 20µM Dopa, or were left untreated (Control). Results represent mean % of GFP+DsRed+ cells in DsRed+ population ± SD from 3 independent experiments; *p<0.05 in comparison to untreated control.

did cause increased RAD51 foci formation in BRCA–proficient cells possibly as a result of PARPi-mediated accumulation of SSBs converted into DSBs in need of repair in dividing cells. Dopa also reduced the ability of the olaparib-treated BRCA1-deficient cells to form RAD51 foci, further indicating that RAD52-mediated HR activity is functional in these cells and is capable of providing protection from the potentially lethal accumulation of DSBs.

Since RAD52 is essential to SSA-mediated DSB repair in addition to RAD52-mediated HR, we compared SSA activity in a BRCA2-proficient and –deficient cell line pair containing SA-GFP reporter cassette (Figure 6B). The SA-GFP cassette contains two GFP fragments with the ISceI endonuclease recognition site situated between two 266 bp homologous sequences, which promotes repair by SSA resulting in restored expression of functional GFP[151]. HR-mediated repair of the ISceI-induced DSB is not possible here because the SA-GFP reporter cassette does not provide the required homologous

template. As expected, RAD52 inhibition significantly reduced repair of DSBs by RAD52-dependent SSA in both BRCA-proficient and –deficient cells, confirming that in addition to RAD52-mediated HR, SSA also protects BRCA-deficient cells from DSB accumulation (Figure 8D).

Additionally, western blot analyses of BRCA1- and BRCA2-deficient cell lines and their BRCA1/2-proficient counterparts were conducted to determine if PARPi or RAD52i effected the expression of their target proteins (Figure 9). While RAD52 expression was downregulated in CAPAN1 BRCA2-defiicent untreated cells compared to BRCA2-proficient counterparts, 24-hour incubation with PARPi and/or RAD52 did not cause additional downregulation of RAD52 expression. Additionally, any PARPi- or RAD52i-associated variability in RAD52 protein expression was only observed in BRCA1/2-proficient cells while no variability was observed in BRCA1/2-defiicent cells. This indicates that both target proteins are expressed in BRCA1/2-defiicent cell lines following exposure to PARPi and/or RAD52i, meaning that the target proteins of both PARPi and RAD52i are available as substrates for their individual inhibitors. These results verify that neither PARPi nor RAD52i downregulate the expression of either target protein compared to untreated controls, indicating functional inhibition of both target proteins by their respective inhibitors.

Overall, we demonstrated here that RAD52 inhibition alone or in combination with PARPi selectively decreased residual HR activity in both BRCA1- and BRCA2-deficient cancer cells, and decreased SSA activity in both BRCA2-proficient and –deficient cells, as expected. BRCA-proficient cell are protected from the decreased SSA

activity by the BRCA-mediated HR pathway. These observations verified that the RAD52-mediated HR pathway is active in BRCA-deficient cells and thus provided justification to continue investigating RAD52 as a target in PARPi-treated BRCA-deficient cells.

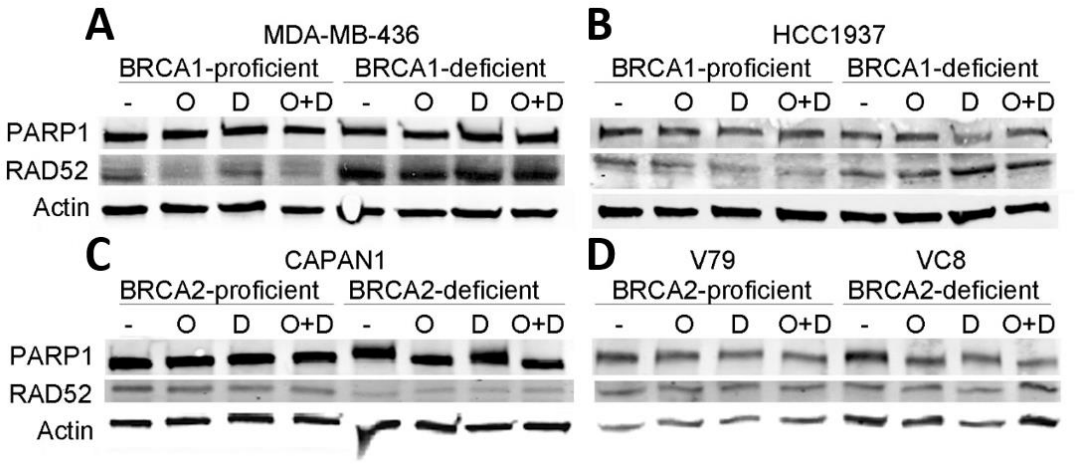

Figure 9. **PARPi and RAD52i did not affect the endogenous expression of PARP1 or RAD52.** Indicated BRCA-proficient or –deficient cell line pairs (**A**) MDA-MB-436, (**B**) HCC1937, (**C**) CAPAN1, (**D**) V79/VC8 were untreated (-) or treated with 5μM olaparib (O), 10μM Dopa (D), or 5μM olaparib + 10μM Dopa (O+D). After 24 hrs exposure to treatment, whole cell lysates were analyzed via western blot to detect RAD52, PARP1, and actin (loading control). Results represent 2-3 independent

RAD52 Inhibition Enhanced the Synthetic Lethal Effect Exerted by PARPi at Targeting BRCA-Deficient Solid Tumor Cell Lines

After verifying that RAD52-mediated HR activity is present and functional in BRCA-deficient cells treated with PARPi, we next sought to test the effectiveness of

using RAD52i in combination with PARPi in a variety of BRCA1- or BRCA2-deficient solid tumor cell lines. To assess the effect of the combination on cell viability following short-term treatment, we treated BRCA1-deficient ovarian (UWB1.289), and breast (MDA-MB-436 and HCC1937) cancer cell lines and the BRCA2-deficient pancreatic cancer cell line (Capan-1) cells for five days with PARPi olaparib in combination with the previously described F79 peptide aptamer[26]. The combination of olaparib and F79 synergistically inhibited cell viability in all four BRCA-deficient cell lines in comparison to individual treatments, while having no effect on the growth of BRCA-proficient counterparts or on immortalized NIH3T3 cells which are also BRCA-proficient (Figure 10).

While the selectivity of F79 at targeting the RAD52 DNA binding domain provides a proof-of-concept for the combination of PARPi and RAD52i, peptide aptamers are generally not stable enough to be considered as potential therapies for patients. Therefore, we tested olaparib in combination with published RAD52is Dopa and D-I03, which both selectively inhibited viability of BRCA-deficient cell in the same manner as F79 when combined with olaparib (Figure 11). This growth inhibitory effect caused by the combination of PARPi + RAD52i correlated with significantly enhanced accumulation of DSBs as detected by neutral comet assay and increased levels of γ-H2AX foci in BRCA1-deficient MDA-MB-436 cells, indicating a selective accumulation of DSBs in these cells (Figure 12). Overall, the selective targeting of BRCA-deficient cell lines when treated with the combination of PARPi and three RAD52i (F79, Dopa, D-I03) was consistent and provides further support for RAD52 as an effective therapeutic target

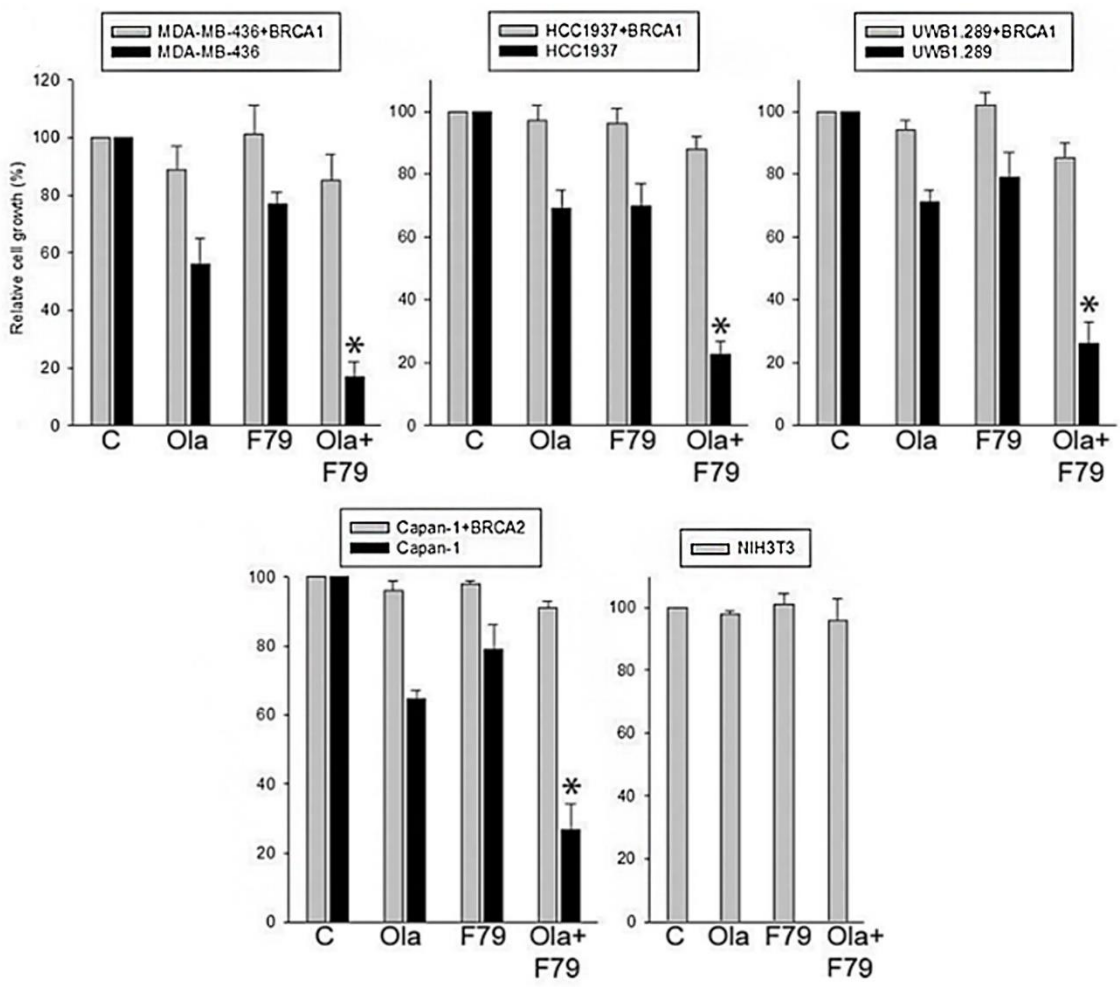

Figure 10. RAD52is enhanced the synthetic lethal effect of PARPi olaparib in BRCA-deficient solid tumor cell lines. Indicated BRCA1/2-deficient cells and BRCA1/2-reconstituted counterparts were treated with 1μM olaparib (Ola) and/or 1μM RAD52 F79 peptide aptamer (F79) added at 0 and 2 days followed by trypan blue counting at day 5. Results represent mean % of trypan blue-negative living cells ± SD relative to untreated counterparts from 3 independent experiments. *, $p<0.04$ and **$p=0.06$ in comparison to cells treated with individual drugs using the response additivity approach.

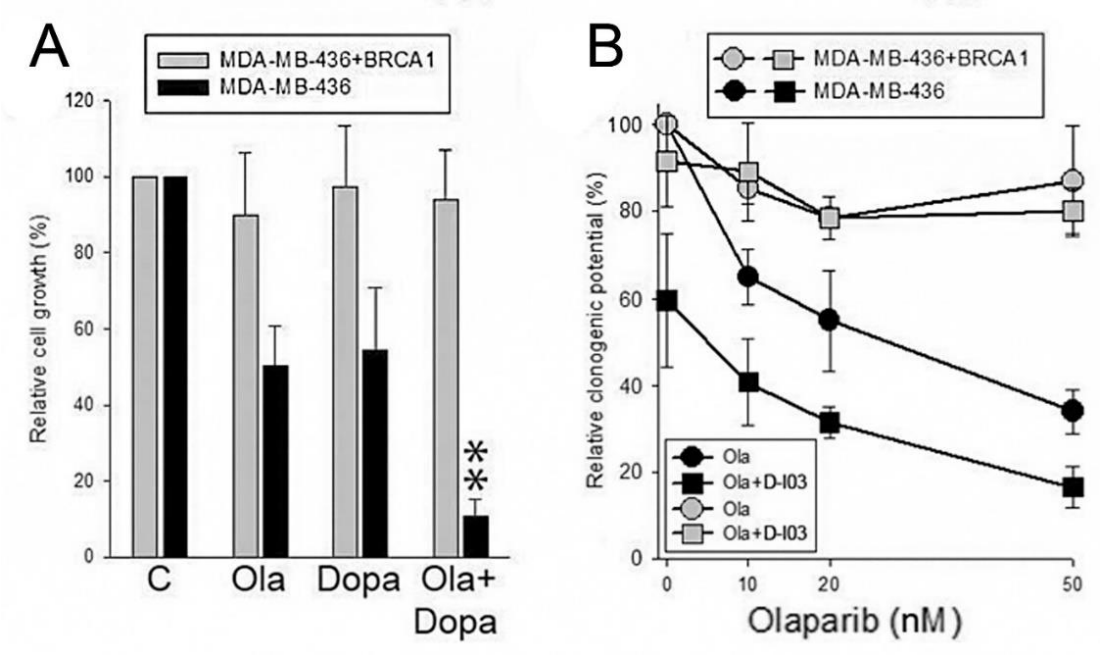

Figure 11. RAD52is Dopa and D-I03 enhanced the synthetic lethal effect of PARPi olaparib in BRCA-deficient solid tumor cell lines. (**A**) MDA-MB-436 BRCA1-deficient cells and BRCA1-reconstituted counterparts were treated with 1μM olaparib (Ola) and 5μM Dopa added on days 0 and 2. Living cells were counted via trypan blue exclusion on day 5. Results are represented as mean % of trypan blue-negative living cells ± SD relative to untreated counterparts from 3 independent experiments. *, $p<0.04$ and **$p=0.06$ in comparison to cells treated with individual drugs using the response additivity approach. (**B**) MDA-MB-436 BRCA1-deficient and BRCA1-proficient cells were treated on days 1 and 3 with increasing concentrations of olaparib in absence or presence of 1 μM D-I03. Results represent mean % of treated clonogenic cells ± SD relative to untreated counterparts from 3 independent experiments.

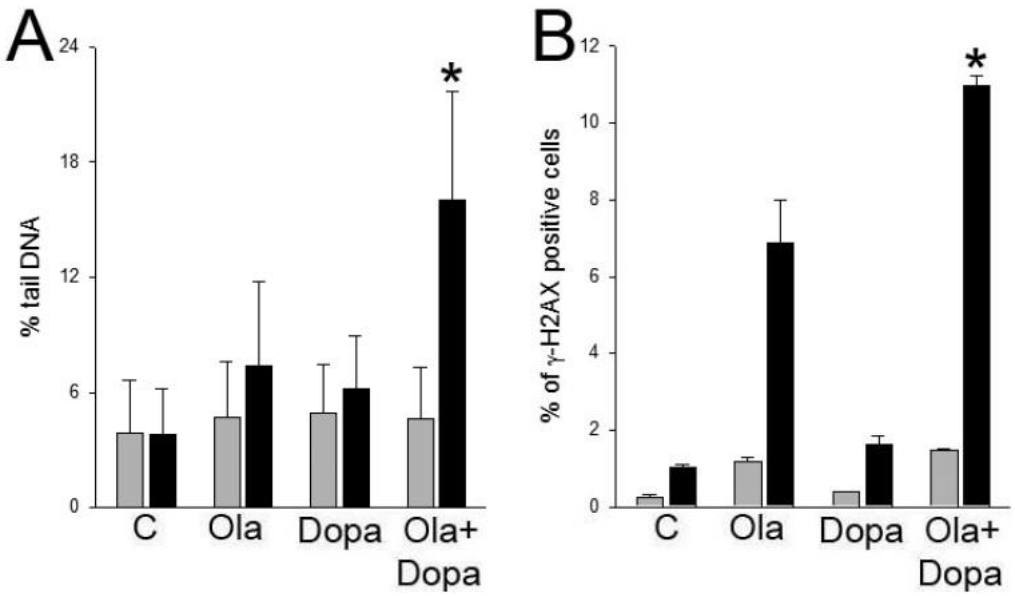

Figure 12. PARPi and RAD52i caused accumulation of DSBs in BRCA-deficient cells. BRCA1-deficient MDA-MB-436 (black bars) cells and BRCA1-reconstituted counterparts (gray bars) were treated with μM Ola and/or 5μM Dopa for 24 hrs followed by detecting of DSBs by (**A**) neutral comet assay and (**B**) γ-H2AX immunofluorescence. Results represent mean % of tail DNA ± SD from 100-150 cells and mean % of γ-H2AX-positive cells ± SD from triplicate experiment. *$p<0.05$ in comparison to cells treated with individual drugs using the response additivity approach.

when used in combination with PARPi in for BRCA-deficient cells.

The lack of success of PARPi in clinical trials is primarily due to patients eventually developing resistance to PARPi either during treatment or after the treatment regimen ceases. To see if BRCA1- or BRCA2-deficient cancers developed resistance following long-term exposure to the combination of PARPi and RAD52i, we exposed

cell lines deficient in BRCA1 (MDA-MB-436 and HCC1937) and BRCA2 (VC8 and Capan-1) to continuous treatment for 28 days with olaparib + RAD52i Dopa. Importantly, continuous long-term exposure of PARPi + RAD52i led to complete eradication of BRCA1 and BRCA2 - deficient cells, while treatments with individual inhibitors only partially inhibited the rate of growth (Figure 13). At the end of 28 days of continuous treatment, cells exposed to the combination of PARPi and RAD52i were

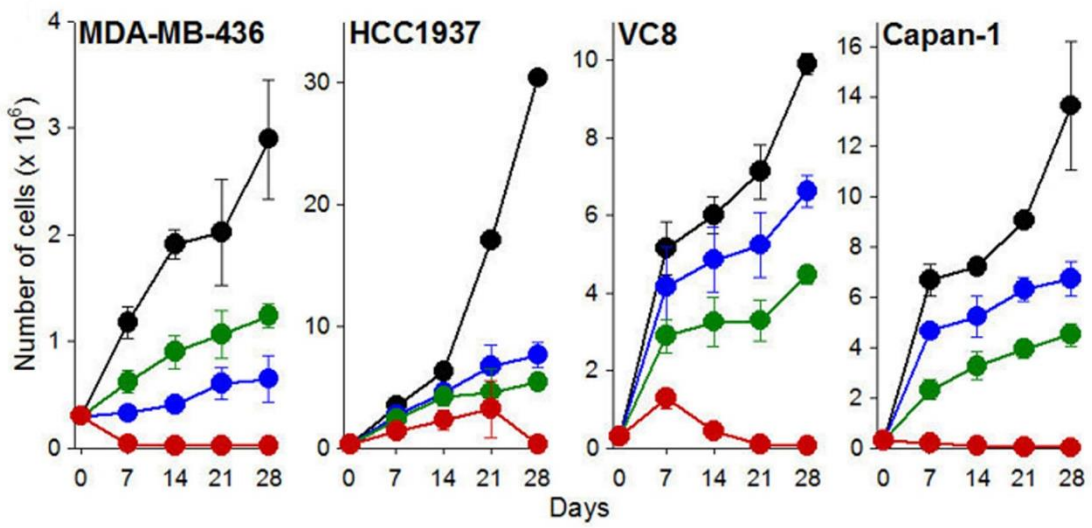

Figure 13. RAD52i abrogated the emergence of potentially resistant clones in BRCA-deficient solid tumor cell lines treated with PARPi olaparib. Indicated BRCA1/2-deficient cells were left untreated (black) or continuously treated with 2.5µM olaparib (blue), 20µM Dopa (green) and olaparib+Dopa (red) for 28 days. Viable cells were identified by Trypan blue exclusion. Results represent mean cumulative number of cells ± SD from triplicate experiments.

washed to ensure complete removal of inhibitors and cultured in inhibitor-free medium for another 14 days. Remarkably, even after 14 days there were no detectable living cells, signifying that they were not able to recover from exposure to the combination.

RAD52i Enhanced the Synthetic Lethal Effect Exerted by PARPi at Targeting BRCA-Deficient Hematopoietic Cell Lines

In addition to testing solid tumor cell lines, we examined the effect of simultaneous treatment with PARPi and RAD52i on leukemia and lymphoma cell lines deficient in BRCA-mediated HR. For the BRCA-mediated HR pathway to successfully recruit and load RAD51 to the DSB site, not only are BRCA1 and BRCA2 required, but PALB2, RAD51, RAD51 paralogs and RAD54 are also equally indispensable. Accordingly, a cell is will have a BRCA-deficient phenotype if any single one of those proteins are knocked down or inhibited. Here, we examined the effect of PARPi and RAD52i on the Nalm6 human leukemia cell line deficient in the BRCA HR pathway gene, RAD54[104].

Short-term treatment of RAD54-/- Nalm6 cells with PARPi olaparib and RAD52i Dopa significantly induced more cell death as determined by both cell viability dye staining and trypan blue exclusion. Additionally, we observed an enhanced accumulation of DSBs specifically in RAD54-/- cells treated with the combination of PARPi and RAD52i as assessed by γ-H2AX immunofluorescence (Figure 14B) and by neutral comet assay (Figure 15). The accumulation of DSBs was associated with selectively decreased cell viability in RAD54-/- cells (Figure 14A, C-D). Furthermore, *RAD54+/+* parental

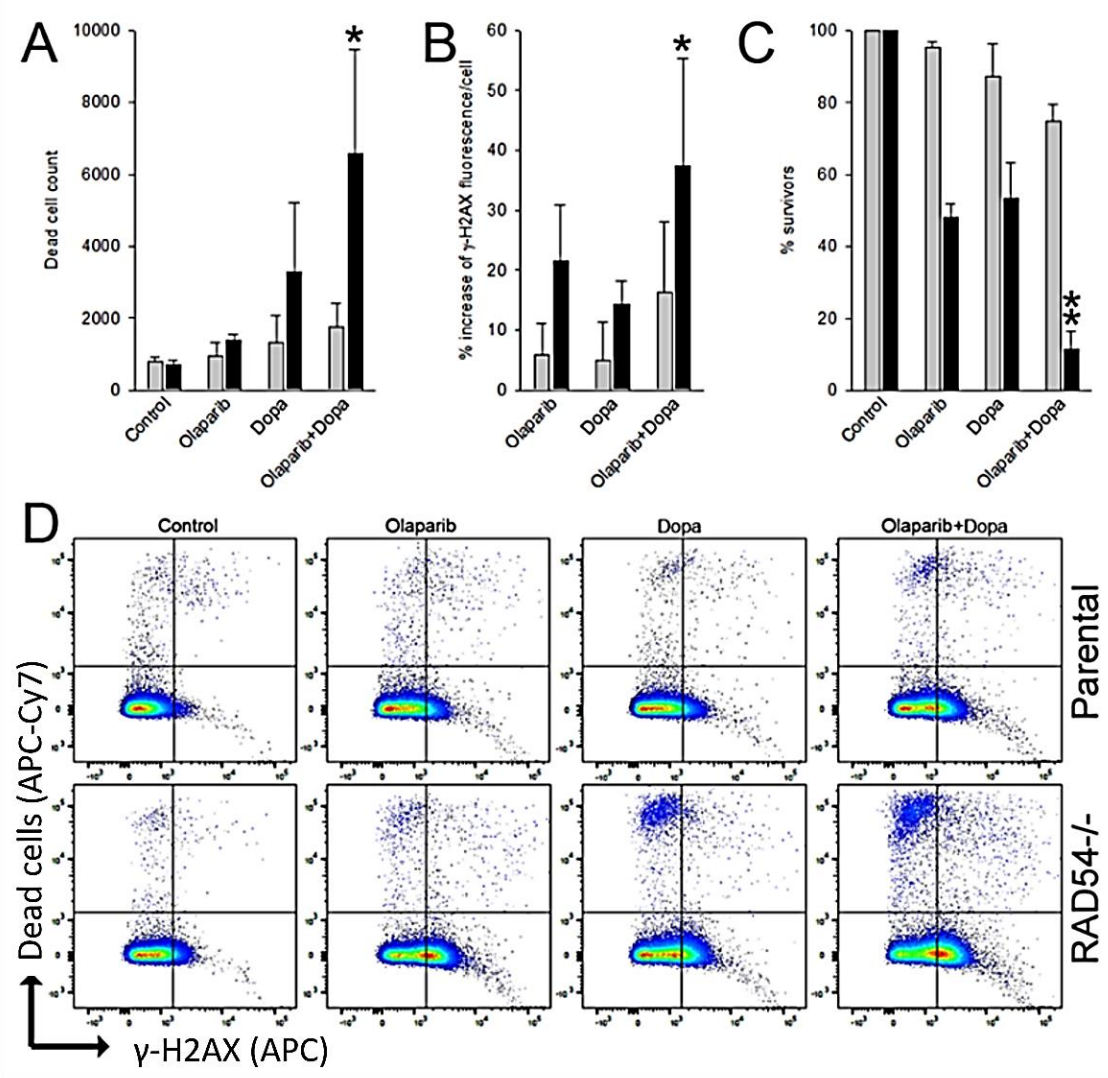

Figure 14. RAD52i enhanced the synthetic lethal effect of PARPi in BRCA pathway-deficient malignant hematopoietic cell lines. (**A-D**) Nalm-6 parental (grey bars) and Nalm-6 RAD54-/- (black bars) cells were left untreated (Control) and treated with 0.3 µM olaparib, 5 µM Dopa, and olaparib + Dopa for 24 h (**A, B**) and 48 h (**C, D**). (**A**) Mean number ± SD of dead cells detected as cells positive for fixable viability staining. (**B**) Mean % increase of cellular γ-H2AX **[Continued]**

[Figure 14 continued] … immunofluorescence ± SD compared to untreated counterparts. (**C**) Mean % of trypan blue-negative living cells ± SD relative to untreated counterparts. (**D**) Representative diagrams illustrate accumulation of γ-H2AX (right quadrangles) and dead cells (upper quadrangles).

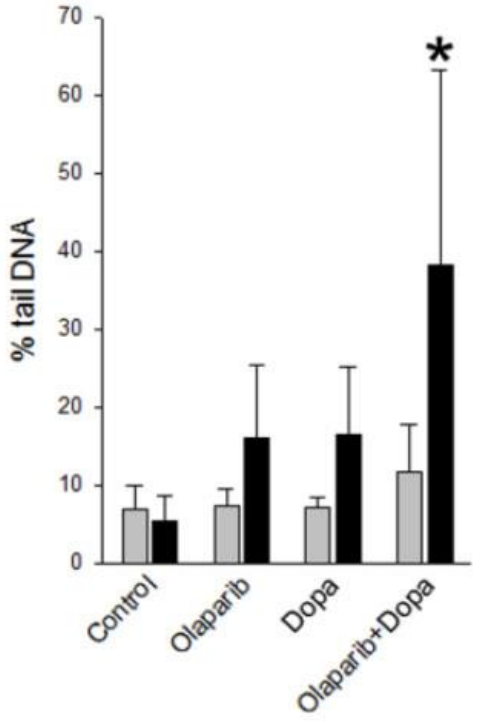

Figure 15. PARPi + RAD52i caused enhanced accumulation of DSBs in RAD54-/- leukemia cells. Nalm-6 parental (grey bars) and Nalm-6 *RAD54-/-* (black bars) cells were left untreated (Control) and treated with 5 μM olaparib, 20 μM Dopa, and olaparib + Dopa for 24 h before DSBs were detected by neutral comet assay. Results represent mean % of tail DNA ± SD from 100-150 cells per treatment group.

cells experienced no significant effects regarding cell viability or DSB accumulation, highlighting the specificity of the combination treatment at targeting cells deficient in BRCA-mediated HR.

For a more clinically relevant treatment model, we sought to determine if leukemias deficient in the BRCA-pathway developed resistance following extended exposure to the combination of PARPi and RAD52i. To test this, we exposed RAD54-/- Nalm6 cells to PARPi olaparib and/or the RAD52i Dopa continuously for 35 days. Continuous exposure to the combination of olaparib and Dopa resulted in the complete elimination of living *RAD54-/-* cells according to trypan blue exclusion, whereas exposure to the individual treatments resulted in initial cell death that the cells eventually recovered from over the duration of the experiment (Figure 16). At the end of 35-day treatment, the olaparib+Dopa-exposed cells were washed to remove all trace of inhibitors and subsequently cultured in fresh inhibitor-free media for an additional 14 days. There were no viable *RAD54-/-* cells detected at the end of the 14-day incubation, demonstrating the notable potency of the combination of PARPi and RAD52i at preventing the development of resistance in BRCA pathway-deficient leukemia following long-term exposure.

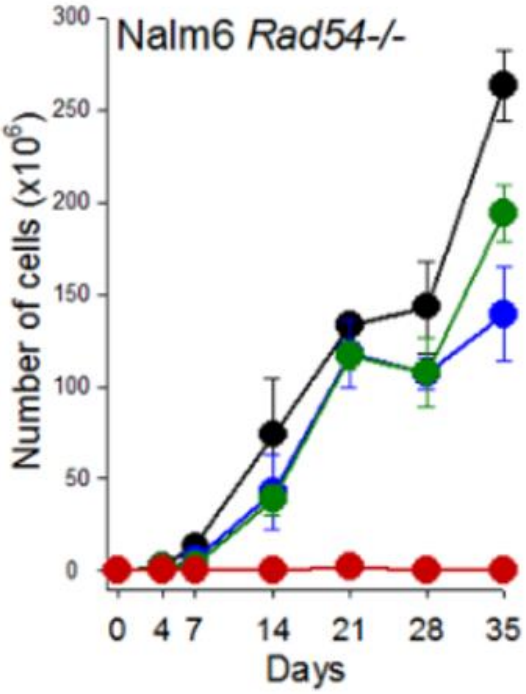

Figure 16. RAD52i in combination with PARPi abrogated the development of potentially resistant clones in BRCA pathway-deficient leukemia cells. Nalm6 RAD54-/- cells were left untreated (black) or continuously treated with 2.5µM olaparib (blue), 20µM Dopa (green) and olaparib+Dopa (red) for 35 days. Viable cells were identified by Trypan blue exclusion. Results represent mean cumulative number of cells ± SD from triplicate experiments Mean cumulative number ± SD of trypan blue-negative living cells. Results in are from 3 independent experiments.

To determine the effect of RAD52i on cells deficient in BRCA-mediated HR that have already developed resistance to PARPi, talazoparib-resistant RAD54-/- Nalm6 cells were developed by culturing the cells under continuous exposure to increasing concentrations of talazoparib until they were fully resistant to 10nM talazoparib. Despite being resistant to PARPi, the cells were still sensitive to treatment with RAD52i Dopa (Figure 17), indicating that RAD52i may still be partially effective at targeting PARPi-resistant clones that have potentially already developed in patients before or during treatment.

Next we sought to use a second BRCA pathway-deficient hematopoietic model to assess for dual synthetic lethality exerted by PARPi + RAD52i. We compared the effects of olaparib and Dopa on BRCA2-deficient Burkitt lymphoma (BL)-derived Epstein-Barr virus (EBV)-positive B-cell lines Mutu and Raji, with BRCA2-proficient EBV-immortalized lymphoblastoid cell lines (LCL1 and LCL2) established from healthy donor cells used as BRCA2-proficient controls[20]. Mutu and Raji express IGH/MYC translocation, which leads to continuous, uncontrolled expression of oncogene MYC, ultimately leading to downregulation of BRCA2 expression[19,20]. Following 72 hours of treatment, the combination exerted a much stronger inhibitory effect on Mutu and Raji when compared to treatment with the individual inhibitors, as assessed by trypan blue exclusion (Figure 18). At the same time, their BRCA2-proficient counterparts were not sensitive to the combination of inhibitors.

To verify that RAD52 inhibition only enhances the effects of PARPi at targeting BRCA-deficient cells, we employed MLL-AF9-positive murine leukemia cells that have

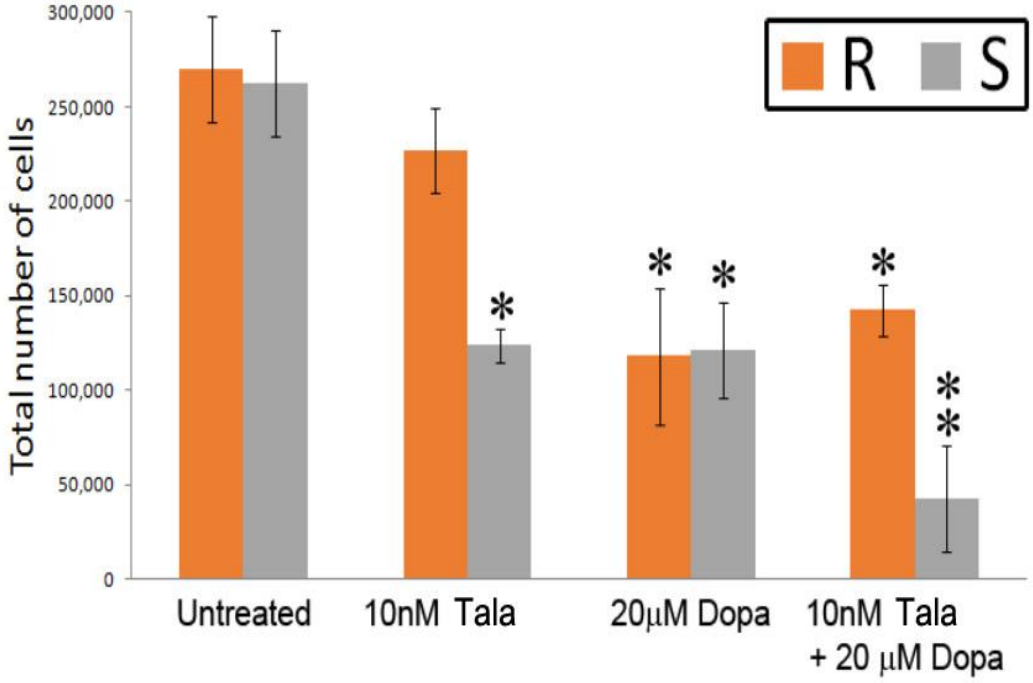

Figure 17. Talazoparib-resistant RAD54-/- Nalm6 leukemia cells are sensitive to RAD52i Dopa. RAD54-/- Nalm6 leukemia cells were continuously exposed to growing concentrations of talazoparib (Tala) until fully resistant to 10nM of the inhibitor. RAD54-/-Nalm6 resistant (R) and RAD54-/- Nalm6 sensitive (S) cells (104/ml) were untreated or treated with the indicated concentrations of Tala and Dopa on day 0 and 2. Living cells were counted via trypan blue exclusion on day 5. Results represent mean ± SD number of living cells from three individual experiments; *$p<0.05$ when compared to corresponding untreated cells, **$p<0.05$ when compared to the cells treated with individual inhibitor.

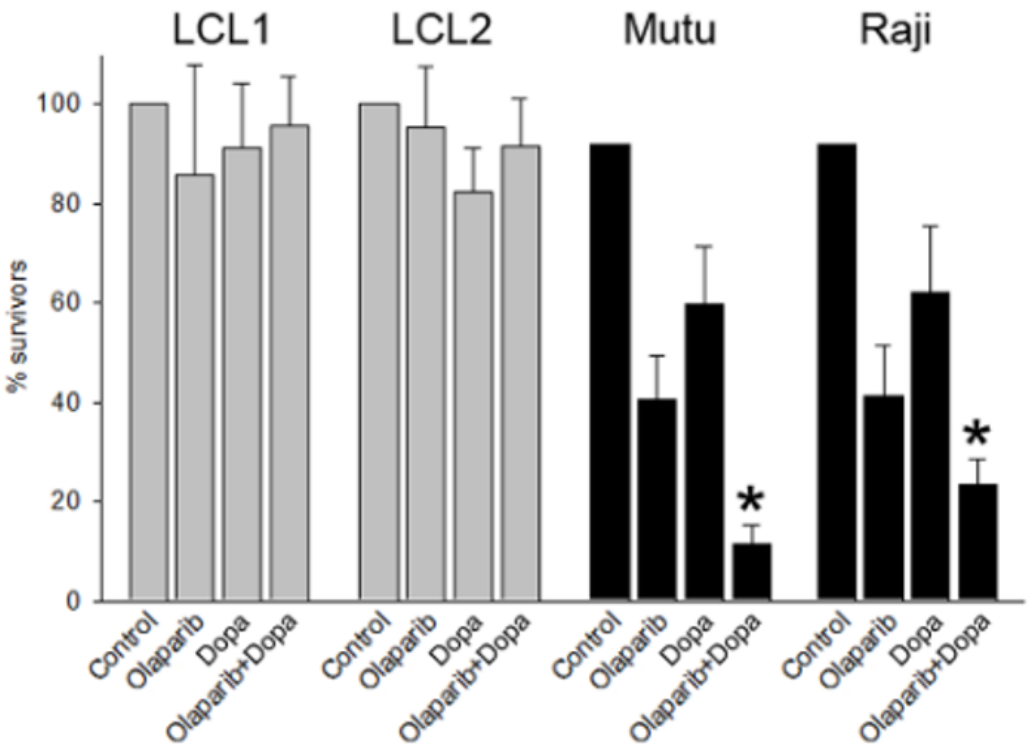

Figure 18. RAD52i enhanced the synthetic lethal effect of PARPi in BRCA pathway-deficient malignant hematopoietic cell lines. BRCA2-deficient BL-derived B-cell lines Mutu and Raji, and control LCL1 and LCL2 cells were treated with 2.5 µM olaparib and/or 5 µM Dopa for 72 h. Results represent mean % of trypan blue-negative living cells ± SD relative to untreated counterparts from triplicate experiments *P<0.05 and ** P<0.03 in comparison to the cells treated with individual drugs using Student t test.

previously been determined to be proficient in all BRCA pathway proteins, but are sensitive to PARPi when used in combination with standard cytotoxic drugs[17,160]. While these cells were sensitive to increasing concentrations of PARPi olaparib as expected, they showed no additional sensitivity when treated with the combination of olaparib and Dopa (Figure 19). These results support the hypothesis that PARPi + RAD52i selectively

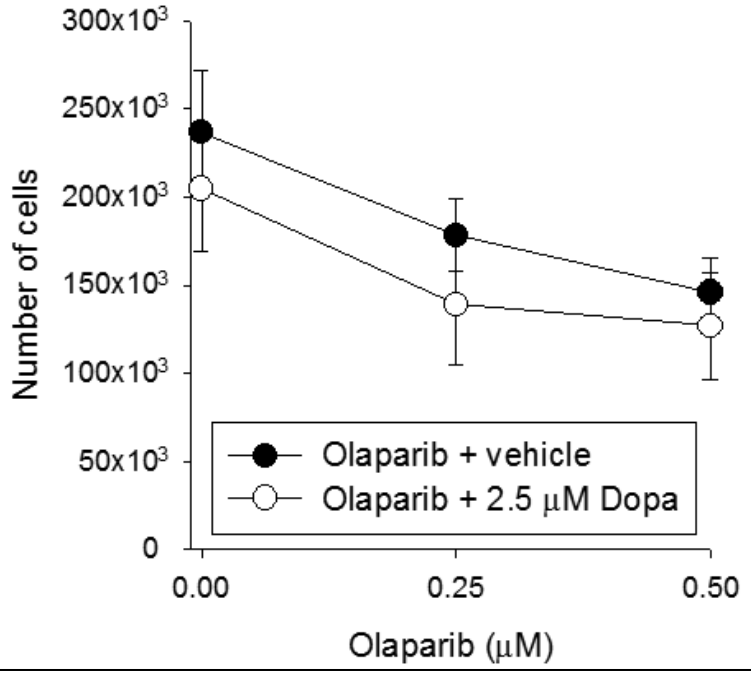

Figure 19. Inhibition of RAD52 did not enhance the effect of PARPi in BRCA-proficient MLL-AF9 –positive leukemia cells. MLL-AF9-positive murine bone marrow cells were treated for 72 hours with the indicated concentrations of olaparib in the absence (vehicle) or presence of 2.5 μM Dopa as assessed by Trypan blue exclusion. Results represent mean ± SD of living cells from 2 independent experiments.

have a synergistic effect in BRCA pathway-deficient cells.

To exclude the possibility that the synergistic effect exerted by the combination of PARPi and RAD52i are caused by off-target effects of the small-molecule inhibitors, we ectopically co-expressed wild type and/or dominant-negative mutants of PARP1 and RAD52 in BRCA1- and BRCA2-deficient cell lines and their BRCA1/2-proficient counterparts, and assessed the effect on cell growth via trypan blue exclusion 14 days after plating (Figure 20). As predicted, the individual expression of either the catalytically inactive PARP1(E988K) mutant or the DNA binding-defective RAD52(F79A) mutant specifically reduced the growth of BRCA1-deficient MDA-MB-436 cells and BRCA2-deficient EUFA423 cells compared to BRCA1/2-deficient cells expressing wild type RAD52 and/or PARP1. Importantly, co-expression of PARP1(E988K) and RAD52(F79A) mutants exerted a synergistic growth inhibitory effect in both MDA-MB-436 cells and EUFA423 cells whereas BRCA1/2-reconstituted counterparts were not affected, which was consistent with effects observed by the combination of PARPi + RAD52i.

In conclusion, we have demonstrated using two different approaches to inactivate PARP1 and RAD52 (via small molecule inhibitors and the expression of dominant negative mutants) in a variety of BRCA pathway-deficient and –proficient cell line pairs that simultaneous inhibition of PARP1 and RAD52 exerts a dual synthetic lethal effect selectively in cells deficient in BRCA-mediated HR by causing a lethal accumulation of DSBs. Importantly, we have also confirmed that prolonged exposure to the combination of PARPi + RAD52i resulted in the complete eradication of BRCA pathway-deficient

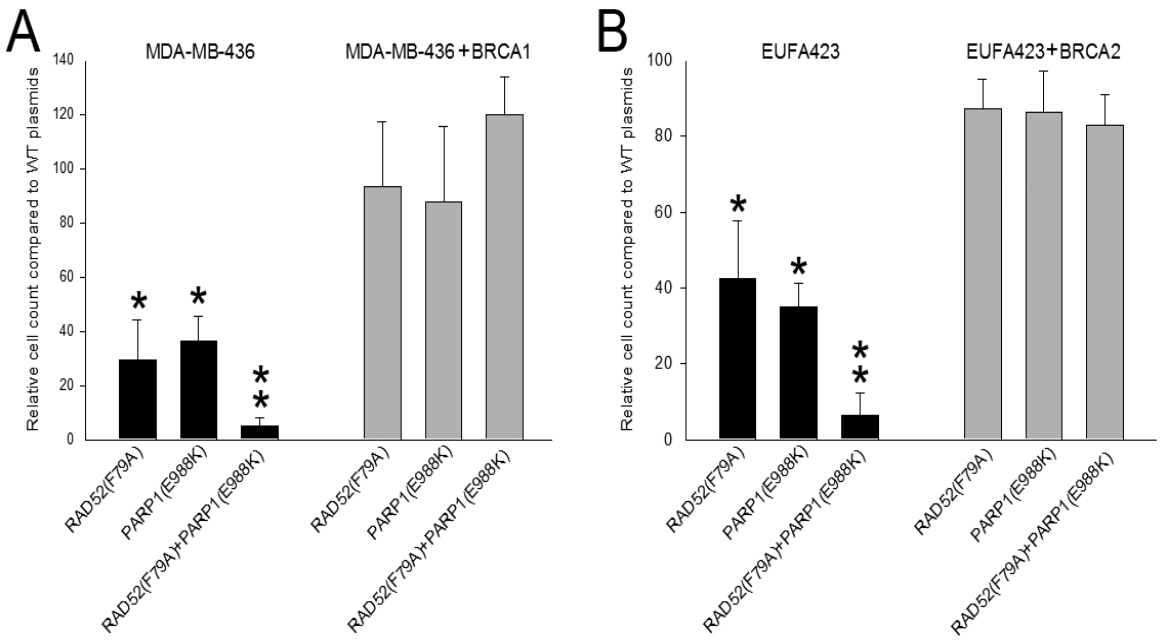

Figure 20. RAD52(F79A) DNA binding deficient mutant enhanced the synthetic lethal effect of PARP1(E988K) catalytically inactive mutant in both BRCA1- and BRCA2-deficient cells. (**A**) BRCA1-deficient (black bars) and BRCA1 reconstituted (gray bars) MBA-MB-436 cells and (**B**) BRCA2-deficient (black bars) and BRCA2 reconstituted (gray bars) EUFA423 cells were transfected to stably express PARP1 and/or RAD52 wild-type or PARP1(E988K) and/or RAD52(F79A) dominant negative mutants. The results represent the growth of the cells expressing dominant-negative mutant(s) relative to these expressing wild-type proteins from at least 3 independent experiments. *$p<0.02$ when compared to BRCA1/2-proficient counterparts using Student t test, and **$p\leq0.01$ when compared to BRCA1/2-deficient cells transfected with individual mutants using the response additivity approach.

cells, preventing the eventual development of a PARPi + RAD52i -resistant population. This effect was selective as the combination did not target BRCA-proficient cells, including MLL-AF9-positive BRCA-proficient cells previously determined to be sensitive to PARPi due to alternative molecular mechanisms. Our data greatly support the approach of simultaneously targeting of PARP1 and RAD52 as a highly robust method for the selective eradication of BRCA-deficient cancer cells.

PARPi + RAD52i Eliminated BRCA-Deficient Primary Leukemia Cells More Efficiently Than Treatment With Individual PARPi or RAD52i

To confirm that the combination of PARPi and RAD52i selectively targets BRCA-deficient primary cells, we tested the combination in leukemia and lymphoma cells obtained from patients that we had previously identified as deficient in BRCA-mediated HR[106]. We and others have reported that the BRCA1/2-deficient phenotype can be induced by several oncogenes that downregulate the expression of BRCA1/2 proteins, such as BCR-ABL1 which downregulates BRCA1 mRNA translation, AML1-ETO which downregulates BRCA2 mRNA expression, and IGH-MYC which downregulates BRCA2 mRNA translation[17-19,106]. It has also been previously reported that the resulting BRCA-deficiency in cells expressing each of these oncogenes has caused them to be significantly sensitized to the synthetic lethal effect induced by individual treatment with both PARP1 and RAD52 inhibitors[17,20,26,106], leading us to hypothesize that the combination of PARPi + RAD52i would exert a synergistic effect on patient samples expressing these oncogenes. To test this, we looked at the effect that PARPi + RAD52i

had on the viability and clonogenicity of various oncogene-induced BRCA1/2-deficient and proficient primary leukemia and lymphoma patient cells, with FLT3(ITD)-positive primary cells used as a BRCA1/2-proficient control since FLT3(ITD) does not inhibit the expression of BRCA1 or BRCA2[106].

The combination of olaparib and Dopa exerted a strong inhibitory effect against primary lin-CD34+ BRCA1/2-deficient leukemia/lymphoma cells expressing BCR-ABL1, AML1-ETO or IGH-MYC, but not against BRCA1/2-proficient normal cells and FLT3(ITD)+ control cells (Figure 21A). Additionally, highly aggressive BCR-ABL1 – positive CML-blast phase (CML-BP) primary cells were sensitive to the combination of sub-optimal concentrations PARPi talazoparib + RAD52i D-I03 (Figure 20B). Importantly, the addition of the BCR-ABL kinase inhibitor imatinib (IM) to the combination of talazoparib + D-I03 resulted in complete eradication of clonogenic CML-BP cells. These results are particularly promising since IM is the current standard care treatment for CML, and although it is an exceptionally effective treatment for CML, it does not cure the disease and consequently patients risk developing resistance over time[161].

We have previously identified primary AML and therapy-related myelodysplastic syndrome (t-MDS) patient samples to be individually either BRCA pathway-proficient and –deficient via microarray analysis and qPCR[26,106]. Here we treated these primary cells with sub-optimal concentrations of PARPi olaparib and/or RAD52i F79 aptamer, and daunorubicin (DNR), a cytotoxic anthracyline drug which is which is commonly used to treat AML. The combination of olaparib + F79 exerted a much stronger inhibitory

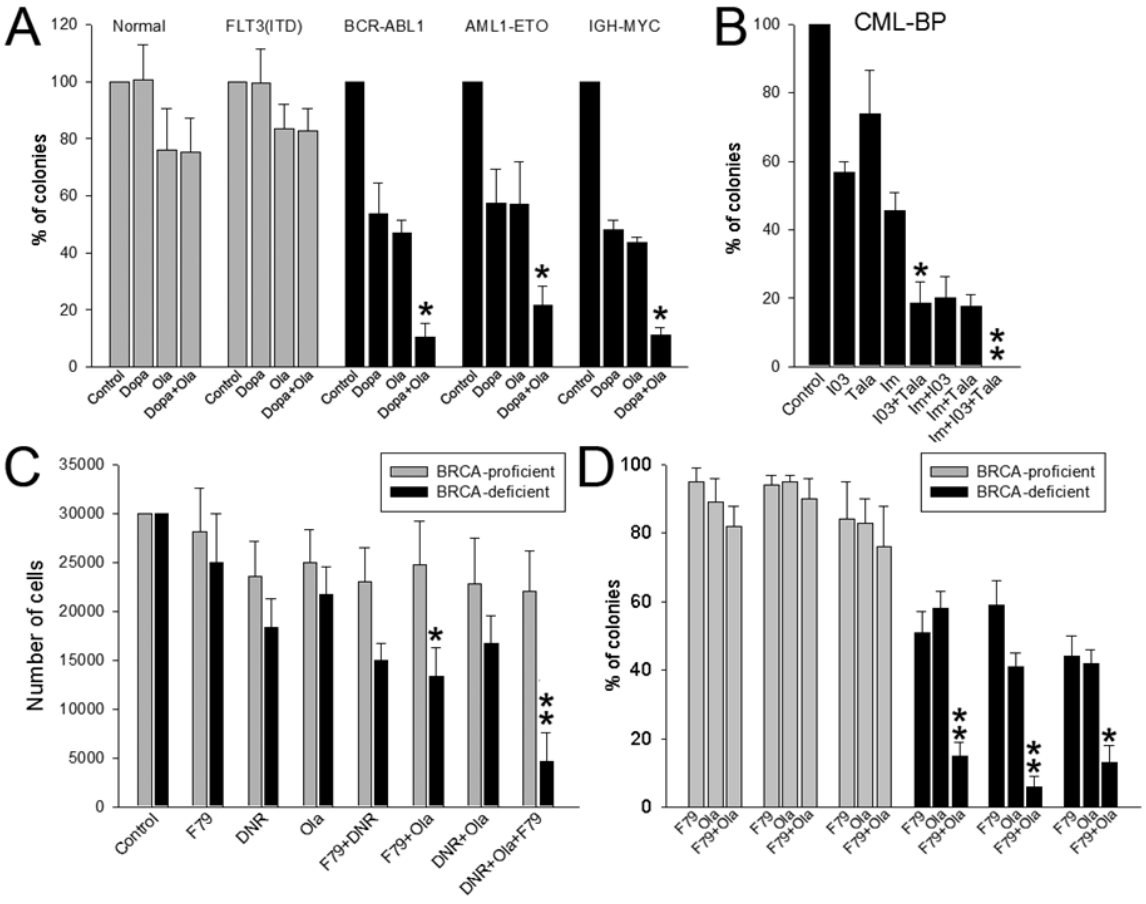

Figure 21. Simultaneous targeting of PARP1 and RAD52 exerted a synergistic synthetic lethal effect against primary patient cells with BRCA1/2-deficient hematopoietic malignancies. (**A**) Lin-CD34+ cells obtained from healthy donors (n=4-8), BRCA-proficient FLT3(ITD) -positive AML (n=3-4), BRCA1-deficient BCR-ABL1 -positive CML-CP (n=3-5), BRCA2-deficient AML1-ETO -positive AML (n=3-6) and BRCA2-deficient IGH-MYC –positive BL cells were treated with 2.5 μM olaparib (Ola) and/or 2.5 μM Dopa. (**B**) BRCA1-deficient BCR-ABL1 –positive CML-BP cells were treated with 2.5 nM talazoparib (Tala), 2.5 μM I03 and/or 1 μM imatinib (Im). (**C**) BRCA pathway-deficient and **[Continued]**

[Figure 21 continued] -proficient AML primary samples (n=3 of each) were treated with 0.125 µg/ml daunorubicin (DNR), 1.25 µM olaparib and/or 1.25 µM F79. (**D**) BRCA pathway -deficient and proficient t-MDS/AML (n=3 of each) were treated with 1.25 µM olaparib and/or 1.25 µM F79. Cells were treated on day 0 and day 2, followed by counting via Trypan blue exclusion on day 3 (**C** and BL cells in **A**) or plating in methylcellulose on day 3; colonies were counted 7-10 days after plating. Results represent mean % ± SD of surviving colonies/cells. *$p<0.05$ in comparison to single and dual treatments, respectively, using Student t test; **$p=0.02$ when compared to DNR + Ola, DNR+F79, Ola, and F79 using the response additivity approach.

effect than individual compounds against AML cells from BRCA pathway-deficient, but not BRCA pathway-proficient patients (Figure 21C-D). Importantly, the triple combination of DNR + olaparib + F79 aptamer exerted a significantly synergistic inhibitory effect on clonogenicity compared to dual combinations of these compounds.

To further justify RAD52 as a therapeutic target in combination with PARPi, we compared the relapse-free survival (RFS) probability of leukemia patients displaying low and high mRNA expression levels of RAD52 and BRCA pathway genes (Figure 22). When comparing RAD52 mRNA expression levels alone, patients with pediatric B-precursor ALL that had low RAD52 expression experienced improved RFS with 75% showing no signs of cancer recurrence after 5 years compared to 50% RFS for patients with high RAD52 levels (Figure 22A). Furthermore, RFS was consistently found to be significantly higher in both MDS and pediatric B-precursor ALL patients expressing low

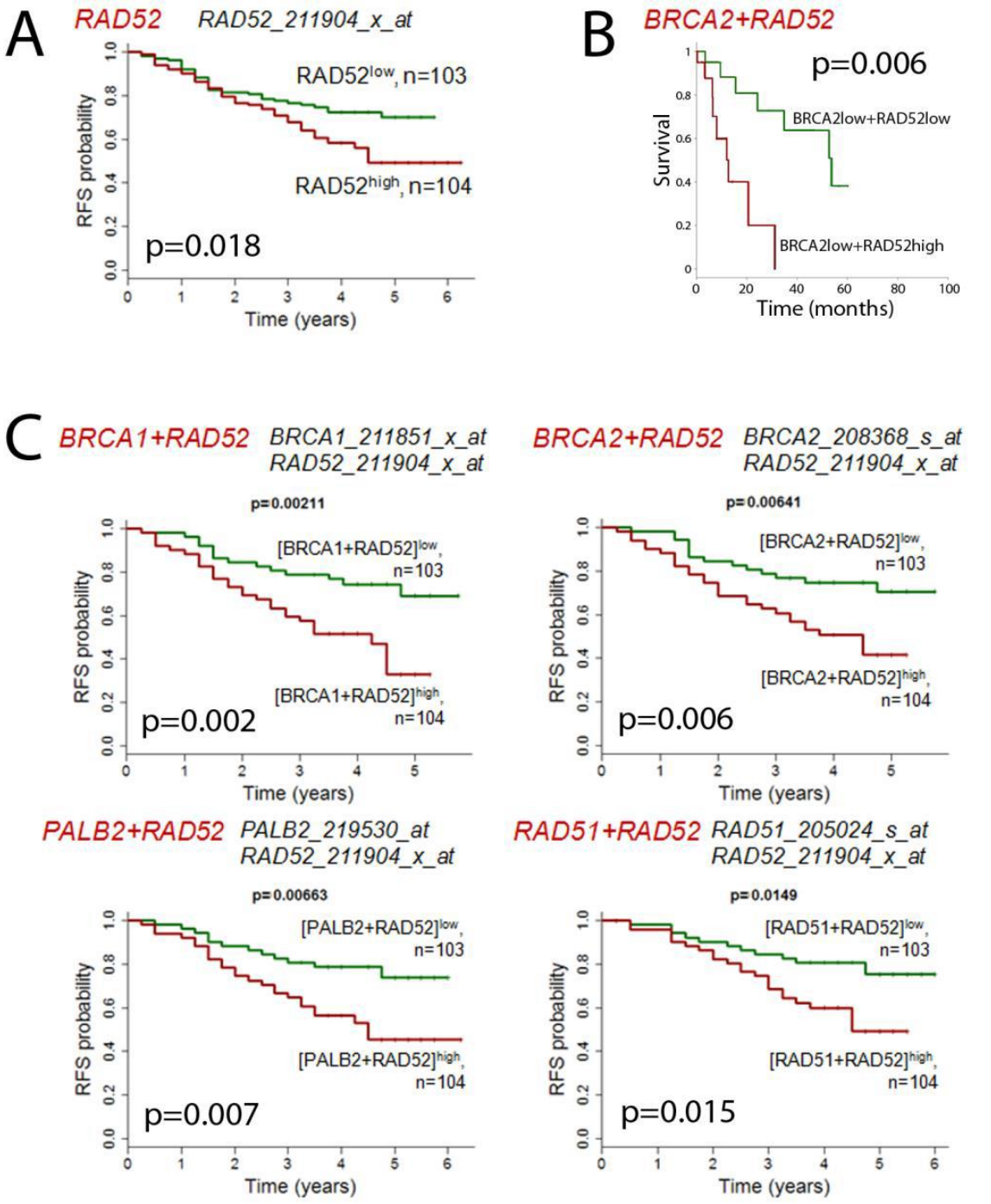

Figure 22. Prognostic value of the expression levels of RAD52 and/or BRCA1, BRCA2, PALB2. (**A**) Kaplan-Meier estimates of relapse free survival [**Continued]**

[Figure 22 continued] …(RFS) for patients with pediatric B-precursor ALL based on higher or lower than the median gene expression values for RAD52 mRNA expression level; p values were calculated from the logrank test. (**B**) Survival of MDS patients displaying downregulation of BRCA2 mRNA (25 percentile) combined with downregulation (25 percentile) or upregulation (75 percentile) of RAD52 mRNA. (**C**) Kaplan-Meier estimates of RFS for patients with pediatric B-precursor ALL based on simultaneous higher or lower than the median mRNA expression values of the indicated pairs of genes. p values were calculated from the logrank test. Analyses were performed using previously published arrays: (**A, C**), and (**B**) PROGene V2 – Pan Cancer Prognostic Database (http://watson.compbio.iupui.edu/chirayu/proggene/database/?url=proggene).

levels of RAD52 and BRCA pathway genes compared to those with leukemias expressing high levels of these genes (Figure 22 B-C). Altogether, RAD52 has consistently proven to be an important target for therapeutic intervention in BRCA-deficient tumors individually and in combination with PARPi.

In conclusion, the combination of PARPi + RAD52i exerted stronger inhibitory effect than individual inhibitors specifically in BRCA-deficient primary leukemia/lymphoma cells. We showed this using primary samples with oncogene-induced BRCA-deficiency in addition to samples from patients determined to be BRCA-deficient based on microarray and qPCR, demonstrating that patients can be predicted to be sensitive to certain combination therapies based on their gene expression profiles. Critically, the addition of standard therapeutic drugs (e.g., IM for CML-BP and DNR for

AML) to the treatment regimen containing sub-optimal doses of PARPi + RAD52i further enhanced the effect of PARPi + RAD52i, suggesting a potentially beneficial therapeutic application of this approach.

Simultaneous Inhibition of PARP1 and RAD52 Exerted a Synergistic Effect Against BRCA-Deficient Mouse Model of Leukemia

To test the effect of PARP1 and RAD52 inhibition through a genetic approach *in vivo*, we first generated *Parp1-/-Rad52-/-* mice to look for any possible toxicity in comparison to mice expressing the wild-type proteins. Notably, *Parp1-/-Rad52-/-* mice do not display any detectable defects in various inspected parameters, including white blood cell (WBC) counts, spleen weight, and immunophenotyping analysis of peripheral blood, spleen, and bone marrow cells (BMCs) (Figure 23). Across all parameters, the *Parp1-/-Rad52-/-* mice were indistinguishable from their wild-type counterparts. We also specifically compared the lin-sca1+c-kit+ (LSK) hematopoietic stem cell (HSC) population between *Parp1-/-Rad52-/-* and wild type mice, and observed that the LSK population was not affected by simultaneous knock out of *Parp1* and *Rad52*, even when under stress from exposure to genotoxic agents such as cisplatin, DNR, and gamma irradiation (Figure 23C). This indicates that *Parp1-/-Rad52-/-* mice do not have a deficiency in HSCs compared to wild type mice, and are thus equally capable of developing leukemia. These results were further validated when comparing hematoxylin and eosin (H&E)-stained tissues from various organs between *Parp1-/-Rad52-/-* and wild type mice, with no notable differences detected between the two (Figure 24).

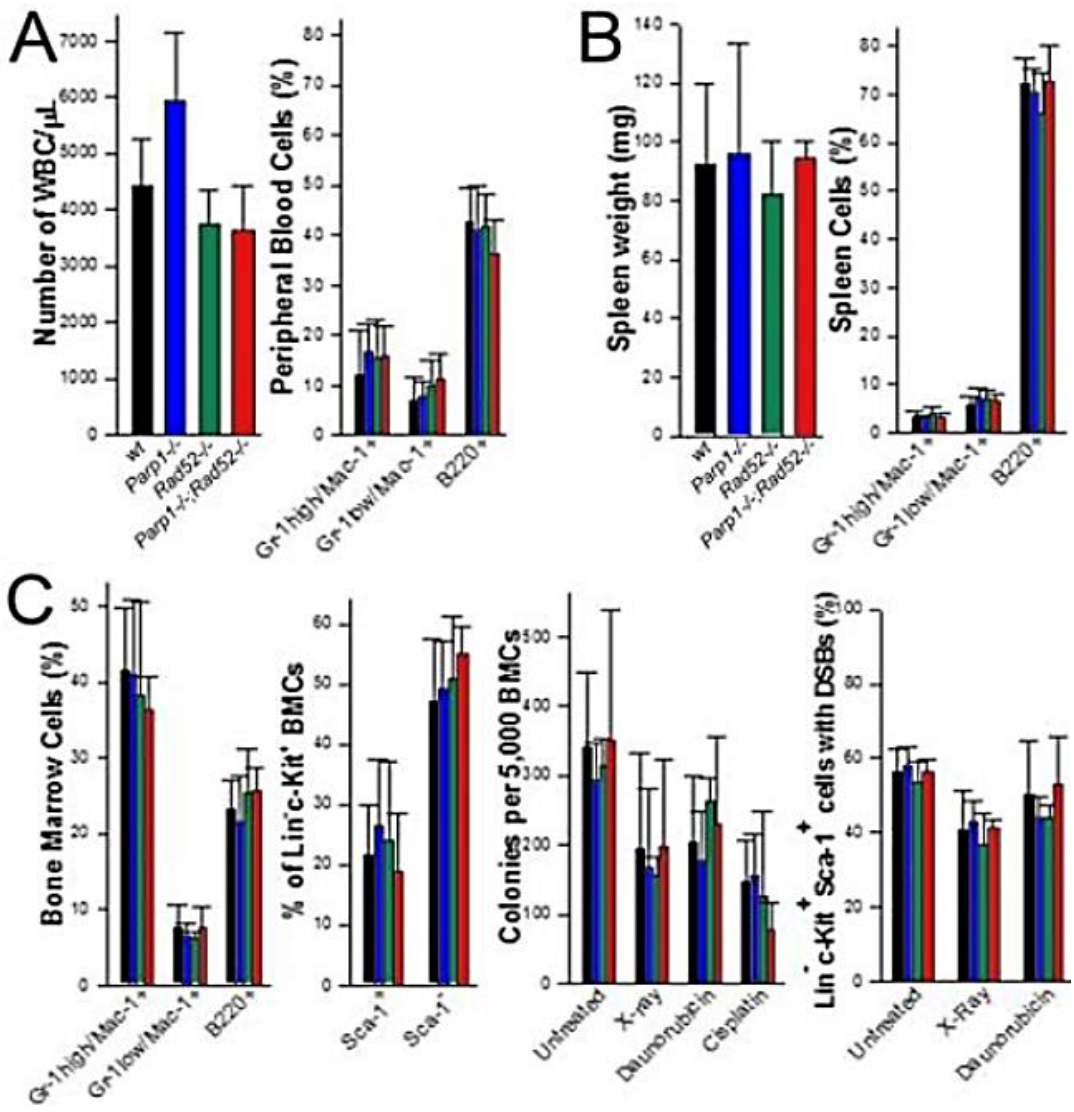

Figure 23. No phenotypic differences between *Parp1-/-Rad52-/-* mice and *Parp1-/-, Rad52-/-* and wild-type animals. (**A**) Peripheral blood parameters: number of white blood cells (WBC)/µL, and % of differentiated myeloid cells and B cells. (**B**) Spleen parameters: spleen weight, and % of differentiated myeloid cells and B cells. (**C**) Bone marrow parameters: % of myeloid cells and B cells, % of Lin-c-Kit+ stem/progenitor **[Continued]**

[Figure 23 continued] …cells, number of colonies per 5,000 BMCs formed by untreated cells and these treated with 1 Gy X-ray, 0.01 μg/ml daunorubicin or 0.4 μg/ml cisplatin, and % of LSK cells with DSBs detected by γ-H2AX immunofluorescence 24 hrs after LSK cells were treated with 1 Gy, 0.01 μg/ml daunorubicin, or were left untreated. Results in **A-C** represent mean ± SD from 3-5 mice/group.

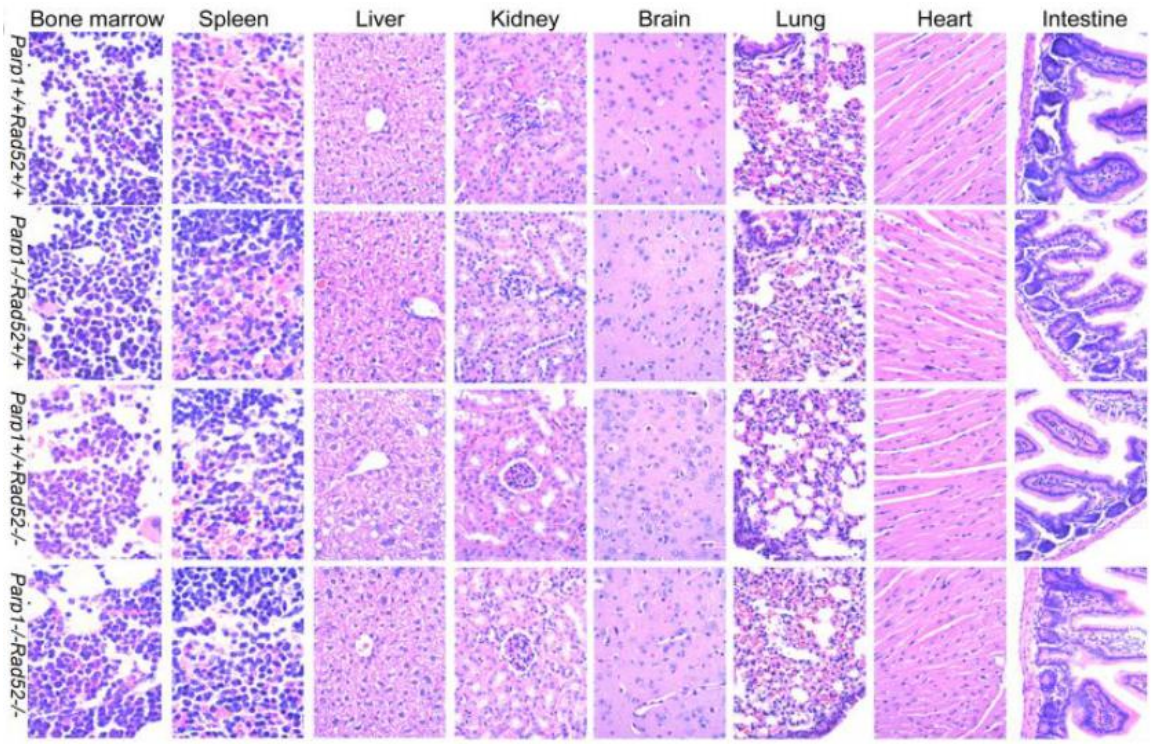

Figure 24. *Parp1-/-Rad52-/-* mice are histologically indistinguishable from *Parp1-/-, Rad52-/-* and wild-type animals. Representative H&E stained tissue sections magnified 100x (bone marrow and spleen) and 40x (liver, kidney, brain, lung, heart, and intestine).

After confirming there were no toxic effects associated with knocking out both *Parp1* and *Rad52 in vivo*, we crossed these mice with a well-established tetracycline- off (Tet-off) SCLtTA/*p210BCR-ABL1* transgenic mouse model of CML-CP, in which BCR-ABL expression is induced under the HSC-specific Stem Cell Locus (SCL) enhancer upon withdrawal of tetracycline (Figure 25)[155]. As a reminder, BCR-ABL is an oncogenic tyrosine kinase that is found in the leukemia cells of almost all CML patients, and it represses the translation of BRCA1 protein while simultaneously promoting its degradation, resulting in leukemia cells that are sensitive to both PARPi and RAD52i[155,162].

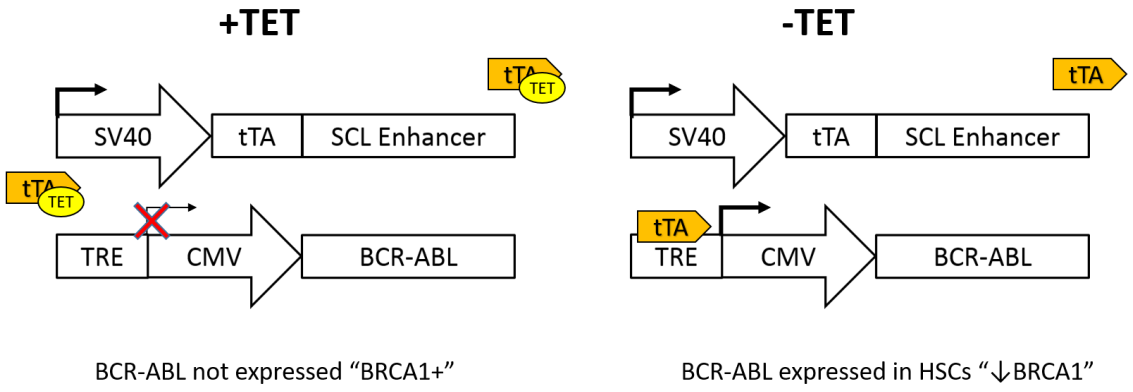

Figure 25. "Tet-off" inducible model of CML-CP. In this model, the tetracycline-controlled transactivator protein (tTA) is constitutively expressed under the SV40 promoter only in HSCs and progenitors which express the SCL enhancer. When tetracycline is present (+TET) it binds to tTA and prevents it from binding to the tetracycline-responsive element (TRE). Removal of tetracycline (-TET) allows tTA to bind to TRE, leading to the expression of BCR-ABL in HSCs/progenitors and the development of a CML-CP-like disease.

To first confirm *in vitro* that the tetracycline-off system worked as expected, we isolated BMCs from *SCLtTA/p210BCR-ABL1* transgenic mice expressing wild type *Parp1* and *Rad52* and exposed them to PARPi olaparib and RAD52i Dopa in the presence or absence of tetracycline, before plating in tetracycline-free methylcellulose. In the absence of tetracycline, individual treatment of PARPi olaparib and RAD52i Dopa resulted in decreased clonogenicity, which was significantly amplified by the combination of olaparib + Dopa with less than 20% of clonogenic cells remaining (Figure 26A). Moreover, this anti-leukemia effect was completely eliminated following continuous exposure to tetracycline, which confirms that BCR-ABL expression is suppressed as expected in the presence of tetracycline, which allows for the translation of BRCA1 to continue unrepressed.

We next cross-bred the *Parp1-/-* and *Rad52-/-* single knockout, and *Parp1-/- Rad52-/-* double knockout mice to generate four groups: *SCLtTA/p210BCR-ABL1/Parp1-/- Rad52-/-*, *SCLtTA/p210BCR-ABL1/Parp1-/-*, *SCLtTA/p210BCR-ABL1/Rad52-/-*, and *SCLtTA/p210BCR-ABL1*. Western blot analysis of BMCs from all four groups of mice cultured in the presence or absence of tetracycline confirmed that the cells expressed BCR-ABL kinase and displayed downregulation of BRCA1 protein only when cultured in the absence of tetracycline, verifying that the Tet-off system was still functioning as expecting for each genotype (Figure 26B). Additionally, we assessed for the relative BCR-ABL-dependent clonogenic potential for each genotype, which was calculated as the difference between number of colonies in the absence (BCR-ABL kinase expressed) or presence (BCR-ABL kinase not expressed) after 7-10 days. BMCs

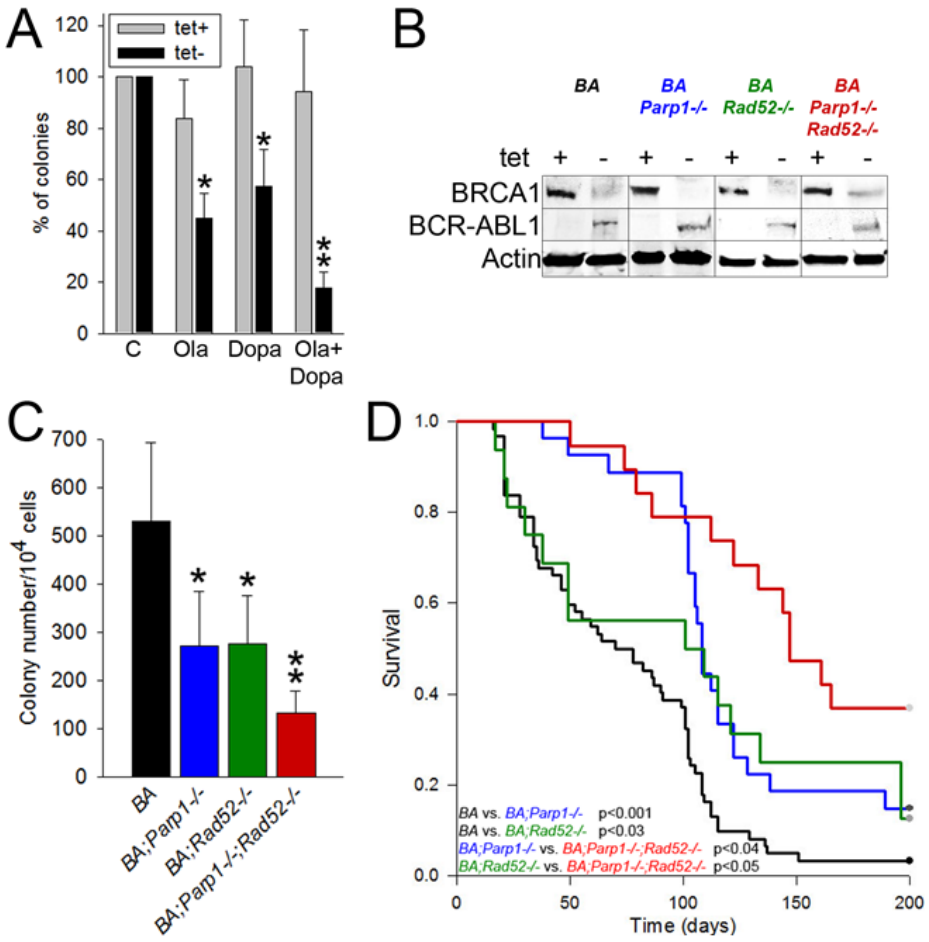

Figure 26. Simultaneous inactivation of PARP1 and RAD52 decreased leukemogenesis and prolonged survival in BRCA1-deficient BCR-ABL transgenic mice. (**A**) Clonogenicity of bone marrow cells isolated from *SCLtTA;p210BCR-ABL1* mice (n=3) to 5μM olaparib (Ola) and/or 20μM 6-OH-dopa (Dopa) in the absence of tetracycline. Results represent mean percentage of clonogenic cells ± SD from 3 mice in triplicates; *p<0.001 in comparison to untreated cells using Student t test, **p=0.016 when compared to individual drugs using the response additivity approach. (**B-D**) *SCLtTA;p210BCR-ABL1;Parp1-/-Rad52-/-* (*BA;Parp1-/-;Rad52-/-*), *SCLtTA;p210BCR-ABL1;* **[Continued]**

[Figure 26 continued] *Parp1-/-* (*BA;Parp1-/-*), *SCLtTA;p210BCR-ABL1;Rad52-/-* (*BA;Rad52-/-*) and *SCLtTA;p210BCR-ABL1* (*BA*) mice were assayed for: (**B**) protein expression of BRCA1, BCR-ABL and actin in the absence (-) or presence (+) of tetracycline, (**C**) clonogenic activity of bone marrow cells from *BA;Parp1-/-;Rad52-/-*, *BA;Parp1-/-*, *BA;Rad52-/-* and *BA* mice (at least 3 mice/group); results show mean ± SD number of BCR-ABL1-dependent colonies ("Tet-" – "Tet+"); *p<0.02 when compared to *BA* and **p<0.05 when compared to *BA;Parp1-/-* and *BA;Rad52-/-*, and (**D**) Kaplan-Meier survival curves of *BA;Parp1-/-;Rad52-/-* (n=19), *BA;Parp1-/-* (n=27), *BA;Rad52-/-* (n=16) and *BA* (n=63) mice following induction of CML-CP-like disease.

isolated from *SCLtTA/p210BCR-ABL1/Parp1-/-Rad52-/-* mice significantly had the lowest BCR-ABL-mediated clonogenic potential when compared to those from *SCLtTA/p210BCR-ABL1/Parp1-/-*, *SCLtTA/p210BCR-ABL1/Rad52-/-*, and *SCLtTA/p210BCR-ABL1* mice (Figure 26C).

To assess the effect of *Parp1-/-Rad52-/-* on the development of CML-CP, we induced expression of BCR-ABL1 by replacing tetracycline-water with regular drinking water at day 0. Mice were euthanized once a moribund state was reached, and immunophenotyping analysis of WBCs were isolated from peripheral blood, bone marrow, and spleen to confirm that each mouse included in the survival curve succumbed to myeloid leukemia (Figure 27). As expected, Kaplan Meier survival curve indicate that in the absence of tetracycline *SCLtTA/p210BCR-ABL1* animals succumbed to CML-CP –

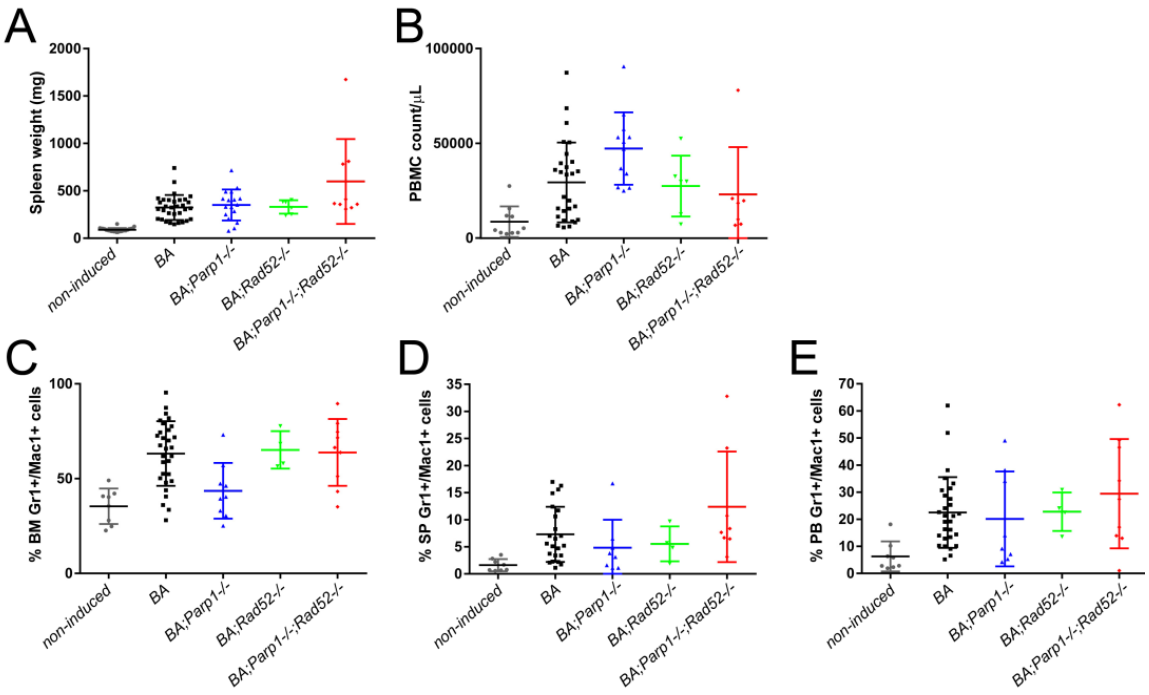

Figure 27. Hematological parameters in transgenic mice indicate they succumbed to CML-like disease: (**A**) spleen weight, (**B**) number of peripheral blood mononuclear cells (PBMC)/µL, and (**C-E**) percent of Gr1+/Mac1+ cells in bone marrow (BM), spleen (SP) and peripheral blood (PB) of all mice (*SCLtTA;p210BCR-ABL1;Parp1-/-Rad52-/-* (*BA;Parp1-/-;Rad52-/-*), *SCLtTA;p210BCR-ABL1;. Parp1-/-* (*BA;Parp1-/-*), *SCLtTA;p210BCR-ABL1;Rad52-/-* (*BA;Rad52-/-*) and *SCLtTA;p210BCR-ABL1* (*BA*)) included in Figure 26D.

like disease in 73.7 ± 5.6 days (Figure 26D, Figure 27). Single knockout *Parp1* and *Rad52* mice displayed delayed development of lethal CML-CP in comparison to *SCLtTA/p210BCR-ABL1* animals ($p<001$ and $p=0.03$, respectively), with *SCLtTA/p210BCR-ABL1/Parp1-/-* mice succumbing in 120.0 ± 8.4 days and *SCLtTA/p210BCR-ABL1/Rad52-/-* mice in 99.9 ± 17.6 days. Most importantly, *SCLtTA/p210BCR- ABL1/Parp1-/-Rad52-/-* mice had a mean survival time of 148.4 ± 11.7 days, which was significantly prolonged in comparison to *SCLtTA/p210BCR-ABL1/Parp1-/-* ($p<0.04$) and *SCLtTA/p210BCR-ABL1/Rad52-/-* ($p<0.05$) animals. Remarkably, 33% of *SCLtTA/p210BCR-ABL1/Parp1-/-Rad52-/-* mice did not develop detectable leukemia and remained healthy throughout the duration of the 200 days of observation, which reveals the ability of dual PARP1 and RAD52 inhibition to outright prevent the onset of the disease in some *SCLtTA/p210BCR-ABL1/Parp1-/-Rad52-/-* mice by overwhelming potential leukemia-initiating cells with lethal DSBs.

To test if the combination of PARPi + RAD52i exerts a synergistic anti-tumor effect *in vivo*, AML patient cells previously determined via microarray analysis to be BRCA-deficient were injected into immunodeficient NSG mice to generate primary AML xenografts. The xenografts were subsequently treated with PARPi talazoparib and RAD52-specific F79 peptide aptamer once a day for 7 consecutive days as previously described[26,106]. Leukemia burden was measured as the percentage of hCD45+ cells in the peripheral blood acquired from tail bleeding at day 35, when the control group was visibly approaching moribund stage. Mice treated with talazoparib and F79 aptamer individually had a reduced percentage of hCD45+ leukemia cells in peripheral blood, but

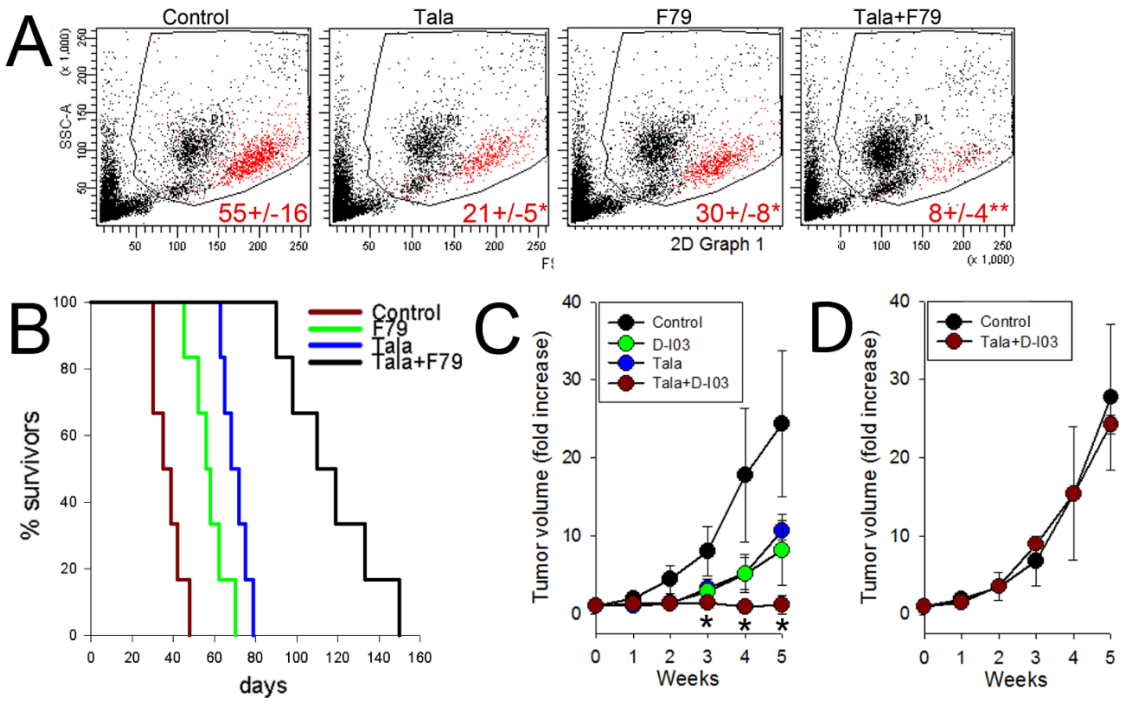

Figure 28. The effect of a combination of PARPi and RAD52i against BRCA1-deficient primary AML xenograft, and BRCA1-deficient breast cancer solid tumor mouse model. NSG mice were inoculated i.v. with 10^6 BRCA1-deficient primary AML xenograft cells. One week later the animals were treated with vehicle (Control), F79 aptamer (F79), talazoparib (Tala) or F79 + Tala (6 mice/group) for 7 consecutive days (6 mice/group). (**A**) Representative plots of PBL from treated mice; mean percentage ± SD of human $CD45^+$ AML cells in peripheral blood leukocytes 3 weeks after leukemia injection; *$p \leq 0.005$ and **$p < 0.001$ in comparison to Control and single compound treatment, respectively, using Student t test. (**B**) Kaplan-Meier survival curves. Results represent mean ± SD fold increase of tumor volume; *$p < 00.05$ when compared to individual agents. (**C**) *Nu/nu* mice were **[Continued]**

Figure 28 continued. …inoculated s.c. with 10^6 BRCA1-deficient MDA-MB-436 cells. Tumor-bearing animals were treated with D-I03, talazoparib (Tala) or D-I03+Tala for 7 consecutive days (3-5 mice/group). Results represent mean ± SD fold increase of tumor volume; *$p<0.05$ when compared to individual agents. (**C**) *Nu/nu* mice were inoculated s.c. with 10^6 BRCA1-proficient MDA-MB-436 cells. Tumor-bearing animals were treated D-I03+Tala for 7 consecutive days (3-5 mice/group).

the combination of talazoparib and F79 aptamer caused an additional 2.6 – 3.8-fold reduction in number of leukemia cells (Untreated mice succumbed to leukemia after 37.3 ± 2.9 days, whereas those treated with F79 aptamer or talazoparib survived for 57.2 ± 3.5 days ($p<0.002$) and 70.3 ± 2.5 days ($p<0.001$), respectively (Figure 28A, B). Combined treatment with talazoparib + F79 aptamer significantly prolonged the survival of leukemic mice to 116.7 ± 9.1 days ($p<0.001$ compared to individual treatments).

Additionally, we tested the effect of PARPi talazoparib combined with RAD52i D-I03 in a solid tumor model *in vivo* by subcutaneously injecting BRCA1-deficient MDA-MB-436 breast cancer cell lines into nu/nu mice. Pharmacokinetic/toxicity studies indicated that maximal tolerated dose of D-I03 is ≥50 mg/kg and t1/2 was 23.4 +/- 17.4 h resulting in >1 μM maximal concentration in peripheral blood. Mice bearing subcutaneous tumors were treated with talazoparib, D-I03, or talazoparib+D-I03 for 7 consecutive days. PARPi and RAD52i when used individually reduced tumor growth in comparison to control vehicle-treated animals whereas the combination of these compounds exerted a stronger effect (Figure 28C). Importantly, talazoparib+D-I03 did

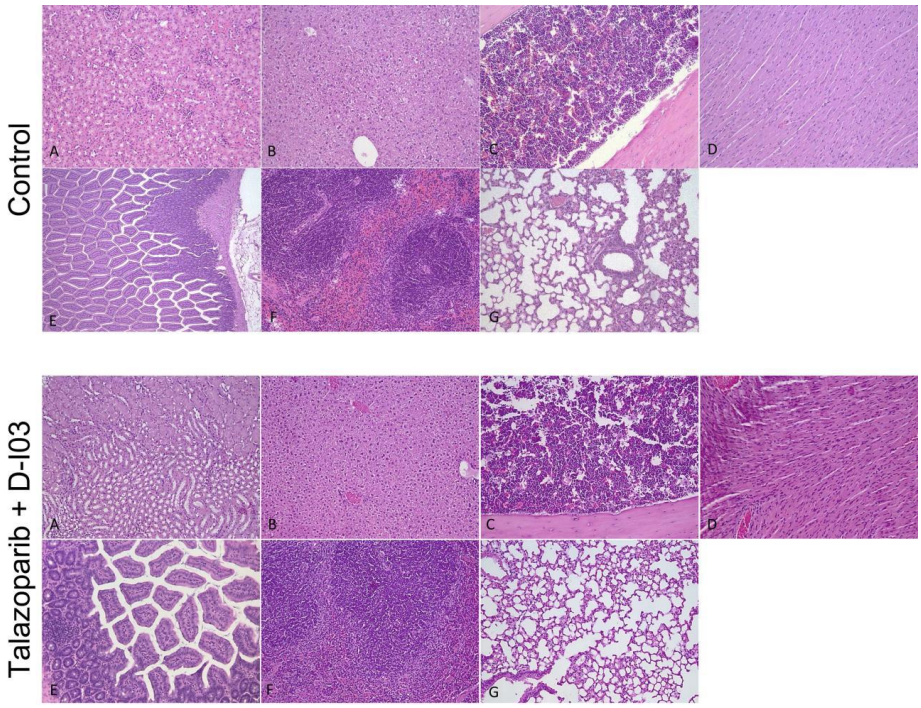

Figure 29. Combination of talazoparib + D-I03 was not toxic to major internal organs. C57Bl/6 mice were treated with vehicle (Control) and talazoparib + D-I03 as described in Figure 26C. Tissue samples were harvested one day after the end of treatment, fixed in formalin, and embedded in paraffin for microscopic evaluation. **Control:** H&E sections of: A) kidney (20x), B) liver (20x), C) tibia bone marrow (20x), D) heart (20x), E) intestine (20x), F) spleen (20x), and G) lung (20x). **Talazoparib + D-I03**: H&E sections of: A) kidney (20x), B) liver (20x), C) tibia bone marrow (20x), D) heart (10x), E) intestine (20x), F) spleen (20x), and G) lung (20x). Results are representative of 5 mice/group.

Parameter		Control	BMN673+D-I03
Peripheral blood	WBC $10^3/\mu L$	6.644±1.877	7.020±2.684
	NE $10^3/\mu L$	1.366±0.699	1.402±0.545
	LY $10^3/\mu L$	4.952±1.051	5.236±1.999
	MO $10^3/\mu L$	0.198±0.086	0.220±0.129
	EO $10^3/\mu L$	0.094±0.104	0.116±0.127
	BA $10^3/\mu L$	0.032±0.036	0.050±0.065
	RBC $10^6/\mu L$	9.114±0.646	8.640±0.630
	HB g/dL	13.240±0.942	12.660±1.555
	HCT %	44.540±3.370	43.400±3.279
	MCV fL	48.860±0.607	50.140±0.598
	MCH pg	14.500±0.339	14.620±0.841
	PLT $10^3/\mu L$	641.000±204.808	825.600±413.964
Bone marrow	White cells/femur ($x10^6$)	11.030±4.260	13.000±1.823
	Lin^-cKit^+ ($x10^6$)	0.203±0.082	0.541±0.181 *
	Lin^-Sca1^+ ($x10^6$)	0.076±0.035	0.152±0.063
	$Lin^-cKit^+Sca1^+$ ($x10^6$)	0.015±0.006	0.065±0.030 *
Spleen weight (g)		0.077±0.008	0.072±0.006
Body weight (g)		19.5±1.400	20.74±0.422

Table 1. Talazoparib + D-I03 did not cause toxicity in hematopoietic organs in C57Bl/6 mice. C57Bl/6 mice (5 mice/group) were treated with vehicle (Control) and talazoparib [0.33mg/kg/day by oral gavage] + D-I03 (50 mg/kg i.p. for 7 days, see Figure 27 C-D). Hematological parameters were examined one day after the end of treatment. Blood was collected into heparinized syringes by cardiac puncture. Peripheral blood parameters (WBC = white blood cells, NE = neutrophils, LY = lymphocytes, MO = monocytes, EO = eosinophils, BA = basophils, RBC = red blood cells, HB = hemoglobin, HCT = hematocrit, MCV = mean red blood cell volume, MCH = mean corpuscular hemoglobin, [**Continued]**

[Table 1 continued] …PLT = platelets) were tested using Hemavet 950FS (Drew) as described before[180]. Lin-cKit+, Lin-Sca1+, and Lin-cKit+Sca1+ cells in bone marrow were counted by flow cytometry as described in Materials and Methods. *$p<0.05$ in comparison to Control.

not exert any significant toxicity against normal tissues and organs (Figure 29; Table 1). Furthermore, the combination of talazoparib and D-I03 had no effect on the growth of BRCA1-proficient MDA-MB-436 tumors in *nu/nu* mice (Figure 28D), providing further support that the combination selectively decreased the tumor volume of BRCA1-deficient MDA-MB-436 tumors.

In conclusion, we have demonstrated using simultaneous genetic and pharmacological inhibition of PARP1 and RAD52 that the combination exerted stronger effect against BRCA-deficient leukemias and solid tumors *in vivo* when compared to individual inhibitors targeting PARP1 or RAD52. Collectively, these data provide strong support for RAD52 as a therapeutic target in PARPi-treated BRCA-deficient cancers.

CHAPTER FOUR

DISCUSSION

Patients with BRCA-deficient tumors often initially respond to PARPi in clinical trials before eventually developing resistance, which eventually leads to cancer relapse[163]. This issue has become more prevalent recently following the publication of multiple studies focused on the identification of the molecular mechanisms behind the development of clinical resistance in patients treated with PARPis[28,136-138] Furthermore, PARPis have been reported to increase the probability of accumulation of additional chromosomal translocations in BRCA-deficient cells, which ultimately may further promote the disease progression[128]. Altogether, since PARPis have become widely used to treat BRCA-deficient cancers, there is an urgent need to develop novel strategies to prevent the development of resistance to PARPi, for example through the development of combination therapies that kill BRCA-deficient cells more rapidly and robustly before resistance mechanisms have the chance to be selected for over time.

There are very few known therapeutic opportunities to potentially reverse acquired resistance to PARPi at this time. These are currently limited to mTOR complex 1 inhibitor rapamycin, CDK12 inhibitor dinaciclib, and NF-κB inhibitor bortezomid[164-166]. Inhibition of P-glycoprotein (P-gp) by treatment with tariquidar may also reverse acquired resistance by preventing the efflux of the PARPi olaparib specifically, as olaparib is the only known PARPi that is a substrate of P-gp [126,167]. The effectiveness of these inhibitors, however, is limited by the molecular mechanisms by which resistance

was acquired. For example, since olaparib is the only PARPi that is a substrate of P-gp, tariquidar would only be effective in olaparib-resistant tumors that were confirmed to be resistant specifically due to upregulated P-gp expression[167]. Furthermore, each of these inhibitors may also aberrantly affect normal cells and thus cause enhanced toxicities and side effects. Therefore, the goal of this dissertation was to come up with an effective combination of inhibitors that would specifically target BRCA-deficient cancer cells while sparing normal, healthy cells, ultimately preventing the development of resistance to PARPi from occurring.

It is well published that PARPis selectively target tumor cells deficient in BRCA-mediated HR repair by causing a lethal accumulation of DSBs which overwhelms the remaining DNA repair pathways in the majority of cells that make up a tumor[168,169]. However, in BRCA-deficient cancers some of these DSBs can still be repaired by both the RAD52-RAD51 alternative HR pathway and RAD52-dependent SSA repair, potentially weakening the synthetic lethal effect of PARPi in some cells[158]. Furthermore, the role of RAD52-mediated DSB repair mechanisms in protecting cells from the toxic accumulation of DSBs is supported by recent reports demonstrating that RAD52 plays an essential role in multiple DSB repair functions including RAD52-mediated HR, single-strand annealing (SSA), break-induced-replication (BIR), and in transcript-RNA-templated DNA recombination and repair[170-173]. Therefore, targeting RAD52 in BRCA-deficient cells will abrogate multiple DNA repair pathways, significantly sensitizing the cells to treatment with PARPi.

We and others have previously demonstrated that inhibition of RAD52 activity caused synthetic lethality to be induced in BRCA-deficient solid tumors and leukemia/lymphoma cells, without exerting toxic effects on normal cells and tissues[23,26,140,148]. To provide additional justification for targeting RAD52 therapeutically, we employed BRCA1/2-proficient and –deficient cell line pairs harboring a DR-GFP reporter cassette to assay for repair of DSBs via HR, which confirmed that RAD52-mediated HR was still active in BRCA1/2-deficient cells and that this activity could be significantly attenuated following exposure to RAD52i. In addition, we confirmed using cells containing SA-GFP cassette that RAD52-depedent SSA activity was significantly attenuated by Dopa, as expected, which further highlights the effectiveness of RAD52i at impairing the ability of BRCA-deficient cells to repair DSBs by targeting multiple repair pathways. Furthermore, we analyzed the RFS probability of ALL and MDS patients displaying low expression levels of RAD52 and genes essential to the BRCA-mediated HR pathway, and found that RFS was significantly higher compared to patients who express high levels of these genes. Altogether, it has been well established that RAD52 is an important therapeutic target for the selective treatment of BRCA-deficient tumors.

In this study we employed two different approaches (small molecule inhibitors targeting RAD52 and PARP1, and dominant-negative RAD52 and PARP1 mutants) to demonstrate *in vitro* that simultaneous inhibition of the two proteins induced a synergistic, dual synthetically lethal effect against a variety of solid tumor and leukemia cell lines deficient in BRCA-mediated HR. This inhibitory effect was associated with an accumulation of DSBs as measured by RAD51 foci formation, γ-H2AX intensity, and

neutral comet tail assays. Not only does the combination of PARPi and RAD52i selectively target highly aggressive BRCA-deficient breast and ovarian cancers, but it also enhances the effectiveness of treatments for other cancers that are deficient in BRCA-mediated repair. We demonstrated that here by using BRCA1/2 -deficient pancreatic cancer, CML, AML, ALL, and Burkitt Lymphoma cell lines and/or primary cells in addition to breast and ovarian cancer cell lines to validate the concept of PARPi + RAD52i-mediated dual synthetic lethality. PARPi + RAD52i was even more selectively potent towards BRCA1/2-deficient cells when used in combination with stand care chemotherapies, while leaving BRCA1/2-proficient cells unharmed.

We also verified that the effect of dual synthetic lethality by PARPi + RAD52is is selectively triggered in BRCA-deficient cells by testing the combination in PARPi-sensitive MLL-AF9 leukemia cells that were previously determined to be BRCA-proficient. Their sensitivity to PARPi is caused by molecular mechanisms unrelated to BRCA-mediated HR-deficiency, and is especially evident when combined with standard cytotoxic therapies[17,160]. However, while these cells were sensitive to PARPi as expected, they did not respond favorably to the combination of PARPi + RAD52i. This is most likely due to the fact that the BRCA pathway is activated in these cells so RAD52-mediated HR and SSA does not play a major role in their repair of DSBs.

The development of resistance PARPi is becoming a common phenomenon following clinical trials. PARPi + RAD52i –mediated dual synthetic lethality is an aggressive therapeutic approach, which may lead to more effective elimination of malignant cells thus limiting/preventing time-dependent drug-induced emergence of

resistant clones[100]. Remarkably, long-term continuous exposure to the combination of PARPi + RAD52i completely prevented the development of resistant clones in all four BRCA1- or BRCA2-deficient solid tumor cell lines tested in addition to RAD54-/- leukemia cell line. Furthermore, sub-optimal doses of PARPi and RAD52i in combination with IM completely eradicated clonogenic primary human CML-BP cells, an advanced and highly aggressive CM.L. PARPi + RAD52i also significantly eradicated clonogenic primary AML cells when used in combination with DNR. The BRCA-proficient clones were unaffected. This observation is especially promising as it demonstrates that the combination of PARPi and RAD52i significantly amplify the effect of IM or DNR, which are both current standard care therapies for their respective diseases. The synergistic effect exerted by PARPi + RAD52i specifically towards BRCA-deficient cells allows for the use of smaller doses in combination with each other and with current standard care therapies to generate a greater effect at targeting BRCA-deficient cells while greatly minimizing toxicity towards normal cells which are BRCA-proficient.

Importantly, we employed three mouse models (transgenic PARP-/-RAD52-/- with inducible CML, BRCA1-deficient AML xenograft, and BRCA1-deficient MDA-MB-436 solid tumor model) that all confirmed the dual synthetic lethal effect we observed *in vitro* in cell lines and primary cells. The AML and breast cancer *in vivo* models highlight the ability of PARPi + RAD52i to specifically target BRCA-deficient cancers in diverse settings, i.e. by targeting a hematopoietic malignancy vs solid tumor.

Additionally, the data generated by the transgenic *SCLtTA/p210BCR-ABL1/Parp1-/-Rad52-/-* mice are especially promising because it demonstrates DSL by knocking out both PARP1 and RAD52 genes. PARPi work by both catalytically inactivating PARP1, and by trapping PARP1 to DSB sites which is extremely cytotoxic. The Kaplan-Meier survival curve of the transgenic mice only represent the effect specifically of PARP1 catalytic inactivation, and the *SCLtTA/p210BCR-ABL1/Parp1-/-Rad52-/-* mice still exhibited significantly prolonged survival compared to both *SCLtTA/p210BCR-ABL1/Parp1-/-* and *SCLtTA/p210BCR-ABL1/Rad52-/-* single knockout mice. It is possible that PARP2 compensated for PARP1 in some of the mice which could explain why some *SCLtTA/p210BCR-ABL1/Parp1-/-Rad52-/-* mice still succumbed to disease eventually, but *Parp1-/-Parp2-/-* mice are embryonic lethal so we could not generate those mice[90]. Importantly, cells and tissues isolated from *Parp1-/-Rad52-/-* mice which were proficient in BRCA-mediated HR repair were not significantly affected by the combination of PARPi and RAD52i, with no adverse effects even following exposure to stressful conditions such as irradiation and treatment with cisplatin, indicating that the combination of PARPi and RAD52i are unlikely to cause side-effects in patients.

One potential limitation of this approach is that due to the heterogeneity of cells within a tumor there is chance that a patient may already have a PARPi-resistant cell at diagnosis. To investigate this issue further, we conducted single-cell RNAseq (scRNAseq) analyses of untreated tumors which did reveal clonal heterogeneity in the expression of DSB repair genes in tumor initiating cells and progenitor cell populations,

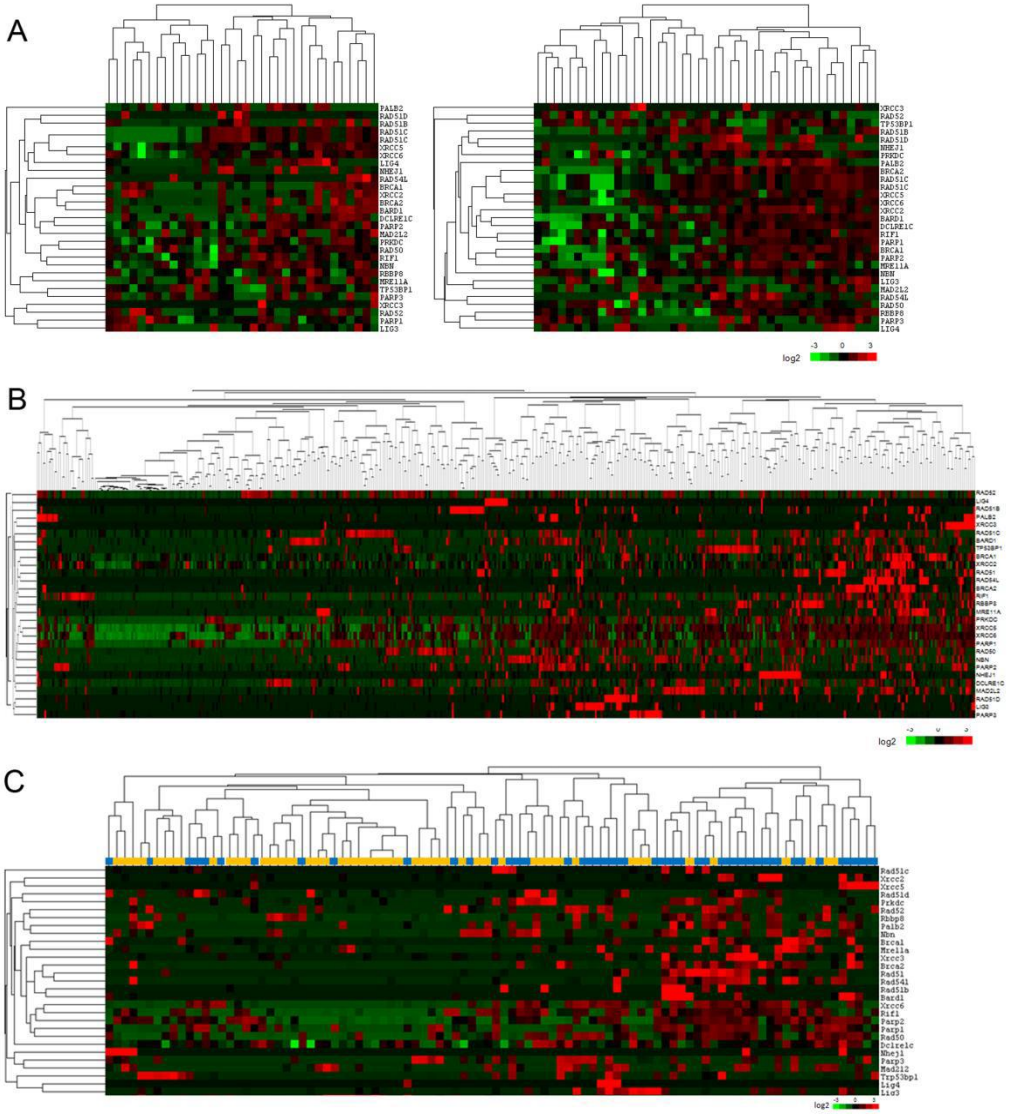

Figure 30. Heterogeneous gene expression patterns of DSB repair genes in single tumor cells identified by single-cell RNA sequencing (scRNAseq). Heatmaps show gene expression values as Z-scores calculated on log2-transformed (RPKM+1) values. (**A, B**) Expression heatmap for DNA repair genes in 34 cells (**A**), and in the replicate batch of 43 cells (**B**) from patient-derived xenograft (PDX) of a lung adenocarcinoma patient (GSE69405)[182]. (**C**) Gene expression profiles in BCR-ABL1-positive CML stem cells (n = 477) obtained from 18 patients with **[continued]**

[Figure 30 continued] …chronic-phase CML at diagnosis (GSE76312)[179]. (**D**) Unsupervised hierarchical clustering of selected DNA repair genes for 96 cells from the c-Kit+ leukemic splenocytes of two independent Flt3ITD/ITD; Dnmt3afl/flMxCre AML mice (GSE77847)[181]; yellow, macrophage/dendritic/neutrophil precursors; blue, hematopoietic stem/progenitor-like cells.

suggesting that PARPi-resistant clones may be already present at diagnosis in some patients (Figure 30). However, PARPi and RAD52i individually induce synthetic lethality in BRCA-deficient cancers by targeting unrelated DNA repair pathways, meaning that it is likely that clones resistant to one inhibitor may still be sensitive to the other. In concordance, we generated talazoparib-resistant *RAD54-/-*Nalm6 leukemia cells and found they were still sensitive to RAD52i Dopa, indicating some of these clones should still be sensitive to an inhibitor such as RAD52i. Additionally, analysis of RFS data of leukemia patients indicated that low RAD52 mRNA expression levels associated with increased survival compared to high expression, and the association was even stronger in patients with low RAD52 expression in combination with low BRCA1, BRCA2, or PALB2 mRNA expression levels. Altogether these data provide further support for the necessity to include RAD52i in treatment regimens targeting BRCA-deficient cancers.

Furthermore, we are proposing PARPi and RAD52i to be used in combination with standard care therapies already in place, as opposed to replacing these therapies. This means that PARPi-resistant clones will still be targeted by other mechanisms in addition to PARPi and RAD52i, further increasing the likelihood that these clones will be

eradicated. In concordance, treatment with the combination of RAD52i D-I03 and IM decreased the number of clonogenic primary CML-BP cells compared to individual treatments of D-I03 or IM. Thus, using RAD52i in combination with PARPi and standard care drugs provides a more effective approach at targeting PARPi-resistant clones already present at diagnosis than only combining PARPi and chemotherapy.

This personalized approach to cancer therapy allows for each patient to receive a combination of drugs tailored specifically to target their cancer based on the specific gene expression profile of their tumor. The combined use of PARPi and RAD52i may be even more effective in patients that express low levels of other possible biomarkers of PARPi-resistance in addition to genes involved in BRCA-mediated HR. For example, low expression levels of MRE11 from the MRN complex have been found to predict sensitivity to PARPi *in vitro* in endometrial carcinomas[174]. MRE11 expression levels are currently being evaluated as a marker for PARPi resistance in clinical trials for prostate, ovarian, and endometrial cancers due to its role in sensing DNA damage that is repaired by both PARP1- and BRCA-mediated pathways[175]. Moreover, the addition of PI3K or PKCβ inhibitor enhanced the effectiveness of a PARPi in BRCA-deficient cancer cells[176,177].

Another recently identified potential biomarker for resistance to PARPi is *Schlafen 11* (SLFN11), with loss of SLFN11 activity correlating with resistance to PARPi in small cell lung cancer (SCLC)[178]. SCLC cell lines and PDXs expressing low levels of SLFN11 were less sensitive to PARPi than those with high expression levels, and that cells with inactivated SLFN11 expression were completely resistant to PARPi.

SLFN11 inhibits replication and induces a prolonged cell cycle arrest during S phase under treatment with the PARPi talazoparib, allowing for the prolonged existence of lethal stalled replication forks, while SLFN11-deficient cells continue cell cycle progression until reaching G2 phase[178]. The identification of additional markers of PARPi and/or RAD52i sensitivity will further enhance the ability to most accurately design a combination therapy to specifically target and eradicate all cells in an individual patient's tumor, thereby decreasing the risk of disease recurrence and the development of resistance over time.

CHAPTER 5

CONCLUSIONS AND FUTURE DIRECTIONS

In conclusion, our data strongly indicate that the simultaneous inhibition of PARP1 and RAD52 will significantly improve the therapeutic outcome of BRCA pathway-deficient malignancies treated with PARPi compared to PARPi monotherapy, while causing no/minimal toxic effects to normal cells and tissues. Importantly, the addition of standard therapeutic drugs, such as IM for CML-BP and DNR for AML, to the treatment regimen containing sub-optimal doses of PARPi + RAD52i further enhanced the dual synthetic lethal effect of PARPi + RAD52i, highlighting the beneficial therapeutic application of this approach. The use of RAD52 as a therapeutic target in PARPi-treated BRCA pathway-deficient cancers was additionally supported *in vivo* using both genetic and pharmacological inhibition of PARP1 and RAD52 in mouse models of leukemia and breast cancer. Moreover, prolonged exposure to the combination of PARPi and RAD52i resulted in complete eradication of cancer cells deficient in BRCA-mediate HR, resulting in the overall prevention of PARPi + RAD52i -resistant clones.

We were also able to successfully predict which primary leukemia samples would be sensitive to the combination of PARPi + RAD52i based on microarray and qPCR analysis of the expression of genes in the BRCA-mediated HR pathway. This provides a way for patients to receive precise, personalized combination therapy regimes based on their unique gene expression profiles. Altogether, our data consistently and clearly demonstrate that inducing dual synthetic lethality by combining PARPi + RAD52i is a

highly robust approach to selectively target BRCA pathway-deficient cancer cells while minimizing toxic effects on normal cells.

To see this approach implemented in clinical trials, the most important step to focus on in the near future is the continued search for and development of specific RAD52i that can be fully developed as anti-cancer drugs. Although there are currently three published RAD52i, two of the three are highly promiscuous inhibitors that would cause too many off-target effects to warrant testing *in vivo*. D-I03 is the only RAD52i thus far to have successfully undergone pharmacokinetic/toxicity studies *in vivo*. For now, additional high throughput screens will need to be conducted to find additional potential "hits" specific to RAD52. Currently, the majority of the high throughput screens are focused on the DNA-binding domain of RAD52. However, it is possible that the RPA-binding domain may also be a useful target for small molecule inhibitors, which is something we may explore in the future. We also plan to continue exploring other potential therapeutic targets involved in various aspects of the DNA damage response, with the ultimate goal of more effectively targeting PARPi-treated BRCA pathway-deficient carcinomas and suppressing the onset of resistance to PARPi.

REFERENCES CITED

1. Yang H, Zhong Y, Peng C, Chen J, Tian D. Important role of indels in somatic mutations of human cancer genes. 2010;11:128-128.

2. O'Neil NJ, Bailey ML, Hieter P. Synthetic lethality and cancer. 2017;18(10):613-623.

3. Nijman SMB. Synthetic lethality: General principles, utility and detection using genetic screens in human cells. 2010;585(1):1-6.

4. Dobzhansky T. Genetics of natural populations .13. recombination and variability in populations of drosophila-pseudoobscura. 1946;31(3):269-290.

5. Miki Y, Swensen J, Shattuckeidens D, et al. A strong candidate for the breast and ovarian-cancer susceptibility gene Brca1. 1994;266(5182):66-71.

6. Wooster R, Bignell G, Lancaster J, et al. Identification of the breast cancer susceptibility gene BRCA2 (vol 378, pg 789, 1995). 1996;379(6567):749-749.

7. Bayraktar S, Glueck S. Systemic therapy options in BRCA mutation-associated breast cancer. 2012;135(2):355-366.

8. Alsop K, Fereday S, Meldrum C, et al. BRCA mutation frequency and patterns of treatment response in BRCA Mutationâ€“Positive women with ovarian cancer: A report from the australian ovarian cancer study group. 2012;30(21):2654-2663.

9. Maxwell KN, Wubbenhorst B, Wenz BM, et al. BRCA locus-specific loss of heterozygosity in germline BRCA1 and BRCA2 carriers. 2017;8(1):319.

10. Li ML, Greenberg RA. Links between genome integrity and BRCA1 tumor suppression. 2012;37(10):418-424.

11. Mersch J, Jackson MA, Park M, et al. Cancers associated with BRCA1 and BRCA2 mutations other than breast and ovarian. 2015;121(2):269-275.

12. Zhang L, Long X. Association of BRCA1 promoter methylation with sporadic breast cancers: Evidence from 40 studies. 2015;5:17869.

13. Ruscito I, Dimitrova D, Vasconcelos I, et al. BRCA1 gene promoter methylation status in high-grade serous ovarian cancer patients--a study of the tumour bank ovarian cancer (TOC) and ovarian cancer diagnosis consortium (OVCAD).

14. Bosviel R, Durif J, Guo J, et al. BRCA2 promoter hypermethylation in sporadic breast cancer. 2012;16(12):707-710.

15. Deutsch E, Jarrousse S, Buet D, et al. Down-regulation of BRCA1 in BCR-ABL-expressing hematopoietic cells. 2003;101(11):4583.

16. Podszywalow-Bartnicka P, Wolczyk M, Kusio-Kobialka M, et al. Downregulation of BRCA1 protein in BCR-ABL1-positive cells depends on tiar-mediated repression of BRCA1 mRNA translation. 2014;124(21).

17. Esposito MT, Zhao L, Fung TK, et al. Synthetic lethal targeting of oncogenic transcription factors in acute leukemia by PARP inhibitors. 2015;21(12):1481-1490.

18. Cho EK, Bang SM, Ahn JY, et al. Prognostic value of AML1/ETO fusion transcripts in patients with acute myelogenous leukemia. 2003;18(1):13-20.

19. Song L, Dai T, Xie Y, et al. Up-regulation of miR-1245 by c-myc targets BRCA2 and impairs DNA repair. 2012;4(2):108-117.

20. Maifrede S, Martin K, Podszywalow-Bartnicka P, et al. IGH/MYC translocation associates with BRCA2 deficiency and synthetic lethality to PARP1 inhibitors. 2017.

21. Chun J, Buechelmaier ES, Powell SN. Rad51 paralog complexes BCDX2 and CX3 act at different stages in the BRCA1-BRCA2-dependent homologous recombination pathway. 2013;33(2):387-395.

22. Jensen RB, Ozes A, Kim T, Estep A, Kowalczykowski SC. BRCA2 is epistatic to the RAD51 paralogs in response to DNA damage. 2013;12(4):306-11.

23. Lok BH, Carley aC, Tchang B, Powell SN. RAD52 inactivation is synthetically lethal with deficiencies in BRCA1 and PALB2 in addition to BRCA2 through RAD51-mediated homologous recombination. 2012;32(30):3552-3558.

24. Qing Y, Yamazoe M, Hirota K, et al. The epistatic relationship between BRCA2 and the other RAD51 mediators in homologous recombination. 2011;7(7):e1002148.

25. Zhao W, Steinfeld JB, Liang F, et al. BRCA1-BARD1 promotes RAD51-mediated homologous DNA pairing. 2017;550(7676).

26. Cramer-Morales K, Nieborowska-Skorska M, Scheibner K, et al. Personalized synthetic lethality induced by targeting RAD52 in leukemias identified by gene mutation and expression profile. 2013;122(7):1293-1304.

27. Nakamura K, Kogame T, Oshiumi H, et al. Collaborative action of Brca1 and CtIP in elimination of covalent modifications from double-strand breaks to facilitate subsequent break repair. 2010;6(1):e1000828.

28. Kondrashova O, Nguyen M, Shield-Artin K, et al. Secondary somatic mutations restoring RAD51C and RAD51D associated with acquired resistance to the PARP inhibitor rucaparib in high-grade ovarian carcinoma. 2017;7(9):984-998.

29. Antoniou AC, Casadei S, Heikkinen T, et al. Breast-cancer risk in families with mutations in PALB2. 2014;371(6):497-506.

30. Hofstatter EW, Domchek SM, Miron A, et al. PALB2 mutations in familial breast and pancreatic cancer. 2011;10(2):10.1007/s10689-011-9426-1.

31. Pelttari LM, Kiiski JI, Ranta S, et al. RAD51, XRCC3, and XRCC2 mutation screening in finnish breast cancer families. 2015;4:92.

32. Loveday C, Turnbull C, Ramsay E, et al. Germline mutations in RAD51D confer susceptibility to ovarian cancer. 2011;43(9):879-882.

33. Pritchard CC, Mateo J, Walsh MF, et al. Inherited DNA-repair gene mutations in men with metastatic prostate cancer. 2016;375(5):443-453.

34. Goodall J, Mateo J, Yuan W, et al. Circulating cell-free DNA to guide prostate cancer treatment with PARP inhibition. 2017;7(9):1006-1017.

35. Soria-Bretones I, SÃ¡ez C, RuÃz-Borrego M, JapÃ³n M,A., Huertas P. Prognostic value of CtIP/RBBP8 expression in breast cancer. 2013;2(6):774-783.

36. Gorringe KL, Choong DYH, Lindeman GJ, Visvader JE, Campbell IG. Breast cancer risk and the BRCA1 interacting protein CTIP. 2008;112(2):351-352.

37. Grabarz A, Barascu A, Guirouilh-Barbat J, Lopez BS. Initiation of DNA double strand break repair: Signaling and single-stranded resection dictate the choice between homologous recombination, non-homologous end-joining and alternative end-joining. 2012;2(3):249-268.

38. Dudas A, Chovanec M. DNA double-strand break repair by homologous recombination. 2004;566(2):131-167.

39. Humphryes N, Hochwagen A. A non-sister act: Recombination template choice during meiosis. 2014;329(1):53-60.

40. Mao Z, Bozzella M, Seluanov A, Gorbunova V. Comparison of nonhomologous end joining and homologous recombination in human cells. 2008;7(10):1765-1771.

41. Lamarche BJ, Orazio NI, Weitzman MD. The MRN complex in double-strand break repair and telomere maintenance. 2010;584(17):3682-3695.

42. Lavin MF, Kozlov S, Gatei M, Kijas AW. ATM-dependent phosphorylation of all three members of the MRN complex: From sensor to adaptor. 2015;5(4):2877-2902.

43. Burma S, Chen BP, Murphy M, Kurimasa A, Chen DJ. ATM phosphorylates histone H2AX in response to DNA double-strand breaks. 2001;276(45):42462-42467.

44. Podhorecka M, Skladanowski A, Bozko P. H2AX phosphorylation: Its role in DNA damage response and cancer therapy. 2010;2010:10.4061/2010/920161.

45. Irminger-Finger I, Ratajska M, Pilyugin M. New concepts on BARD1: Regulator of BRCA pathways and beyond. 2016;72:1-17.

46. Chen L, Nievera CJ, Lee AY, Wu X. Cell cycle-dependent complex formation of BRCA1·CtIP·MRN is important for DNA double-strand break repair. 2008;283(12):7713-7720.

47. Chen L, Nievera CJ, Lee AY, Wu X. Cell cycle-dependent complex formation of BRCA1·CtIP·MRN is important for DNA double-strand break repair. 2008;283(12):7713-7720.

48. Zhang F, Ma J, Wu J, et al. PALB2 links BRCA1 and BRCA2 in the DNA-damage response. 2009;19(6):524-529.

49. Somyajit K, Saxena S, Babu S, Mishra A, Nagaraju G. Mammalian RAD51 paralogs protect nascent DNA at stalled forks and mediate replication restart. 2015;43(20):9835-9855.

50. Taylor MRG, Spirek M, Ma CJ, et al. A polar and nucleotide-dependent mechanism of action for RAD51 paralogs in RAD51 filament remodeling. 2016;64(5):926-939.

51. Taylor MRG, Spirek M, Chaurasiya KR, et al. Rad51 paralogs remodel pre-synaptic Rad51 filaments to stimulate homologous recombination. 2015;162(2):271-286.

52. Mazin AV, Alexeev AA, Kowalczykowski SC. A novel function of Rad54 protein: STABILIZATION OF THE Rad51 NUCLEOPROTEIN FILAMENT. 2003;278(16):14029-14036.

53. Mazin AV, Bornarth CJ, Solinger JA, Heyer W, Kowalczykowski SC. Rad54 protein is targeted to pairing loci by the Rad51 nucleoprotein filament. ;6(3):583-592.

54. Kass EM, Jasin M. Collaboration and competition between DNA double-strand break repair pathways. 2010;584(17):3703-3708.

55. Raderschall E, Golub E, Haaf T. Nuclear foci of mammalian recombination proteins are located at single-stranded DNA regions formed after DNA damage. 1999;96(5):1921-1926.

56. Takata M, Sasaki M, Tachiiri S, et al. Chromosome instability and defective recombinational repair in knockout mutants of the five Rad51 paralogs. 2001;21(8):2858-2866.

57. Park J, Zhang F, Andreassen PR. PALB2: The hub of a network of tumor suppressors involved in DNA damage responses. 2014;1846(1):263-275.

58. McCarthy EE, Celebi JT, Baer R, Ludwig T. Loss of Bard1, the heterodimeric partner of the Brca1 tumor suppressor, results in early embryonic lethality and chromosomal instability. 2003;23(14):5056-5063.

59. Ozden O, Bishehsari F, Bauer J, et al. Expression of an oncogenic BARD1 splice variant impairs homologous recombination and predicts response to PARP-1 inhibitor therapy in colon cancer. 2016;6:26273.

60. Sartori AA, Lukas C, Coates J, et al. Human CtIP promotes DNA end resection. 2007;450(7169):509-514.

61. Rijkers T, Van den Ouweland J, Morolli B, et al. Targeted inactivation of mouse RAD52 reduces homologous recombination but not resistance to ionizing radiation. 1998;18(11):6423-6429.

62. Lok BH, Powell SN. Molecular pathways: Understanding the role of Rad52 in homologous recombination for therapeutic advancement. 2012;18(23):6400-6406.

63. Jensen RB, Carreira A, Kowalczykowski SC. Purified human BRCA2 stimulates RAD51-mediated recombination. 2010;467(7316):678-U62.

64. Wray J, Liu J, Nickoloff JA, Shen Z. Distinct RAD51 associations with RAD52 and BCCIP in response to DNA damage and replication stress. 2008;68(8):2699-2707.

65. Frankenberg-Schwager M, Gebauer A, Koppe C, Wolf H, Pralle E, Frankenberg D. Single-strand annealing, conservative homologous recombination, nonhomologous DNA end joining, and the cell cycle-dependent repair of DNA double-strand breaks induced by sparsely or densely ionizing radiation. 2009;171(3):265-273.

66. Howard SM, Yanez DA, Stark JM. DNA damage response factors from diverse pathways, including DNA crosslink repair, mediate alternative end joining. 2015;11(1):e1004943.

67. Dueva, R., Iliakis,G. Alternative pathways of non-homologous end joining (NHEJ) in genomic instability and cancer. 2013;2(3).

68. Jiang W, Crowe JL, Liu X, et al. Differential phosphorylation of DNA-PKcs regulates the interplay between end-processing and end-ligation during nonhomologous end-joining. 2015;58(1):172-185.

69. Keijzers G, Maynard S, Shamanna RA, Rasmussen LJ, Croteau DL, Bohr VA. The role of RecQ helicases in non-homologous end-joining. 2014;49(6):463-472.

70. Chang HHY, Lieber MR. Structure-specific nuclease activities of artemis and the artemis: DNA-PKcs complex. 2016;44(11):4991-4997.

71. Boboila C, Jankovic M, Yan CT, et al. Alternative end-joining catalyzes robust IgH locus deletions and translocations in the combined absence of ligase 4 and Ku70. 2010;107(7):3034-3039.

72. Parsons J, Dianova I, Allinson S, Dianov G. Poly(ADP-ribose) polymerase-1 protects excessive DNA strand breaks from deterioration during repair in human cell extracts. 2005;272(8):2012-2021.

73. Wang M, Wu W, Wu W, et al. PARP-1 and ku compete for repair of DNA double strand breaks by distinct NHEJ pathways. 2006;34(21):6170-6182.

74. Perrault R, Wang H, Wang M, Rosidi B, Iliakis G. Backup pathways of NHEJ are suppressed by DNA-PK. 2004;92(4):781-794.

75. Soni A, Siemann M, Pantelias GE, Iliakis G. Marked contribution of alternative end-joining to chromosome-translocation-formation by stochastically induced DNA double-strand-breaks in G(2)-phase human cells. 2015;793:2-8.

76. Gottipati P, Vischioni B, Schultz N, et al. Poly(ADP-ribose) polymerase is hyperactivated in homologous recombination-defective cells. 2010;70(13):5389-98.

77. Karanam K, Kafri R, Loewer A, Lahav G. Quantitative live cell imaging reveals a gradual shift between DNA repair mechanisms and a maximal use of HR in mid S phase. 2012;47(2):320-9.

78. Caldecott KW. Mammalian single-strand break repair: Mechanisms and links with chromatin. 2007;6(4):443-453.

79. De Vos M, Schreiber V, Dantzer F. The diverse roles and clinical relevance of PARPs in DNA damage repair: Current state of the art. 2012;84(2):137-146.

80. Rouleau M, Patel A, Hendzel MJ, Kaufmann SH, Poirier GG. PARP inhibition: PARP1 and beyond. 2010;10(4):293-301.

81. Boehler C, Gauthier LR, Mortusewicz O, et al. Poly(ADP-ribose) polymerase 3 (PARP3), a newcomer in cellular response to DNA damage and mitotic progression. 2011;108(7):2783-2788.

82. Nagy Z, Kalousi A, Furst A, Koch M, Fischer B, Soutoglou E. Tankyrases promote homologous recombination and check point activation in response to DSBs. 2015;12(2):e1005791.

83. Pines A, Mullenders LH, van Attikum H, Luijsterburg MS. Touching base with PARPs: Moonlighting in the repair of UV lesions and double-strand breaks. 2013;38(6):321-330.

84. Horvath EM, ZsengellÃ©r Z,K., Szabo C. Quantification of PARP activity in human tissues: Ex vivo assays in blood cells, and immunohistochemistry in human biopsies. 2011;780:267-275.

85. Carter-O'Connell I, Jin H, Morgan RK, David LL, Cohen MS. Engineering the substrate specificity of ADP-ribosyltransferases for identifying direct protein targets. 2014;136(14):5201-5204.

86. Ghosh R, Roy S, Kamyab J, Dantzer F, Franco S. Common and unique genetic interactions of the poly(ADP-ribose) polymerases PARP1 and PARP2 with DNA double-strand break repair pathways. 2016;45:56-62.

87. Beck C, Boehler C, Barbat JG, et al. PARP3 affects the relative contribution of homologous recombination and nonhomologous end-joining pathways. 2014;42(9):5616-5632.

88. Munnur D, Ahel I. Reversible mono-ADP-ribosylation of DNA breaks. 2017;284(23):4002-4016.

89. Zarkovic G, Belousova EA, Talhaoui I, et al. Characterization of DNA ADP-ribosyltransferase activities of PARP2 and PARP3: New insights into DNA ADP-ribosylation. 2017;46(5):2417-2431.

90. Boehler C, Gauthier L, Yelamos J, Noll A, Schreiber V, Dantzer F. Phenotypic characterization of parp-1 and parp-2 deficient mice and cells. 2011;780:313-336.

91. Wei H, Yu X. Functions of PARylation in DNA damage repair pathways. 2016;14(3):131-139.

92. Strom C,E., Johansson F, UhlÃ©n M, Szigyarto CA, Erixon K, Helleday T. Poly (ADP-ribose) polymerase (PARP) is not involved in base excision repair but PARP inhibition traps a single-strand intermediate. 2011;39(8):3166-75.

93. Ying S, Chen Z, Medhurst AL, et al. DNA-PKcs and PARP1 bind to unresected stalled DNA replication forks where they recruit XRCC1 to mediate repair. 2016;76(5):1078.

94. Ying S, Hamdy FC, Helleday T. Mre11-dependent degradation of stalled DNA replication forks is prevented by BRCA2 and PARP1. 2012;72(11):2814-2821.

95. Bryant HE, Petermann E, Schultz N, et al. PARP is activated at stalled forks to mediate Mre11-dependent replication restart and recombination. 2009;28(17):2601-2615.

96. Helleday T, Petermann E, Lundin C, Hodgson B, Sharma RA. DNA repair pathways as targets for cancer therapy. 2008;8(3):193-204.

97. Mortusewicz O, Ame J, Schreiber V, Leonhardt H. Feedback-regulated poly(ADP-ribosyl)ation by PARP-1 is required for rapid response to DNA damage in living cells. 2007;35(22):7665-7675.

98. Gottschalk AJ, Timinszky G, Kong SE, et al. Poly(ADP-ribosyl)ation directs recruitment and activation of an ATP-dependent chromatin remodeler. 2009;106(33):13770-13774.

99. Timinszky G, Till S, Hassa PO, et al. A macrodomain-containing histone rearranges chromatin upon sensing PARP1 activation. 2009;16(9):923-U41.

100. Sonnenblick A, de Azambuja E, Azim HA, Jr., Piccart M. An update on PARP inhibitors-moving to the adjuvant setting. 2015;12(1):27-41.

101. Meehan RS, Chen AP. New treatment option for ovarian cancer: PARP inhibitors. 2016;3(1):3.

102. Yang L, Huang K, Li X, et al. Identification of poly(ADP-ribose) polymerase-1 as a cell cycle regulator through modulating Sp1 mediated transcription in human hepatoma cells. 2013;8(12):e82872.

103. Iglehart JD, Silver DP. Synthetic lethality — A new direction in cancer-drug development. 2009;361(2):189-191.

104. McCabe N, Turner NC, Lord CJ, et al. Deficiency in the repair of DNA damage by homologous recombination and sensitivity to poly(ADP-ribose) polymerase inhibition. 2006;66(16):8109-15.

105. Czyz M, Toma M, Gajos-Michniewicz A, et al. PARP1 inhibitor olaparib (lynparza) exerts synthetic lethal effect against ligase 4-deficient melanomas. 2016;7(46):75551-75560.

106. Nieborowska-Skorska M, Sullivan K, Dasgupta Y, et al. Gene expression and mutation-guided synthetic lethality eradicates proliferating and quiescent leukemia cells. 2017;127(6):2392-2406.

107. Curtin NJ, Szabo C. Therapeutic applications of PARP inhibitors: Anticancer therapy and beyond. 2013;34(6):1217-1256.

108. Murai J, Huang SN, Renaud A, et al. Stereospecific PARP trapping by BMN 673 and comparison with olaparib and rucaparib. 2014;13(2):433.

109. Pfizer Inc. Talazoparib. Talazoparib Significantly Extends Progression-Free Survival in Phase 3 Embraca Trial of Patients with Metastatic Breast Cancer. 2017. https://www.pfizer.com/news/press-release/press-release-detail/talazoparib_significantly_extends_progression_free_survival_in_phase_3_embraca_trial_of_patients_with_metastatic_breast_cancer

110. Wahlberg E, Karlberg T, Kouznetsova E, et al. Family-wide chemical profiling and structural analysis of PARP and tankyrase inhibitors. 2012;30(3):283-+.

111. Murai J, Pommier Y. Classification of PARP inhibitors based on PARP trapping and catalytic inhibition, and rationale for combinations with topoisomerase I inhibitors and alkylating agents. In: Curtin NJ, Sharma RA, eds. *PARP inhibitors for cancer therapy.* Cham: Springer International Publishing; 2015:261-274.

112. Kim G, Ison G, McKee AE, et al. FDA approval summary: Olaparib monotherapy in patients with deleterious germline BRCA-mutated advanced ovarian cancer treated with three or more lines of chemotherapy. 2015;21(19):4257-4261.

113. U.S. Food and Drug Administration. FDA approves olaparib tablets for maintenance treatment in ovarian cancer. 2017. https://www.fda.gov/Drugs/InformationOnDrugs/ApprovedDrugs/ucm572143.htm

114. U.S. Food and Drug Administration. FDA approves olaparib for germline BRCA-mutated metastatic breast cancer. https://www.fda.gov/Drugs/InformationOnDrugs/ApprovedDrugs/ucm592357.htm. Updated January, 2018.

115. Dockery LE, Gunderson CC, Moore KN. Rucaparib: The past, present, and future of a newly approved PARP inhibitor for ovarian cancer. 2017;10:3029-3037.

116. U.S. Food and Drug Administration. FDA approves maintenance treatment for recurrent epithelial ovarian, fallopian tube or primary peritoneal cancers. March 2017. Available from: https://www.fda.gov/NewsEvents/Newsroom/PressAnnouncements/ucm548948.htm.

117. Cadoo KA, Aghajanian C, Fraser C, Milner A, Kolvenbag G. A phase 2 study to assess olaparib by homologous recombination deficiency status in patients with platinum-sensitive, relapsed, ovarian, fallopian tube, or primary peritoneal cancer. 2017;35(15):TPS5606-TPS5606.

118. Wang Y, Wang P, Wang Y, Yang G, Zhang A, Miao Z. An update on poly(ADP-ribose)polymerase-1 (PARP-1) inhibitors: Opportunities and challenges in cancer therapy. 2016;59(21):9575-9598.

119. Ohmoto A, Yachida S. Current status of poly(ADP-ribose) polymerase inhibitors and future directions. 2017;10:5195-5208.

120. Ledermann JA, Harter P, Gourley C, et al. Overall survival in patients with platinum-sensitive recurrent serous ovarian cancer receiving olaparib maintenance monotherapy: An updated analysis from a randomised, placebo-controlled, double-blind, phase 2 trial. 2016;17(11):1579-1589.

121. Kamel D, Gray C, Walia JS, Kumar V. PARP inhibitor drugs in the treatment of breast, ovarian, prostate and pancreatic cancers: An update of clinical trials. 2018;19(1):21-37.

122. Livraghi L, Garber JE. PARP inhibitors in the management of breast cancer: Current data and future prospects. 2015;13:188.

123. Bitler BG, Watson ZL, Wheeler LJ, Behbakht K. PARP inhibitors: Clinical utility and possibilities of overcoming resistance. 2017;147(3):695-704.

124. Ricks TK, Chiu H, Ison G, et al. Successes and challenges of PARP inhibitors in cancer therapy. 2015;5:222.

125. ter Brugge P, Kristel P, van dB, et al. Mechanisms of therapy resistance in patient-derived xenograft models of BRCA1-deficient breast cancer. 2016;108(11):djw148-djw148.

126. Rottenberg S, Jaspers JE, Kersbergen A, et al. High sensitivity of BRCA1-deficient mammary tumors to the PARP inhibitor AZD2281 alone and in combination with platinum drugs. 2008;105(44):17079-17084.

127. Li X, Delzer J, Voorman R, de Morais SM, Lao Y. Disposition and drug-drug interaction potential of veliparib (ABT-888), a novel and potent inhibitor of poly(ADP-ribose) polymerase. 2011;39(7):1161.

128. Bunting SF, CallÃ©n E, Wong N, et al. 53BP1 inhibits homologous recombination in *Brca1*-deficient cells by blocking resection of DNA breaks. ;141(2):243-254.

129. Jaspers JE, Kersbergen A, Boon U, et al. Loss of 53BP1 causes PARP inhibitor resistance in Brca1-mutated mouse mammary tumors. 2013;3(1):68-81.

130. Bouwman P, Aly A, Escandell JM, et al. 53BP1 loss rescues BRCA1 deficiency and is associated with triple-negative and BRCA-mutated breast cancers. 2010;17(6):688-695.

131. Bouwman P, Jonkers J. Molecular pathways: How can BRCA-mutated tumors become resistant to PARP inhibitors? 2014;20(3):540.

132. Sakai W, Swisher EM, Karlan BY, et al. Secondary mutations as a mechanism of cisplatin resistance in BRCA2-mutated cancers. 2008;451(7182):1116-1120.

133. Edwards SL, Brough R, Lord CJ, et al. Resistance to therapy caused by intragenic deletion in BRCA2. 2008;451(7182):1111-1115.

134. Sakai W, Swisher EM, Jacquemont C, et al. Functional restoration of BRCA2 protein by secondary *BRCA2* mutations in *BRCA2*-mutated ovarian carcinoma. 2009;69(16):6381.

135. Norquist B, Wurz KA, Pennil CC, et al. Secondary somatic mutations restoring BRCA1/2 predict chemotherapy resistance in hereditary ovarian carcinomas. 2011;29(22):3008-3015.

136. Barber LJ, Sandhu S, Chen L, et al. Secondary mutations in BRCA2 associated with clinical resistance to a PARP inhibitor. 2013;229(3):422-429.

137. Quigley D, Alumkal JJ, Wyatt AW, et al. Analysis of circulating cell-free DnA identifies multiclonal heterogeneity of BRCA2 reversion mutations associated with resistance to PARP inhibitors. 2017;7(9):999-1005.

138. Weigelt B, Comino-Mendez I, de Bruijn I, et al. Diverse BRCA1 and BRCA2 reversion mutations in circulating cell-free DNA of therapy-resistant breast or ovarian cancer. 2017;23(21):6708-6720.

139. Oza AM, Tinker AV, Oaknin A, et al. Antitumor activity and safety of the PARP inhibitor rucaparib in patients with high-grade ovarian carcinoma and a germline or

somatic BRCA1 or BRCA2 mutation: Integrated analysis of data from study 10 and ARIEL2. 2017;147(2):267-275.

140. Feng Z, Scott SP, Bussen W, et al. Rad52 inactivation is synthetically lethal with BRCA2 deficiency. 2011;108(2):686-691.

141. Fujimori A, Tachiiri S, Sonoda E, et al. Rad52 partially substitutes for the Rad51 paralog XRCC3 in maintaining chromosomal integrity in vertebrate cells. 2001;20(19):5513-5520.

142. Sullivan K, Cramer-Morales K, McElroy DL, et al. Identification of a small molecule inhibitor of RAD52 by structure-based selection. 2016;11(1):e0147230.

143. Viana R, Aguado C, Esteban I, et al. Role of AMP-activated protein kinase in autophagy and proteasome function. 2008;369(3):964-968.

144. Chandramouly G, McDevitt S, Sullivan K, et al. Small-molecule disruption of RAD52 rings as a mechanism for precision medicine in BRCA-deficient cancers. 2015;22(11):1491-1504.

145. Simeonov A, Kulkarni A, Dorjsuren D, et al. Identification and characterization of inhibitors of human apurinic/apyrimidinic endonuclease APE1. 2009;4(6):e5740.

146. Kladova OA, Bazlekowa-Karaban M, Baconnais S, et al. The role of the N-terminal domain of human apurinic/apyrimidinic endonuclease 1, APE1, in DNA glycosylase stimulation. 2018;64:10-25.

147. Domanskyi A, Geissler C, Vinnikov IA, et al. Pten ablation in adult dopaminergic neurons is neuroprotective in parkinson's disease models. 2011;25(9):2898-2910.

148. Huang F, Goyal N, Sullivan K, et al. Targeting BRCA1-and BRCA2-deficient cells with RAD52 small molecule inhibitors. 2016;44(9):4189-4199.

149. Moynahan M, Cui T, Jasin M. Homology-directed DNA repair, mitomycin-C resistance, and chromosome stability is restored with correction of a Brca1 mutation. 2001;61(12):4842-4850.

150. Saeki H, Siaud N, Christ N, et al. Suppression of the DNA repair defects of BRCA2-deficient cells with heterologous protein fusions. 2006;103(23):8768-8773.

151. Stark JM, Pierce AJ, Oh J, Pastink A, Jasin M. Genetic steps of mammalian homologous repair with distinct mutagenic consequences. 2004;24(21):9305-16.

152. Scully R, Ganesan S, Vlasakova K, Chen J, Socolovsky M, Livingston D. Genetic analysis of BRCA1 function in a defined tumor cell line. 1999;4(6):1093-1099.

153. Johnson N, Johnson SF, Yao W, et al. Stabilization of mutant BRCA1 protein confers PARP inhibitor and platinum resistance. 2013;110(42):17041-17046.

154. Slupianek A, Schmutte C, Tombline G, et al. BCR/ABL regulates mammalian RecA homologs, resulting in drug resistance. 2001;8(4):795-806.

155. Koschmieder S, Gottgens B, Zhang P, et al. Inducible chronic phase of myeloid leukemia with expansion of hematopoietic stem cells in a transgenic model of BCR-ABL leukemogenesis. 2005;105(1):324-34.

156. Bolton-Gillespie E, Schemionek M, Klein H, et al. Genomic instability may originate from imatinib-refractory chronic myeloid leukemia stem cells. 2013;121(20):4175-83.

157. Manfredi M, Brandi J, Conte E, et al. IEF peptide fractionation method combined to shotgun proteomics enhances the exploration of rice milk proteome. 2017;537:72-77.

158. Liu J, Heyer W. Who's who in human recombination: BRCA2 and RAD52. 2011;108(2):441-442.

159. Slinker B. The statistics of synergism. 1998;30(4):723-731.

160. Maifrede S, Martinez E, Nieborowska-Skorska M, et al. MLL-AF9 leukemias are sensitive to PARP1 inhibitors combined with cytotoxic drugs. 2017;1(19):1467-1472.

161. Cortes J, Goldman JM, Hughes T. Current issues in chronic myeloid leukemia: Monitoring, resistance, and functional cure. 2012;10(Suppl 3):S-1-S-13.

162. Dkhissi F, Aggoune D, Pontis J, et al. The downregulation of BAP1 expression by BCR-ABL reduces the stability of BRCA1 in chronic myeloid leukemia. 2015;43(9):775-780.

163. Lord CJ, Ashworth A. Mechanisms of resistance to therapies targeting BRCA-mutant cancers. 2013;19(11):1381-1388.

164. Sun C, Zhang F, Xiang T, et al. Phosphorylation of ribosomal protein S6 confers PARP inhibitor resistance in BRCA1-deficient cancers. 2014;5(10):3375-3385.

165. Johnson SF, Cruz C, Greifenberg AK, et al. CDK12 inhibition reverses de novo and acquired PARP inhibitor resistance in BRCA wild-type and mutated models of triple-negative breast cancer. 2016;17(9):2367-2381.

166. Nakagawa Y, Sedukhina AS, Okamoto N, et al. NF-kappa B signaling mediates acquired resistance after PARP inhibition. 2015;6(6):3825-3839.

167. Lawlor D, Martin P, Busschots S, et al. PARP inhibitors as P-glyoprotein substrates. ;103(6):1913-1920.

168. Bryant H, Schultz N, Thomas H, et al. Specific killing of BRCA2-deficient tumours with inhibitors of poly(ADP-ribose) polymerase. 2005;434(7035):913-917.

169. Farmer H, McCabe N, Lord C, et al. Targeting the DNA repair defect in BRCA mutant cells as a therapeutic strategy. 2005;434(7035):917-921.

170. Sotiriou SK, Kamileri I, Lugli N, et al. Mammalian RAD52 functions in break-induced replication repair of collapsed DNA replication forks. 2016;64(6):1127-1134.

171. Hanamshet K, Mazina OM, Mazin AV. Reappearance from obscurity: Mammalian Rad52 in homologous recombination. 2016;7(9):63.

172. Mazina OM, Keskin H, Hanamshet K, Storici F, Mazin AV. Rad52 inverse strand exchange drives RNA-templated DNA double-strand break repair. 2017;67(1):19-+.

173. Keskin H, Shen Y, Huang F, et al. Transcript-RNA-templated DNA recombination and repair. 2014;515(7527):436-+.

174. Koppensteiner R, Samartzis EP, Noske A, et al. Effect of MRE11 loss on PARP-inhibitor sensitivity in endometrial cancer in vitro. 2014;9(6):e100041.

175. Ganguly B, Dolfi SC, Rodriguez-Rodriguez L, Ganesan S, Hirshfield KM. Role of biomarkers in the development of PARP inhibitors. 2015;8:15-25.

176. Juvekar A, Burga LN, Hu H, et al. Combining a PI3K inhibitor with a PARP inhibitor provides an effective therapy for BRCA1-related breast cancer. 2012;2(11):1048-1063.

177. McGrail DJ, Lin CC, Garnett J, et al. Improved prediction of PARP inhibitor response and identification of synergizing agents through use of a novel gene expression signature generation algorithm. 2017;3(1):8.

178. Lok BH, Gardner EE, Schneeberger VE, et al. PARP inhibitor activity correlates with SLFN11 expression and demonstrates synergy with temozolomide in small cell lung cancer. 2017;23(2):523-535.

179. Giustacchini A, Thongjuea S, Barkas N, et al. Single-cell transcriptomics uncovers distinct molecular signatures of stem cells in chronic myeloid leukemia. 2017;23(6):692-702.

180. Nieborowska-Skorska M, Maifrede S, Dasgupta Y, et al. Ruxolitinib-induced defects in DNA repair cause sensitivity to PARP inhibitors in myeloproliferative neoplasms. 2017;130(26):2848-2859.

181. Meyer SE, Qin T, Muench DE, et al. Dnmt3a haploinsufficiency transforms Flt3-ITD myeloproliferative disease into a rapid, spontaneous, and fully-penetrant acute myeloid leukemia. 2016;6(5):501-515.

182. Kim K, Lee HW, Lee H, et al. Single-cell mRNA sequencing identifies subclonal heterogeneity in anti-cancer drug responses of lung adenocarcinoma cells. 2015;16(1):127.